A COMPREHENSIVE COMPARISON BETWEEN ANGLES-ONLY INITIAL ORBIT DETERMINATION TECHNIQUES

A Thesis

by

ANDREW VERNON SCHAEPERKOETTER

Submitted to the Office of Graduate Studies of
Texas A&M University
in partial fulfillment of the requirements for the degree of

MASTER OF SCIENCE

December 2011

Major Subject: Aerospace Engineering

A COMPREHENSIVE COMPARISON BETWEEN ANGLES-ONLY INITIAL ORBIT DETERMINATION TECHNIQUES

A Thesis

by

ANDREW VERNON SCHAEPERKOETTER

Submitted to the Office of Graduate Studies of
Texas A&M University
in partial fulfillment of the requirements for the degree of

MASTER OF SCIENCE

Approved by:

Chair of Committee,	Daniele Mortari
Committee Members,	John Junkins
	Ergun Akleman
Head of Department,	Dimitris Lagoudas

December 2011

Major Subject: Aerospace Engineering

ABSTRACT

A Comprehensive Comparison

between Angles-only Initial Orbit Determination Techniques. (December 2011)

Andrew Vernon Schaeperkoetter, B.S., University of Kansas

Chair of Advisory Committee: Dr. Daniele Mortari

During the last two centuries many methods have been proposed to solve the angles-only initial orbit determination problem. As this problem continues to be relevant as an initial estimate is needed before high accuracy orbit determination is accomplished, it is important to perform direct comparisons among the popular methods with the aim of determining which methods are the most suitable (accuracy, robustness) for the most important orbit determination scenarios. The methods tested in this analysis were the Laplace method, the Gauss method (suing the Gibbs and Herrick-Gibbs methods to supplement), the Double R method, and the Gooding method. These were tested on a variety of scenarios and popular orbits.

A number of methods for quantifying the error have been proposed previously. Unfortunately, many of these methods can overwhelm the analyst with data. A new method is used here that has been shown in previous research by the author. The orbit error is here quantified by two new general orbit error parameters identifying the capability to capture the orbit shape and the orbit orientation.

The study concludes that for nearly all but a few cases, the Gooding method best estimates the orbit, except in the case for the polar orbit for which it depends on the

observation interval whether one uses the Gooding method or the Double R method. All the methods were found to be robust with respect to noise and the initial guess (if required by the method). All the methods other than the Laplace method suffered no adverse effects when additional observation sites were used and when the observation intervals were unequal. Lastly for the case when the observer is in space, it was found that typically the Gooding method performed the best if a good estimate is known for the range, otherwise the Laplace method is generally best.

To My Friends, Family, and For the Greater Glory of God

ACKNOWLEDGMENTS

Firstly, I'd like to thank my advisor, Dr. Mortari, for all his encouragement and support, particularly during this trying time. I further would like to thank the members of my thesis committee, Dr. Junkins and Dr. Akleman. Thank you also to my fellow graduate students, who provided a great deal of support through helping me to understand the computer programs and previous research that enables my own and patiently answering my questions. Thank you to my dear friends who have made me feel at home and given me the strength and will to persevere through this work. Thank you to my family, who through their raising and upbringing, I fell in love with learning and pushing my abilities, in addition to their ever-generous love which is a constant source of support. Finally, but most importantly, thank you to the Lord God who has blessed me with life, intelligence, and wondrous opportunities.

TABLE OF CONTENTS

Page

CHAPTER Page

LIST OF FIGURES

FIGURE Page

FIGURE Page

FIGURE Page

FIGURE Page

FIGURE Page

NOMENCLATURE

Acronyms

GEO	Geostationary Earth Orbit
HEO	Highly Elliptical Orbit
IOD	Initial Orbit Determination
LEO	Low Earth Orbit
NSDC	Near-Earth Differential Corrector

Roman Letters

a	Semi-Major Axis, Gauss Intermediate Parameter
b	Semi-Minor Axis
B	Gibbs Intermediate Parameter
c	Gauss constants
C	Scalar Projection Parameter, Direction Cosine Matrix
C_e	Double R Intermediate Elliptical Orbit Parameter
C_h	Double R Intermediate Hyperbolic Orbit Parameter
C_Ψ	Double R Intermediate Parameter
d	Orbit Shape Error, Gauss Intermediate Parameter
D	Laplace, Gooding, and Gibbs Intermediate Parameter
e	Eccentricity
E	Eccentric Anomaly
f	Orbit Propagation Function, Gooding Intermediate Parameter
F	Double R Evaluation Function, Hyperbolic Anomaly
g	Orbit Propagation Function, Gooding Intermediate Parameter

h	Angular Momentum
i	Inclination, Imaginary Number
L	Line-of-sight Vector
L_g	Gibbs Intermediate Parameter
M	Mean Anomaly, Gauss Intermediate Parameter
n	Mean Motion
N	Gibbs Intermediate Parameter
p	Semi-Latus Rectum
P	Vector Towards Perigee
Q	Vector to Complete Coordinate System with W and P
r	Radial Position
s	Double R Intermediate Parameter
S	Gibbs Intermediate Parameter
S_e	Double R Intermediate Elliptical Orbit Parameter
S_e	Double R Intermediate Hyperbolic Orbit Parameter
t	Time, Vector to Complete Coordinate System with $\hat{h}$ and $\hat{r}$
v	Velocity
w	Gooding Intermediate Parameter
W	Orbit Plane Vector in the Direction of the Angular Momentum
(x, y, z)	Cartesian coordinates

Greek Letters

α	Right Ascension
δ	Declination, Double R Radius Adjustment Parameter, Orbit Attitude Error

ε	General Orbital Error Descriptor
θ	Gooding Intermediate Parameter
λ	Double R Orbit Multiplier
μ	Standard Gravitational Parameter
ν	Gooding Intermediate Parameter, Gaussian Random Number
ρ	Range
τ	Modified Time Variable
φ	True Anomaly
Φ	Orbit Orientation Error
ω	Argument of Perigee
$\omega_{\oplus}$	Earth's Angular Velocity
Ω	Right Ascension of the Ascending Node

Subscript

OI	Orbital to Inertial Frame
$site$	Observation Site

Superscript

T	Transpose

CHAPTER I

INTRODUCTION

A. Statement of Problem

Initial Orbit Determination (IOD) continues to be an important component of a number of different issues in astrodynamics. An estimation of the orbit is needed immediately after a satellite is launched. Additionally, IOD is needed whenever a new object is detected from a ground-based or space-based observer, so that possible future collisions can be avoided. Once IOD has been performed on a satellite, precision orbit determination can then be used to propagate the orbit into the future as needed. Precision orbit determination can of course work better when a better estimate is provided by IOD. Furthermore, in some cases not all IOD methods will provide an estimate at all, or if it does, the estimate can be wildly off. Thus it is important to determine which IOD method will consistently provide an accurate estimation of the observed satellite's orbit.

B. Background

The problem of IOD has been pondered by some of the greatest minds in the past few centuries. Initially, the problem was approached by Laplace and Gauss to determine the orbits of celestial bodies such as planets and asteroids. In the modern era, this problem became more important with the dawn of the Space Race and intercontinental ballistic missiles. The IOD problem remains an essential task in modern times as estimates must be made of the satellite orbital elements before precision orbit deter-

---

This thesis follows the style of *Journal of the Astronautical Sciences*.

mination and the performance of maneuvers. A variety of IOD methods have been devised, incorporating various kinds of measurements, including ranges, angles, and range rates. Angles-only approaches still remain imperative to develop and research as they are being considered for space-based determination for satellites and space debris, particularly through the use of cameras.

Laplace developed the first IOD method in 1780, when range information was unavailable. Laplace used 3 sets of angular measurements from a location and fitted the second satellite position while being reasonably close for the other two. Unfortunately, for near-Earth satellites, Laplace's method produces inaccurate estimates, but is frequently used for heliocentric orbits. It was also very mathematically complex, making the method difficult to use in practicality in an age before calculators.

Need arose for a usable IOD scheme in 1801 when the minor planet Ceres was discovered. The minor planet was lost due to it going behind the sun and an IOD technique was needed to find it again. Thus, Gauss developed his own angles-only method which was subsequently successfully used to relocate Ceres. Gauss's method did not compute the entire orbit but rather just the position. Later Gibbs would create his own technique that could be used in conjunction with the Gauss method to determine the velocity in 1889. The Gibbs technique was best used when possessing widely-spaced observations but struggled with closely-spaced observations. As a result, Herrick modified the Gibbs technique using a Taylor series approximation in the derivation, creating the Herrick-Gibbs method, which is better at the closely-spaced observations.

The age of computers and the ability to perform more mathematically intensive computations, Escobal developed his own method [1], titled the Double R method, which is particularly excellent for widely-spaced observations, though an estimate of the initial and final radii must be provided. Lastly, Gooding developed his own

method [2] which utilizes a solution to Lambert's problem to gradually minimize the angular differences between the observations and the estimated position.

Vallado [3] provides a very good summary of the various algorithms proposed and employed in IOD. The algorithms tested in this research are coded largely based on the description provided in Vallado [3], supplemented with Escobal [1] for the Double R algorithm for the hyperbolic cases. Furthermore, Vallado [3] also gives clear derivations for each of the algorithms, except for the Double R method which can be found in Escobal [1].

It is important to realize that while the 3-angles IOD techniques are the most popular in literature, frequently the majority of the time many more observations are available, creating a dense spread of observations. Much literature has been created discussing the use of these additional observations through a variety of means. If an IOD method determines the orbit within an acceptable accuracy, these additional observations can be used in a Kalman Filter or the method of least squares to refine the parameters of the orbit. Frequently, though, IOD methods have not successfully determined the orbit with acceptable accuracy historically on the first try [4]. As a result, a multitude of methods have been created that can utilize more than the minimum number (3) of observations [5][6][7][8][9]. Furthermore, as radar is being used more frequently, additional information such as range is known as well, leading to techniques that incorporate both range and angle measurements to determine the orbit. Additionally, algorithms have been created to determine which observations should be used of a batch to determine the orbit with the best accuracy [10].

The field of angles-only IOD remains particularly relevant for an observer in orbit with an increasing need for space situational awareness. Thus, methods of IOD capable of performing space-based IOD have been researched and developed. Space-based IOD presents added difficulties because the observer is in orbit as well. Several

methods have been researched and proposed [5][11][12].

Some work has been done previously on analyzing the success of different methods in response to different scenarios and as different parameters are changed. Karimi [7] performs analysis comparing the Gauss and Double R to his own method when faced with different simple scenarios where the observation interval was not varied within a particular scenario. The analysis was simple in that only the scalar position error was studied. Both methods failed for the coplanar case. Furthermore, for a LEO orbit and a polar orbit, both Gauss and Double R perform comparably well. Additionally, sensitivity analysis was performed. Karimi finds that for increasing noise, the Gauss method using a series form of the f and g functions performed worse than the Double R method and the Gauss method using the exact functions when the noise decreased. A small amount of analysis was performed when the observation interval was varied for a particular LEO orbit. The Double R method and Gauss exact method continued to improve in accuracy while the Gauss series method decreased in accuracy after a certain point.

Celletti and Pinzari [13] perform a comparison between the Gauss and Laplace methods by studying a large variety of randomly created heliocentric orbits. When this analysis was completed, it was found that the Gauss method determined the inclination better while the Laplace method did better for the semi-major axis. Both determined the eccentricity with roughly the same accuracy. In general, the Gauss method performed better. The solutions found by the methods were found to be near to each other. Additionally, while randomly created orbits have some advantages, it doesn't directly address the more peculiar orbits explicitly which is a necessary component to compare the two methods. Additionally, this research does not address the orbits of artificial satellites around the Earth. This work was expanded later to observe the effects of varying the observation intervals, sometimes making them

unequally spaced [14]. The study however just observed the frequency of convergence without presenting much data on the relative accuracies of the different methods. The objects studied were asteroid belt objects (which the Gauss method was stated to be best for) and Kuiper belt objects (which the Laplace method did the best at). In general, the rate of convergence increased with decreasing observation interval, but little can be said as to the effects of unequal observation intervals since the total observation times varied.

Taff [4] quite strongly rejects the Gauss method and its historical idealization. Taff believes that the near legendary story of the rediscovery of Ceres has unfairly biased the world towards the Gauss method, which he claims to rarely work on only 3 observations. Taff then proceeds to tell the story of the determination of the orbit of Chiron, where the initial estimate was wildly off compared to the final resulting estimate, which was only achieved through gather enough observations. Taff, Randall, and Stansfield states that the Gauss method is really only good for nearly circular orbits and in general only to be used as a method of last resort [15]. Rather, Taff, Randall, and Stansfield endorses the use of the Laplace method for its possibility of greater accuracy, along with proposed improvements to the Laplace method. No direct comparison of the two methods is found in the study (though part of this is because he uses multiple observations). Related to this work though, Taff, Randall, and Stansfield were unable to achieve convergence on a Molniya orbit at apogee using his Laplace method [15]. Taff, Randall, and Stansfield then divides the scenarios into four portions, dependent upon their angular speeds. When the angular speed is greater than 50"/s, then he endorses the Laplace method. When the speed is between 20-50"/s and near the equator use Laplace, but if nearer the poles (above 20° North or below 20° South) then use Gauss. If the speed is lower than 20"/s and not near stationary use Gauss, but if it is near-stationary, then use a method called NSDC

(Near-Stationary Differential Corrector).

In a later work, Taff [16] cautions against using the Laplace method when possessing only a small amount of data. Rather, Taff, as well as others [17], encourages obtaining a large amount of data to numerically differentiate to obtain the derivatives involved with the method and to smooth the polynomial. Taff further states that the radius of convergence for the Gauss method is relatively small and that the observation intervals must be carefully selected as the orbit becomes more eccentric. Furthermore, when used operationally, Taff stated that one almost needed to know half of the elements (mean anomaly, semi-major axis, and eccentricity) for the method to operate smoothly. Taff then again endorses the use of the Laplace method as best when there is an abundance of data, though it is more sensitive to measurement errors. This noise can be compensated for with a greater density of data. He does note that the Gauss method is useful for more noisy data.

C. Summary of Work

With this array of tools available for both Earth-based and space-based IOD, it is important to systematically analyze each method and its performances for the most classic orbit determination scenarios. While generalizations have been made previously [18], particularly about the closeness of the observations, a systematic analysis of how the methods respond to different scenarios has not yet been undertaken. Furthermore, the different orbital elements might be best estimated by a combination of methods, thus requiring a combination of different methods for optimal results. As the importance of space situational surveillance and the awareness of orbital debris grow, space-based initial orbit determination also should be considered . The goal of this research is to understand which method would be most accurate given a particu-

lar scenario. Portions of this work have previously been presented by Schaeperkoetter and Mortari [19].

D. Original Contributions of Work

This analysis first uses a new method to quantify error between an estimated orbit and the true orbit. The advantage to this quantification of error allows for one to more easily understand where the IOD method failed. This is compared to when Cartesian coordinates are used, which are difficult to interpret, and compared to when Keplerian elements which can overwhelm the analyst. This work then tests the methods under a variety of different orbital scenarios to quantify the accuracy and convergence performance of each method, creating a comprehensive survey of all the methods.

E. Outline of Thesis

In Chapter II, the different IOD methods will be further explained and fully derived. In Chapter III, the methodology of comparing the different orbits will be more fully explained, beginning with a summary of previous orbit error descriptions employed to compare IOD methods. Then a new orbit error description method will be proposed. Finally, the different orbit scenarios that will be employed will be discussed. In Chapter IV, the results of the analysis will be shown and discussed, first discussing the particular orbit scenario results and then the parameter variation scenario results. Additionally, the robustness of the methods is tested, testing the sensitivity to both the initial guess (if required), the measurement error, and when the observations are unequally spaced. In Chapter V, the final conclusions of the thesis will be presented. Then in Appendix A, supplementary charts will be presented.

CHAPTER II

IOD METHODS

As stated before, several IOD methods shall be used to estimate the initial orbit determination results. The apparent strengths and weaknesses of the different methods shall be revealed through the scenarios selected. For this research, the Laplace method, the Gauss method, the Double R iteration method, and the Gooding method will all be used. Both the Gibbs and Herrick-Gibbs methods will be used to refine the velocity estimate found by the Gauss method.

The following equation defines the line-of-sight vector using angular measurements of the declination and right ascension. This line-of-sight vector will be foundational for all of the IOD methods.

$$\hat{L} = \begin{Bmatrix} \cos\delta\cos\alpha \\ \cos\delta\sin\alpha \\ \sin\delta \end{Bmatrix} \tag{2.1}$$

The line-of-sight vector can be related to the observer's location and the satellite's location by the following equation.

$$\vec{r} = \rho\hat{L} + \vec{r}_{site} \tag{2.2}$$

An expression for the radius magnitude can be found by taking the scalar product of this last equation with itself.

$$r = \sqrt{\rho^2 + 2\rho\hat{L}\cdot\vec{r}_{site} + r_{site}^2} \tag{2.3}$$

These equations will serve as the foundation for the different IOD methods.

A. Laplace Method

Laplace developed the Laplace method in 1780 to estimate the middle position and velocity using three observations each at a different time. The Laplace method requires only the initial angular measurements and not any initial guesses. After several algebraic manipulations, a solution can be found for the position and velocity of the observed satellite. It is also possible to expand this method to include more observations by adding higher order derivatives to the derivation, thus enabling the accuracy to be improved, particularly for near-Earth satellites. The Laplace method is most often used for heliocentric orbits and historically important as the first IOD method developed. It is typically not very good at near-Earth orbits. Karimi and Mortari [20] proposes several improvements to the Laplace method to eliminate the need to use an 8^{th} order polynomial, find a solution for all three positions rather than just the middle position, and to use additional measurements.

First, Eqn. (2.2) is differentiated twice to create the velocity and acceleration equations.

$$\dot{\vec{r}} = \dot{\rho}\hat{L} + \rho\dot{\hat{L}} + \dot{\vec{r}}_{site} \tag{2.4}$$

$$\ddot{\vec{r}} = \ddot{\rho}\hat{L} + 2\dot{\rho}\dot{\hat{L}} + \rho\ddot{\hat{L}} + \ddot{\vec{r}}_{site} \tag{2.5}$$

Combining Eqn. (2.5) and the fundamental equation of astrodynamics, the following equation is reached.

$$-\frac{\mu}{r^3}(\rho\hat{L} + \vec{r}_{site}) = \ddot{\rho}\hat{L} + 2\dot{\rho}\dot{\hat{L}} + \rho\ddot{\hat{L}} + \ddot{\vec{r}}_{site} \tag{2.6}$$

Collecting the ρ-derivatives on one side, the following equation is derived.

$$\ddot{\rho}\hat{L} + 2\dot{\rho}\dot{\hat{L}} + \rho\left(\ddot{\hat{L}} + \frac{\mu}{r^3}\hat{L}\right) = -\ddot{\vec{r}}_{site} - \frac{\mu}{r^3}\vec{r}_{site} \tag{2.7}$$

The Lagrange interpolation formula, below,

$$\vec{r}(t) = \sum_{i=1}^{n} \vec{r}_i \prod_{k \neq i} \frac{t - t_k}{t_i - t_k} \tag{2.8}$$

is then used to have an approximate expression for the line-of-sight vector at any time, t.

$$\hat{L}(t) = \frac{(t-t_2)(t-t_3)}{(t_1-t_2)(t_1-t_3)}\hat{L_1} + \frac{(t-t_1)(t-t_3)}{(t_2-t_1)(t_2-t_3)}\hat{L_2} + \frac{(t-t_1)(t-t_2)}{(t_3-t_1)(t_3-t_2)}\hat{L_3} \tag{2.9}$$

This is differentiated twice to produce two of the derivatives necessary for equation (2.7).

$$\dot{\hat{L}}(t) = \frac{2t-t_2-t_3}{(t_1-t_2)(t_1-t_3)}\hat{L_1} + \frac{2t-t_1-t_3}{(t_2-t_1)(t_2-t_3)}\hat{L_2} + \frac{2t-t_1-t_2}{(t_3-t_1)(t_3-t_2)}\hat{L_3} \tag{2.10}$$

$$\ddot{\hat{L}}(t) = \frac{2}{(t_1-t_2)(t_1-t_3)}\hat{L_1} + \frac{2}{(t_2-t_1)(t_2-t_3)}\hat{L_2} + \frac{2}{(t_3-t_1)(t_3-t_2)}\hat{L_3} \tag{2.11}$$

The following equation will convert all the t's to a modified time variable, τ, thus simplifying the equation.

$$\tau_i = t_i - t_2 \tag{2.12}$$

Next, the derivatives for the observer's vector need to be found. If all the obser-

vations occur at the same location, the following equations can be used for the r_{site_2} derivatives if the angular rate is known (e.g., observations from Earth).

$$\dot{\hat{r}}_{site_2} = \vec{\omega}_{\oplus} \times \vec{r}_{site_2} \tag{2.13}$$

$$\ddot{\hat{r}}_{site_2} = \vec{\omega}_{\oplus} \times \dot{\vec{r}}_{site_2} \tag{2.14}$$

Alternatively, the more general formulation can be used to estimate the derivatives, again using the Lagrange interpolation formula.

$$\dot{\hat{r}}_{site_2} = -\frac{\tau_3}{\tau_1(\tau_1 - \tau_3)}\vec{r}_{site_1} - \frac{\tau_3 + \tau_1}{\tau_1\tau_3}\vec{r}_{site_2} - \frac{\tau_1}{\tau_3(\tau_3 - \tau_1)}\vec{r}_{site_3} \tag{2.15}$$

$$\dot{\hat{r}}_{site_2} = \frac{2}{\tau_1(\tau_1 - \tau_3)}\vec{r}_{site_1} + \frac{2}{\tau_1\tau_3}\vec{r}_{site_2} + \frac{2}{\tau_3(\tau_3 - \tau_1)}\vec{r}_{site_3} \tag{2.16}$$

Now, these equations can be substituted into Eqn. (2.7), as all the variables except for the range, the derivatives, and magnitude of the position, r. The position magnitude is the most difficult component to find. For the moment, however, assume that r is known. First, it is desirable to convert the three equations for each observed time of Eqn. (2.7) into matrix form.

$$\begin{bmatrix} \hat{L} & 2\dot{\hat{L}} & \ddot{\hat{L}} + \frac{\mu}{r^3}\hat{L} \end{bmatrix} \begin{Bmatrix} \ddot{\rho} \\ \dot{\rho} \\ \rho \end{Bmatrix} = -\left[\ddot{\vec{r}}_{site} + \frac{\mu}{r^3}\vec{r}_{site}\right] \tag{2.17}$$

To solve for the range and its derivatives, the determinant and Cramer's rule are used. Thus the determinant, D, is found.

$$D = \begin{vmatrix} \hat{L} & 2\dot{\hat{L}} & \ddot{\hat{L}} + \frac{\mu}{r^3}\hat{L} \end{vmatrix} \tag{2.18}$$

Using matrix rules, the determinant is simplified first by subtracting the product of μ/r^3 and the first column from the third column. Then the *coefficient* is factored out of the second second column resulting in the following equation.

$$D = 2 \begin{vmatrix} \hat{L} & 2\dot{\hat{L}} & \ddot{\hat{L}} \end{vmatrix} \tag{2.19}$$

Cramer's rule is then applied using Eqn. (2.7). Because the third column represents the range from the observer, the column is replaced with the right-hand side of Eqn. (2.7), while factoring a -1 out of the column, producing the following equation.

$$D\rho = -2 \begin{vmatrix} \hat{L} & 2\dot{\hat{L}} & \ddot{\vec{r}}_{site} + \frac{\mu}{r^3}\vec{r}_{site} \end{vmatrix} \tag{2.20}$$

This is then split into two determinants.

$$D\rho = -2 \begin{vmatrix} \hat{L} & 2\dot{\hat{L}} & \ddot{\vec{r}}_{site} \end{vmatrix} - 2\frac{\mu}{r^3} \begin{vmatrix} \hat{L} & 2\dot{\hat{L}} & \vec{r}_{site} \end{vmatrix} \tag{2.21}$$

The first determinant shall be considered D_1 and the second determinant shall be considered D_2. The range is then solved for, producing the final equation.

$$\rho = \frac{-2D_1}{D} - \frac{2\mu D_2}{r^3 D} \tag{2.22}$$

It is possible for the determinant to be 0, which will prevent the algorithm from proceeding. Escobal [1] determines that this will only occur when the observation site lies on the great circle of the satellite's orbit.

Now it is necessary to find the middle radius magnitude to determine ρ. To accomplish this, the previous equation is substituted into Eqn. (2.3).

$$r_2^2 = \left(\frac{-2D_1}{D} - \frac{2\mu D_2}{r_2^3 D}\right)^2 + 2\left(\frac{-2D_1}{D} - \frac{2\mu D_2}{r_2^3 D}\right)\hat{L}_2 \cdot \vec{r}_{site_2} + r_{site_2}^2 \tag{2.23}$$

Multiplying everything out and letting C be defined as below, the following eighth-order polynomial is produced.

$$C = \hat{L}_2 \cdot \vec{r}_{site_2} \tag{2.24}$$

$$r_2^8 + \left(\frac{4CD_1}{D} - \frac{4D_1^2}{D^2} - r_{site_2}^2 \right) r_2^6 + \mu \left(\frac{4CD_2}{D} - \frac{8D_1D_2}{D^2} \right) r_2^3 - \frac{4\mu^2 D_2^2}{D^2} = 0 \tag{2.25}$$

Multiple roots of this equation can exist. Prussing and Conway [21] have determined that the correct root must be among the real roots, though this still can result in multiple roots. To determine which of these roots is true, more observations must be processed or *a priori* information must be used.

Having found r, Eqn. (2.22) can then be solved for the range.

To fully determine the orbit, the velocity must be found. Again, Cramer's rule is again used. Since the middle term on the left-hand side in Eqn. (2.7) is the velocity component, the right-hand side of Eqn. (2.7) is entered into that column.

$$D\dot{\rho} = \begin{vmatrix} \hat{L} & \ddot{\vec{r}}_{site} + \frac{\mu}{r^3}\vec{r}_{site} & \ddot{\hat{L}} \end{vmatrix} \tag{2.26}$$

The determinant is again split.

$$D\dot{\rho} = -\begin{vmatrix} \hat{L} & \ddot{\vec{r}}_{site} & \ddot{\hat{L}} \end{vmatrix} - \frac{\mu}{r^3} \begin{vmatrix} \hat{L} & \vec{r}_{site} & \ddot{\hat{L}} \end{vmatrix} \tag{2.27}$$

The first determinant shall be D_3 and the second shall be D_4. The equation is then solved for the range rate.

$$\dot{\rho} = -\frac{D_3}{D} - \frac{\mu D_4}{r^3 D} \tag{2.28}$$

With the range rate and using the previously found derivatives, these known variables can be entered into Eqn. (2.4) which had been found previously.

$$\vec{v}_2 = \dot{\rho}\hat{L}_2 + \rho\dot{\hat{L}}_2 + \dot{\vec{r}}_{site_2} \tag{2.29}$$

B. Gauss Method

Gauss developed the Gauss method in 1801 to find the the position (Gauss was not concerned with finding the velocity). However, the method can be easily extended to find the velocity as well, using extension methods such as Gibbs, Herrick-Gibbs, or a solution to Lambert's Problem (only using 2 position vectors). To successfully apply the method, Long et al. [18] suggests that the orbital arc between observations be less than 60°. Vallado [3] observes that when the angular separation is less than 10°, the method works particularly well. The method begins with the assumption that all the position vectors lie in a single plane. The Gauss method can be divided into two separate methods, Gauss Series and Gauss Exact, to identify the f and g functions employed. Gauss Series uses a Taylor Series approximation of the f and g functions and is non-iterative, as derived in Escobal [1], obtaining a method to find the velocity. Gauss Exact is an iterative method that uses a method to refine the velocity estimate using an estimate of the radius vectors. The method then proceeds to iteratively solve for both the radius and velocity using the exact f and g functions. The Gauss methods require only the initial measurements and not any initial guesses. When the analysis was performed, the Gauss Exact and Gauss Series methods both produced nearly the same results, so only the Gauss Series derivation and results will be shown. When using this method, it was decided to only use the Gibbs and Herrick-Gibbs methods for finding the velocity.

The Gauss method begins with the assumption that all three position vectors lie in a plane. Because this assumption is made, the following equation is valid for some unknown particular values of c_1, c_2, and c_3.

$$c_1\vec{r}_1 + c_2\vec{r}_2 + c_3\vec{r}_3 = \vec{0} \tag{2.30}$$

First, the equation is then multiplied by taking the cross product of the first position vector and then a second equation is produced by taking the cross product of the third position vector (assuming that c_2 is not zero).

$$\vec{r}_1 \times \vec{r}_3(c_1) = \vec{r}_2 \times \vec{r}_3(-c_2) \tag{2.31}$$

$$\vec{r}_1 \times \vec{r}_3(c_1) = \vec{r}_2 \times \vec{r}_3(-c_2) \tag{2.32}$$

Next the f and g functions can be used to relate the second position and velocity with the position of either the first or third position.

$$\vec{r}_i = f_i\vec{r}_2 + g_i\vec{v}_2, \qquad i = 1, 3 \tag{2.33}$$

Letting c_2 be -1 for convenience and substituting in the results from the f and g functions, the following expressions are found for the coefficients.

$$c_1 = \frac{\vec{r}_2 \times (f_3\vec{r}_2 + g_3\vec{v}_2)}{(f_1\vec{r}_2 + g_1\vec{v}_2) \times (f_3\vec{r}_2 + g_3\vec{v}_2)} = \frac{g_3}{f_1g_3 - f_3g_1} \tag{2.34}$$

$$c_3 = \frac{(f_1\vec{r}_2 + g_1\vec{v}_2) \times \vec{r}_2}{(f_1\vec{r}_2 + g_1\vec{v}_2) \times (f_3\vec{r}_2 + g_3\vec{v}_2)} = \frac{-g_1}{f_1g_3 - f_3g_1} \tag{2.35}$$

Since the velocity at the second position is not known, an alternative method of the f and g equations can be used, called the Series Forms. Similar to the Laplace

method, the equation, $\tau_i = t_i - t_2$, is used to create modified time parameters. Also, for the sake of simplicity, the coefficient u is equal to μ/r_2^3. These new formulations are then inserted into the coefficient equations.

$$c_1 = \frac{g_3}{f_1 g_3 - f_3 g_1} \approx \frac{\tau_3}{\tau_3 - \tau_1} + \frac{u\tau_3((\tau_3 - \tau_1)^2 - \tau_3^2)}{6(\tau_3 - \tau_1)} = a_1 + a_{1_u} u \tag{2.36}$$

$$c_3 = \frac{-g_1}{f_1 g_3 - f_3 g_1} \approx \frac{\tau_1}{\tau_3 - \tau_1} + \frac{u\tau_1((\tau_3 - \tau_1)^2 - \tau_1^2)}{6(\tau_3 - \tau_1)} = a_3 + a_{3_u} u \tag{2.37}$$

While this does give us approximate solutions for the coefficients, the ranges have not yet been found. Thus, returning to Eqn. (2.30), Eqn. (2.2) is substituted in.

$$c_1(\vec{\rho}_1 + \vec{r}_{site_1}) + c_2(\vec{\rho}_2 + \vec{r}_{site_2}) + c_3(\vec{\rho}_3 + \vec{r}_{site_3}) = \vec{0} \tag{2.38}$$

The different terms are then separated.

$$c_1\vec{\rho}_1 + c_2\vec{\rho}_2 + c_3\vec{\rho}_3 = -c_1\vec{r}_{site_1} - c_2\vec{r}_{site_2} - c_3\vec{r}_{site_3} \tag{2.39}$$

This can then be further seperated into matrix form so that the ranges can be solved for.

$$\begin{bmatrix} \hat{L}_1 & \hat{L}_2 & \hat{L}_3 \end{bmatrix} \begin{Bmatrix} c_1\rho_1 \\ c_2\rho_2 \\ c_3\rho_3 \end{Bmatrix} = \begin{bmatrix} \vec{r}_{site_1} & \vec{r}_{site_2} & \vec{r}_{site_3} \end{bmatrix} \begin{Bmatrix} -c_1 \\ -c_2 \\ -c_3 \end{Bmatrix} \tag{2.40}$$

The ranges can be solved for by multiplying both sides by the inverse of the line-of-sight vector matrix. This inverse, M, can be given by the following equation,

where $L_i = L_{x_i}\hat{I} + L_{y_i}\hat{J} + L_{z_i}\hat{K}$.

$$L^{-1} = \frac{\begin{bmatrix} L_{y_2}L_{z_3} - Ly_3L_{z_2} & -L_{y_1}L_{z_3} + L_{y_3}L_{z_1} & L_{y_1}L_{z_2} - L_{y_2}L_{z_1} \\ -L_{x_2}L_{z_3} + Lx_3L_{z_2} & L_{x_1}L_{z_3} - Lx_3L_{z_1} & -L_{x_1}L_{z_2} - Lx_2L_{z_1} \\ L_{x_2}L_{y_3} - Lx_3L_{y_2} & -L_{x_1}L_{y_3} + Lx_3L_{y_1} & L_{x_1}L_{y_2} - Lx_2L_{y_1} \end{bmatrix}}{|L|} \tag{2.41}$$

$$\begin{Bmatrix} c_1\rho_1 \\ c_2\rho_2 \\ c_3\rho_3 \end{Bmatrix} = L^{-1} \begin{bmatrix} \vec{r}_{site_1} & \vec{r}_{site_2} & \vec{r}_{site_3} \end{bmatrix} \begin{Bmatrix} -c_1 \\ -c_2 \\ -c_3 \end{Bmatrix} \tag{2.42}$$

Now, the middle range can be determined. The term, $L^{-1}r_{site}$, is designated as M. For computational reasons, it is easiest to keep the coefficients in the form of $a_i + a_{i_u}u$.

$$\rho_2 = M_{21}a_1 - M_{22} + M_{23}a_3 + (M_{21}a_{1u} + M_{23}a_{3_u})u = d_1 + d_2u \tag{2.43}$$

Substituting this into Eqn. (2.3) results in another eighth-order polynomial in r_2. This equation can again be solved.

$$r_2^8 - (d_1^2 + 2Cd_1 + r_{site_2}^2)r_2^6 - 2\mu(Cd_2d_1d_2)r_2^3 - \mu^2d_2^2 = 0 \tag{2.44}$$

where

$$C = \hat{L}_2 \cdot \vec{r}_{site_2} \tag{2.45}$$

Solving Eq. (2.44) can give an initial estimate for r and subsequently ρ. If greater

accuracy is desirable, the method can be further developed to include the Herrick-Gibbs or Gibbs methods. Using Eqn. (2.2) and the solved ranges, the positions at each observation time can be estimated. From these, the Gibbs or Herrick-Gibbs methods can be used to find an estimate for $\vec{v}_2$. Knowing the position and velocity, this information can be used to calculate the semi-latus rectum, p. This can be utilized in the exact f and g functions.

$$f_i = 1 - \left(\frac{r_i}{p}\right)(1 - \cos(\Delta\varphi_i)) \qquad i = 1, 3 \tag{2.46}$$

and

$$g_i = \frac{r_i r_2 \sin(\Delta\varphi_i)}{\sqrt{\mu p}} \qquad i = 1, 3 \tag{2.47}$$

Using these exact forms of the f and g functions, Eqn. (2.36) and equation (2.37) can be used to calculate the coefficients. Again, the matrix calculations in Eqn. (2.42) can be performed to calculate the ranges.

This process of estimating the ranges can be repeated until the ranges converge. With the converged range, Eqn. (2.2) can be used to calculate the position for the three observation times. These three positions can then be entered into the Gibbs or Herrick-Gibbs methods to generate the second velocity.

C. Double R Iteration Method

The Double R iteration method was first published by Escobal in 1965 [1]. While the previous methods may be capable of handling observations spread very far apart, there are scenarios when the methods fail to converge upon a good solution. The advantage of the Double R iteration method is that the method is designed to be able to solve problems where there might be very large intervals between observations.

Long et al. [18] states that the Double R method is effective for measurements that spanned less than a complete orbit. The method iterates around estimates of the magnitudes of the radius vectors, estimates which must be initially provided to the algorithm by the user. A Newton-Raphson iteration process using the numerical partial derivatives is employed to converge upon the radius magnitudes. As stated, the Double R iteration method requires that an estimate of the initial and final radii be made.

First, one begins again with the relationship between the observer and the satellite, relationship that follows from Eqn. (2.2).

$$\vec{\rho}_i = \vec{r}_i - \vec{r}_{site_i} \tag{2.48}$$

The scalar product of this equation is taken with itself, with the variable C_{ψ_i} used to simplify the relationship.

$$\rho_i^2 + \rho_i C_{\psi_i} + (r_{site_i}^2 - r_i^2) = 0 \tag{2.49}$$

where

$$C_{\psi_i} = 2\hat{L}_i \cdot \vec{r}_{site_i} \tag{2.50}$$

Then the equation is solved for the range, ρ.

$$\rho_i = \frac{-C_{\psi_i} + \sqrt{C_{\psi_i}^2 - 4({r_{site_i}}^2 - r_i^2)}}{2} \tag{2.51}$$

At this point, r_1 and r_2 are assumed to be known. At the beginning of this method, estimates for these parameters must be supplied. To assist in the determination of r_3, the following parameter is calculated, which is perpendicular to the plane

formed by the vectors of the first and second position. (The sign for $\hat{W}$ is negative for retrograde orbits).

$$\hat{W} = \frac{\vec{r}_1 \times \vec{r}_2}{|\vec{r}_1 \times \vec{r}_2|} \tag{2.52}$$

Working under the assumption of the two-body problem, all the positions are in the same plane. Thus, as a result, the following must be true.

$$\vec{r}_3 \cdot \hat{W} = 0 \tag{2.53}$$

Substituting in Eqn. (2.2) into Eqn. (2.53) and solving for the range results in the following equation.

$$\rho_3 = \frac{-\vec{r}_{site_3} \cdot \hat{W}}{\hat{L}_3 \cdot \hat{W}} \tag{2.54}$$

Consequently, all three positions can be calculated with the correct radiis.

It is desirable to use the information from the difference in true anomalies, using the following equations, which will to find the correct radii.

$$\cos(\varphi_j - \varphi_k) = \frac{\vec{r}_j \cdot \vec{r}_k}{|\vec{r}_j \cdot \vec{r}_k|} \tag{2.55}$$

and

$$\sin(\varphi_j - \varphi_k) = s\sqrt{1 - \cos^2(\varphi_j - \varphi_k)} \tag{2.56}$$

where

$$s = \pm\frac{x_k y_j - x_j y_k}{|x_k y_j - x_j y_k|} \tag{2.57}$$

where the positive sign in s is for a prograde orbit and a negative sign is for a

retrograde orbit.

Now a method for updating the estimates for r_1 and r_2 must be developed. To accomplish this, the resultant time intervals between the first and second position, and the second and third position must be found so they can be compared to the true time intervals. The following equation is given by Gauss and derived in the Gibbs derivation.

$$p = \frac{c_1 r_1 + c_3 r_3 - r_2}{c_1 + c_3 - 1} \tag{2.58}$$

where the coefficients are given by:

$$c_1 \equiv \frac{r_2 \sin(\varphi_3 - \varphi_2)}{r_1 \sin(\varphi_3 - \varphi_1)} \tag{2.59}$$

and

$$c_3 \equiv \frac{r_2 \sin(\varphi_2 - \varphi_1)}{r_3 \sin(\varphi_3 - \varphi_1)} \tag{2.60}$$

The previous set of equations were not used by Gauss in his derivation because they result in being poorly defined when the first and third observation are close together. A similar equation can be given by dividing the numerator and denominator of Eqn. (2.58) by c_1 (resulting in multiplying the equation by 1):

$$p = \frac{r_1 + c_{r_3} r_3 - c_{r_1} r_2}{1 + c_{r_3} - c_{r_1}} \tag{2.61}$$

where:

$$c_{r1} \equiv \frac{r_1 \sin(\varphi_3 - \varphi_1)}{r_2 \sin(\varphi_3 - \varphi_2)} \tag{2.62}$$

and

$$c_{r3} \equiv \frac{r_1 \sin(\varphi_2 - \varphi_1)}{r_3 \sin(\varphi_3 - \varphi_2)} \tag{2.63}$$

The second set of equations removes the singularity when the first and third observation have a true anomaly difference of π. Eqn. (2.58) is used when the true anomaly difference between the first and third observation is more than π while Eqn. (2.61) is used when the difference is less than or equal to π. Together, these find the semi-latus rectum, p, for all cases.

The product of the eccentricity and the cosine of the true anomaly, $e\cos(\varphi_i)$, at each observation time can then be determined using the equation for a conic.

$$e\cos(\varphi_i) = \frac{p}{r_i} - 1 \tag{2.64}$$

To determine the eccentricity, it is desirable to determine the product, $e\sin(\varphi_i)$. To accomplish this, trigonometric identities are used to expand $e\sin(\varphi_1 + \varphi_2 - \varphi_2)$.

$$e\sin\varphi_1 = \frac{cos(\varphi_2 - \varphi_1)(e\cos\varphi_1) - (e\cos\varphi_2)}{\sin(\varphi_2 - \varphi_1)} \tag{2.65}$$

$$e\sin\varphi_2 = \frac{-cos(\varphi_2 - \varphi_1)(e\cos\varphi_2) + (e\cos\varphi_1)}{\sin(\varphi_2 - \varphi_1)} \tag{2.66}$$

These equations are used so long as $(\varphi_2 - \varphi_1) \neq \pi$. Also,

$$e\sin\varphi_1 = \frac{cos(\varphi_3 - \varphi_2)(e\cos\varphi_2) - (e\cos\varphi_3)}{\sin(\varphi_3 - \varphi_1)} \tag{2.67}$$

$$e\sin\varphi_2 = \frac{-cos(\varphi_3 - \varphi_2)(e\cos\varphi_3) + (e\cos\varphi_2)}{\sin(\varphi_2 - \varphi_1)} \tag{2.68}$$

as long as $(\varphi_3 - \varphi_1) \neq \pi$.

Using an additional trigonometric identity , the eccentricity can be calculated,

followed by the semi-major axis, a.

$$e^2 = (e\cos\varphi_2)^2 + (e\sin\varphi_2)^2 \tag{2.69}$$

$$a = \frac{p}{(1-e^2)} \tag{2.70}$$

At this point the method seperates to two different branches, dependent upon the eccentricity. If the orbit is hyperbolic, the later derivation should be followed. The derivation for an elliptical orbit follows.

It is desirable to first calculate the mean motion with the equation below.

$$n = \mu^{1/2} a^{-3/2} \tag{2.71}$$

First, the commonly derived equations to relate the true anomaly to the eccentric anomaly are given below.

$$\sin E = \frac{r}{p}\sqrt{1-e^2}\sin\varphi \tag{2.72}$$

$$\cos E = \frac{r}{p}(e + \cos\varphi) \tag{2.73}$$

From the previous equations the following relationship can be found.

$$S_e \equiv (e\sin E_2) = \frac{r_2}{p}\sqrt{1-e^2}(e\sin\varphi_2) \tag{2.74}$$

$$C_e \equiv (e\cos E_2) = \frac{r_2}{p}(e^2 + (e\cos\varphi_2)) \tag{2.75}$$

Using these equations, the following forms can be found by using the trigonometric identity and expanding forms such as $\sin(E_3 - E_2 + E_2)$.

$$\sin(E_3 - E_2) = \frac{r_3}{\sqrt{ap}} \sin(\varphi_3 - \varphi_2) - \frac{r_3}{p}[1 - \cos(\varphi_3 - \varphi_2)]S_e \tag{2.76}$$

$$\cos(E_3 - E_2) = 1 - \frac{r_3 r_2}{ap}[1 - \cos(\varphi_3 - \varphi_2)] \tag{2.77}$$

$$\sin(E_2 - E_1) = \frac{r_1}{\sqrt{ap}} \sin(\varphi_2 - \varphi_1) - \frac{r_1}{p}[1 - \cos(\varphi_2 - \varphi_1)]S_e \tag{2.78}$$

$$\cos(E_2 - E_1) = 1 - \frac{r_2 r_1}{ap}[1 - \cos(\varphi_2 - \varphi_1)] \tag{2.79}$$

Using these equations and Kepler's equation, $M = E - e \sin E$, the following equations are reached.

$$M_3 - M_2 = E_3 - E_2 + 2S_e \sin^2\left(\frac{E_3 - E_2}{2}\right) - C_e \sin(E_3 - E_2) \tag{2.80}$$

$$M_1 - M_2 = -(E_2 - E_1) + 2S_e \sin^2\left(\frac{E_2 - E_1}{2}\right) - C_e \sin(E_2 - E_1) \tag{2.81}$$

Using the knowledge that $M_k - M_2 = n(t_k - t_2)$, the following equations are then developed, where the overhead bars denote that the differences were calculated using the estimated parameters.

$$\bar{t}_3 - \bar{t}_2 = \frac{M_3 - M_2}{n} \tag{2.82}$$

$$\bar{t}_1 - \bar{t}_2 = \frac{M_1 - M_2}{n} \tag{2.83}$$

Knowing that these should be equivalent to the time intervals from the obser-

vations themselves, the following function is created to take the difference between the time interval as a result of the estimated orbit and the time interval from the observations.

$$F_1 \equiv \tau_1 - \left(\frac{M_1 - M_2}{n}\right) \tag{2.84}$$

$$F_2 \equiv \tau_3 - \left(\frac{M_3 - M_2}{n}\right) \tag{2.85}$$

These must be forced to zero over the course of the iterations so that the time intervals between the true observations is equal to the time interval between the estimated orbit positions. The time interval, τ, is defined below:

$$\tau_1 = t_1 - t_2 \tag{2.86}$$

$$\tau_3 = t_3 - t_2 \tag{2.87}$$

where the times are those from the true observations. The equations for F_1 and F_2 can be made more broadly applicable by adding an additional term to these equations when the observations occur over the course of more than one orbital period.

$$F_1 = \tau_1 - \left(\frac{M_1 - M_2}{n}\right) + \left(\frac{2\pi}{n}\right)\lambda \tag{2.88}$$

and

$$F_2 = \tau_3 - \left(\frac{M_3 - M_2}{n}\right) - \left(\frac{2\pi}{n}\right)\lambda \tag{2.89}$$

where λ is an integer denoting the number of orbits.

When the F_i functions are made equal to zero, convergence has been reached.

Thus, the iterations should progressively force these functions to zero. A linear approximation of F_i can be given by taking the first-order Taylor series expansion.

$$-F_i = \left(\frac{\partial F_i}{\partial r_1}\right) dr_1 + \left(\frac{\partial F_i}{\partial r_2}\right) dr_2 \tag{2.90}$$

The differentials are then replaced with finite differences, which can then be used to create a system of linear equations using F_1 and F_2.

$$\Delta r_1 = -\frac{\Delta_1}{\Delta} \tag{2.91}$$

$$\Delta r_2 = -\frac{\Delta_2}{\Delta} \tag{2.92}$$

where

$$\Delta \equiv \left(\frac{\partial F_1}{\partial r_1}\right)\left(\frac{\partial F_2}{\partial r_2}\right) - \left(\frac{\partial F_2}{\partial r_1}\right)\left(\frac{\partial F_1}{\partial r_2}\right) \tag{2.93}$$

$$\Delta_1 \equiv \left(\frac{\partial F_2}{\partial r_2}\right) F_1 \left(\frac{\partial F_1}{\partial r_2}\right) F_2 \tag{2.94}$$

$$\Delta_2 \equiv \left(\frac{\partial F_1}{\partial r_1}\right) F_2 \left(\frac{\partial F_2}{\partial r_1}\right) F_1 \tag{2.95}$$

To solve these equations, the partial derivatives, $\frac{\partial F_i}{\partial r}$, must be known, which would then allow for r_i to be corrected iteratively. These partial derivatives can be approximated numerically.

$$\frac{\partial F_i}{\partial r_1} \cong \frac{F_i(r_1 + \delta r_1, r_2) - F_i(r_1, r_2)}{\delta r_1} \tag{2.96}$$

$$\frac{\partial F_i}{\partial r_2} \cong \frac{F_i(r_1, r_2 + \delta r_2) - F_i(r_1, r_2)}{\delta r_2} \tag{2.97}$$

Eqns. (2.96) and (2.97) will produce the four necessary partial derivatives which can then be entered into Eqns. (2.93), (2.94), and (2.95), correcting the radii guesses. The increment inside the partial derivatives, δr_i, is chosen to be .005% of the radii, per the recommendations of Escobal citepEscobal.

$$(r_i)_{j+1} = (r_i)_j + (\Delta r_i)_j, \qquad j = 1, 2, ..., q \tag{2.98}$$

where q is the number of iterations.

Once the radii have been converged upon, they can be used to estimate the velocity, first by finding the f and g coefficients for the f and g functions. The radii is considered to be converged when the update to the radii, Δr, becomes less than 1.0×10^{-6}.

$$f = 1 - \frac{a}{r_2}[1 - \cos(E_3 - E_2)] \tag{2.99}$$

$$g = \tau_3 - \frac{a^{3/2}}{\mu^{1/2}}[E_3 - E_2 \sin(E_3 - E_2)] \tag{2.100}$$

Then manipulating the f and g functions and solving for the velocity, the following equation is reached.

$$\dot{\vec{r}}_2 = \frac{\vec{r}_3 - f\vec{r}_2}{g} \tag{2.101}$$

Thus the elliptical orbital elements are fully determined.

This orbit estimation algorithm is completed when the hyperbolic case is included in the algorithm. It is necessary not only for when the orbit is truly hyperbolic, but

far more commonly, when the initial guess gives a hyperbolic orbit and only gradually converges upon an elliptical orbit.

For the hyperbolic case, the derivation picks up with an alternative mean motion equation.

$$n = \mu^{1/2}(-a)^{-3/2} \tag{2.102}$$

The previous analogous equations of Eqns. (2.74) and (2.75) are then replaced with the similar equations of:

$$S_h = \frac{r_2}{p}\sqrt{e^2-1}(e\sin\varphi_2) \tag{2.103}$$

$$C_h = \frac{r_2}{p}(e^2 + (e\cos\varphi_2)) \tag{2.104}$$

The Eqns. (2.103) and (2.104) can then be used to determine the differences in terms of the hyperbolic anomaly.

$$\sinh(F_3 - F_2) = \frac{r_3}{\sqrt{-ap}}\sin(\varphi_3 - \varphi_2) - \frac{r_3}{p}[1 - \cos(\varphi_3 - \varphi_2)]S_h \tag{2.105}$$

$$\cosh(F_3 - F_2) = 1 - \frac{r_3 r_2}{-ap}[1 - \cos(\varphi_3 - \varphi_2)] \tag{2.106}$$

$$\sinh(F_2 - F_1) = \frac{r_1}{\sqrt{-ap}}\sin(\varphi_2 - \varphi_1) + \frac{r_1}{p}[1 - \cos(\varphi_2 - \varphi_1)]S_h \tag{2.107}$$

$$\cosh(F_2 - F_1) = 1 - \frac{r_2 r_1}{ap}[1 - \cos(\varphi_2 - \varphi_1)] \tag{2.108}$$

The differences in the hyperbolic anomaly are then solved for:

$$F_3 - F_2 = \log(\sinh(F_3 - F_2) + [\sinh^2(F_3 - F_2) + 1]^{1/2}) \tag{2.109}$$

$$F_2 - F_1 = \log(\sinh(F_2 - F_1) + [\sinh^2(F_2 - F_1) + 1]^{1/2}) \tag{2.110}$$

Eqns. (2.109) and (2.110) can then be used in the hyperbolic version of Kepler's equation to produce.

$$M_3 - M_2 = -(F_3 - F_2) + 2S_h \sinh^2\left(\frac{F_3 - F_2}{2}\right) + C_h \sinh(F_3 - F_2) \tag{2.111}$$

$$M_1 - M_2 = (F_2 - F_1) + 2S_h \sinh^2\left(\frac{F_2 - F_1}{2}\right) - C_h \sinh(F_2 - F_1) \tag{2.112}$$

The algorithm then starts at Eqns. (2.88). After convergence upon the radii is obtained, it is again necessary to use different f and g coefficients to calculate the velocity.

$$f = -\frac{\sqrt{-\mu a}}{r_2 r_3} \sinh(F_3 - F_2) \tag{2.113}$$

$$g = 1 - \frac{a}{r_3}(1 - \cosh(F_3 - F_2)) \tag{2.114}$$

From these hyperbolic f and g coefficients, Eqns. (2.101) can be used to calculate the velocity.

D. Gooding Method

The Gooding method was proposed by Gooding in 1993 [2] for the minimum (3) number of measurements. The method requires initial estimates of the first and third ranges ($\tilde{\rho}_1 and \tilde{\rho}_3$) as well as an estimate must be made of whether the orbit is retrograde or prograde. If the wrong guess is made, the method will not converge.

The method begins with two guesses of the scalar range from the observation site to the position at the first and third observation times. With these guesses, the radius vectors at the first and third observation times are then calculated. With the knowledge of these two vectors and the $t_3 - t_1$ time of flight, a Lambert solver is then used to compute the orbit. Using this orbit, a Keplerian propagator estimates the radius vector at the second observation time ($\vec{R}_2$). In the ideal case of perfect measurements and if the initial estimates ($\tilde{\rho}_1 and \tilde{\rho}_3$) were correct, then the unit vector of $\vec{R}_2$ will coincide with the second measurement. In the real case with noise in the measurements, a shooting method is then proposed to minimize the error: the angular difference between the second measurement and the one predicted (orbit) by the Lambert solver. This minimization is then made using nonlinear numerical optimizers (e.g., fmincon() in MATLAB, Nelder-Mead).

Recently, the Gooding method has been extended for N-measurements [5] with $N > 3$, though this will not be employed in the work presented. Modifications have also been proposed as the Gooding method is based on the assumption that the first and third measurements have no error [5]. This requires the additional use of a second nonlinear optimization that include in the cost function also the errors of the first and third measurements.

E. Gibbs Method

Josiah Gibbs proposed his technique in 1889 [22] so that the velocity could be found using three position vectors (previously Lambert's Problem only made use of two). The Gibbs method is primarily based upon geometry. Using three time-sequential vectors, the velocity can be found for the middle position. The method works well for observations which have an angular separation greater than 1 degree. When the observations are closer than this interval, the Herrick-Gibbs method [23] should be used, as proposed by Sam Herrick which uses a Taylor series approach to the Gibbs method.

The Gibbs method is very similar to the formulation for the Gauss method. This method begins with two assumptions. First, the vectors should be in time-sequential order. The second assumption is that the three observations are coplanar. The derivation follows the derivation of Bate, Mueller, and White [24].

The Gibbs method begins with the following equation, similar to the Gauss method.

$$c_1\vec{r}_1 + c_2\vec{r}_2 + c_3\vec{r}_3 = \vec{0} \tag{2.115}$$

Three cross-products are made, the previous equation with $\vec{r}_1$, with $\vec{r}_2$, and with $\vec{r}_3$. This results in the three following equations.

$$c_2\vec{r}_1 \times \vec{r}_2 = c_3\vec{r}_3 \times \vec{r}_1 \tag{2.116}$$

$$c_1\vec{r}_1 \times \vec{r}_2 = c_3\vec{r}_2 \times \vec{r}_3 \tag{2.117}$$

$$c_1\vec{r}_3 \times \vec{r}_1 = c_2\vec{r}_2 \times \vec{r}_3 \tag{2.118}$$

Now, the scalar product is made with Eqn. (2.115) and with the eccentricity vector.

$$\vec{e} \cdot c_1\vec{r}_1 + \vec{e} \cdot c_2\vec{r}_2 + \vec{e} \cdot c_3\vec{r}_3 = 0 \tag{2.119}$$

This can then be simplified with the formula: $\vec{e} \cdot \vec{r} = er\cos\varphi$. Substituting this formula into the previous equation and rearranging the terms results in the following:

$$p = r(1 + e\cos\varphi) = r + re\cos\varphi = r + \vec{e} \cdot \vec{r} \tag{2.120}$$

which can be again rearranged to be

$$\vec{e} \cdot \vec{r}_i = p - r_i \tag{2.121}$$

This can be substituted into Eqn. (2.119).

$$c_1(p - r_1) + c_2(p - r_2) + c_3(p - r_3) = 0 \tag{2.122}$$

This should then be multiplied by the cross product, $\vec{r}_3 \times \vec{r}_1$.

$$\vec{r}_3 \times \vec{r}_1 c_1(p - r_1) + \vec{r}_3 \times \vec{r}_1 c_2(p - r_2) + \vec{r}_3 \times \vec{r}_1 c_3(p - r_3) = \vec{0} \tag{2.123}$$

Then, using the expressions found earlier, Eqns. (2.116),(2.117), and (2.118) are substituted in to remove all the variables except for c_2.

$$c_2\vec{r}_2 \times \vec{r}_3(p - r_1) + c_2\vec{r}_3 \times \vec{r}_1(p - r_2) + c_2\vec{r}_1 \times \vec{r}_2(p - r_3) = \vec{0} \tag{2.124}$$

The coefficient c_2 can then be divided out of the equation, leaving

$$p(\vec{r}_1 \times \vec{r}_2 + \vec{r}_2 \times \vec{r}_3 + \vec{r}_3 \times \vec{r}_1) = r_1(\vec{r}_2 \times \vec{r}_3) + r_2(\vec{r}_3 \times \vec{r}_1) + r_3(\vec{r}_1 \times \vec{r}_2) \tag{2.125}$$

For further development of the Gibbs method, the vector part of the left-hand side of the equation is defined as $\vec{D}$ and the right-hand side is defined as $\vec{N}$.

$$\vec{D} = \vec{r}_1 \times \vec{r}_2 + \vec{r}_2 \times \vec{r}_3 + \vec{r}_3 \times \vec{r}_1 \tag{2.126}$$

$$\vec{N} = r_1(\vec{r}_2 \times \vec{r}_3) + r_2(\vec{r}_3 \times \vec{r}_1) + r_3(\vec{r}_1 \times \vec{r}_2) = p\vec{D} \tag{2.127}$$

Both of these vectors are perpendicular to the plane formed by the three vectors. It is necessary to here define the perifocal coordinate system. A vector $\hat{P}$ points in the direction of the perigee while $\hat{W}$ points in the direction of the angular momentum. Hence, the following must be true:

$$\hat{P} = \frac{\vec{e}}{|\vec{e}|} \tag{2.128}$$

$$\hat{W} = \frac{\vec{N}}{|\vec{N}|} \tag{2.129}$$

Because these vectors are orthogonal to each other, they can define a third vector to complete the coordinate system as:

$$\hat{Q} = \hat{W} \times \hat{P} = \frac{\vec{N} \times \vec{e}}{|\vec{N}||\vec{e}|} \tag{2.130}$$

The definition for $\hat{N}$ is then substituted in.

$$Ne\hat{Q} = \vec{N} \times \vec{e} = r_1(\vec{r}_2 \times \vec{r}_3) \times \vec{e} + r_2(\vec{r}_3 \times \vec{r}_1) \times \vec{e} + r_3(\vec{r}_1 \times \vec{r}_2) \times \vec{e} \tag{2.131}$$

This is simplified using the rule of triple cross products and simplified to be:

$$Ne\hat{Q} = r_1(\vec{r}_2 \cdot \vec{e})\vec{r}_3 - r_1(\vec{r}_3 \cdot \vec{e})\vec{r}_2 + r_2(\vec{r}_3 \cdot \vec{e})\vec{r}_1 - r_2(\vec{r}_1 \cdot \vec{e})\vec{r}_3 + r_3(\vec{r}_1 \cdot \vec{e})\vec{r}_2 - r_3(\vec{r}_2 \cdot \vec{e})\vec{r}_1 \tag{2.132}$$

Again, using Eqn. (2.127), the previous equation is again simplified.

$$Ne\hat{Q} = p[(r_2 - r_3)\vec{r}_1 + (r_3 - r_1)\vec{r}_2 + (r_1 - r_2)\vec{r}_3] = p\vec{S} \tag{2.133}$$

Knowing that $Ne = pS$ and that $N = pD$, the eccentricity can be solved for with the following equation.

$$e = \frac{S}{D} \tag{2.134}$$

From the derivation of the trajectory equation, the following formula is recalled.

$$\dot{\vec{r}}_2 \times \vec{h} = \mu \left(\frac{\vec{r}_2}{r_2} + \vec{e} \right) \tag{2.135}$$

With this formula, two cross products are formed on each side of the equation with the angular momentum, resulting in

$$\vec{h} \times (\dot{\vec{r}}_2 \times \vec{h}) = \mu \left(\frac{\vec{h} \times \vec{r}_2}{r_2} + \vec{h} \times \vec{e} \right) \tag{2.136}$$

which can be reduced to

$$h^2 \vec{v}_2 = \mu \left(\frac{\vec{h} \times \vec{r}_2}{r_2} + \vec{h} \times \vec{e} \right) \tag{2.137}$$

Remembering that $\vec{h} = h\hat{W}$ and $\vec{e} = e\hat{P}$, these equations are then substituted in.

$$\vec{v}_2 = \frac{\mu}{h}\left(\frac{\hat{W}\times\vec{r}_2}{r_2} + e\hat{W}\times\hat{P}\right) = \frac{\mu}{h}\left(\frac{\hat{W}\times\vec{r}_2}{r_2} + e\hat{Q}\right) \tag{2.138}$$

Recalling that $N = pD$ and $h = \sqrt{\mu p}$, the following equation is also derived.

$$h = \sqrt{\frac{N\mu}{D}} \tag{2.139}$$

Combining Eqn. (2.139) with Eqn. (2.134) in conjunction with the knowledge that $\hat{Q}$ is a unit vector in the direction of $\vec{S}$ and that $\hat{W}$ is a unit vector in the direction of $\vec{D}$, the following equation can be derived.

$$\vec{v}_2 = \frac{1}{r_2}\sqrt{\frac{\mu}{ND}}\vec{D}\times\vec{r}_2 + \sqrt{\frac{\mu}{ND}}\vec{S} \tag{2.140}$$

This is simplified by defining the following quantities:

$$\vec{B} \equiv \vec{D}\times\vec{r}_2 \tag{2.141}$$

$$L_g \equiv \sqrt{\frac{\mu}{ND}} \tag{2.142}$$

resulting in

$$\vec{v}_2 = \frac{L_g}{r_2}\vec{B} + L_g\vec{S} \tag{2.143}$$

Thus the goal of calculating the middle velocity has been achieved.

F. Herrick-Gibbs Method

The Herrick-Gibbs method is an extension of the Gibbs method. It is not as robust as the Gibbs method but it fulfills a gap in the capabilities of the Gibbs method. As

previously stated, the Gibbs method is best for observations that do not include short-arcs. In contrast, the Herrick-Gibbs method, using a Taylor series approximation approach, is very good when used for short-arcs. As would be expected for a Taylor-series approximation, as the time interval grows larger (and the arcs consequently become longer), the approximation becomes less and less accurate. However, as the arcs shrink, the problem becomes less and less observable and it becomes more and more dominated by measurement error.

The derivation begins with the Taylor series approximation centered around the second position vector.

$$\vec{r}(t) = \vec{r}_2 + \dot{\vec{r}}_2(t - t_2) + \frac{\ddot{\vec{r}}_2(t - t_2)^2}{2!} + \frac{\dddot{\vec{r}}_2(t - t_2)^3}{3!} + \frac{\ddddot{\vec{r}}_2(t - t_2)^4}{4!} + ... \tag{2.144}$$

The appropriate time differences are then substituted into the equation for the first and third position vectors.

$$\vec{r}_1 = \vec{r}_2 + \dot{\vec{r}}_2\Delta t_{12} + \frac{\ddot{\vec{r}}_2\Delta t_{12}^2}{2!} + \frac{\dddot{\vec{r}}_2\Delta t_{12}^3}{3!} + \frac{\ddddot{\vec{r}}_2\Delta t_{12}^4}{4!} + ... \tag{2.145}$$

$$\vec{r}_3 = \vec{r}_2 + \dot{\vec{r}}_2\Delta t_{32} + \frac{\ddot{\vec{r}}_2\Delta t_{32}^2}{2!} + \frac{\dddot{\vec{r}}_2\Delta t_{32}^3}{3!} + \frac{\ddddot{\vec{r}}_2\Delta t_{32}^4}{4!} + ... \tag{2.146}$$

Again, the goal of the Herrick-Gibbs method is to find the middle velocity vector. To accomplish this, terms of 5th or higher order will be ignored in the Taylor series approximation. Next, multiply Eqn. (2.145) by $(-\Delta t_{32}^2)$ and Eqn. (2.146) by (Δt_{12}^2), after which the sum of the two resulting equations is taken, leaving

$$\begin{aligned} -\vec{r}_1\Delta t_{32}^2 + \vec{r}_3\Delta t_{12}^2 &= \vec{r}_2(-\Delta t_{32}^2 + \Delta t_{12}^2) + \dot{\vec{r}}_2(-\Delta t_{32}^2\Delta t_{12} + \Delta t_{12}^2\Delta t_{32}) \\ &\quad + \frac{\dddot{\vec{r}}_2}{6}(-\Delta t_{32}^2\Delta t_{12}^3 + \Delta t_{12}^2\Delta t_{32}^3) \\ &\quad + \frac{\ddddot{\vec{r}}_2}{24}(-\Delta t_{32}^2\Delta t_{12}^4 + \Delta t_{12}^2\Delta t_{32}^4) \end{aligned} \tag{2.147}$$

In the desire to simplify this equation, the following quantities were found and substituted into the previous equation.

$$\Delta t_{12}^2\Delta t_{32} - \Delta t_{32}^2\Delta t_{12} = \Delta t_{12}\Delta t_{32}\Delta t_{13} \tag{2.148}$$

$$\Delta t_{12}^2\Delta t_{32}^3 - \Delta t_{32}^2\Delta t_{12}^3 = \Delta t_{12}^2\Delta t_{32}^2\Delta t_{31} \tag{2.149}$$

$$\Delta t_{12}^2\Delta t_{32}^4 - \Delta t_{32}^2\Delta t_{12}^4 = \Delta t_{12}^2\Delta t_{32}^2\Delta t_{31}(\Delta t_{32} + \Delta t_{12}) \tag{2.150}$$

After the substitution is completed and the terms are rearranged, the following equation is obtained.

$$\begin{aligned} \dot{\vec{r}}_2(\Delta t_{12}\Delta t_{32}\Delta t_{31}) &= \vec{r}_1\Delta t_{32}^2 + \vec{r}_2(-\Delta t_{32}^2 + \Delta t_{12}^2) - \vec{r}_3\Delta t_{12}^2 \\ &\quad + \frac{\dddot{\vec{r}}_2}{6}(\Delta t_{12}^2\Delta t_{32}^2\Delta t_{31}) \\ &\quad + \frac{\ddddot{\vec{r}}_2}{24}(\Delta t_{12}^2\Delta t_{32}^2\Delta t_{31}(\Delta t_{32} + \Delta t_{12})) \end{aligned} \tag{2.151}$$

It is now necessary to find the quantities for the derivatives, as all other values needed to find the velocity have been found. To accomplish this, return to Eqns. (2.145) and (2.146) and take the derivative of each twice to result in the following equations.

$$\ddot{\vec{r}}_1 = \ddot{\vec{r}}_2 + \dddot{\vec{r}}_2 \Delta t_{12} + \frac{\ddddot{\vec{r}}_2}{2} \Delta t^2/12 + ... \tag{2.152}$$

$$\ddot{\vec{r}}_3 = \ddot{\vec{r}}_2 + \dddot{\vec{r}}_2 \Delta t_{32} + \frac{\ddddot{\vec{r}}_2}{2} \Delta t^2/32 + ... \tag{2.153}$$

Similar to the process performed earlier, Eqn. (2.152) is multiplied by $(-\Delta t_{32})$ and Eqn. (2.153) is multiplied by (Δt_{12}), after which the sum is taken, thus eliminating the third derivative in the equation.

$$-\ddot{\vec{r}}_1 \Delta t_{32} + \ddot{\vec{r}}_3 \Delta t_{12} = \ddot{\vec{r}}_2(-\Delta t_{32} + \Delta t_{12}) + \frac{\ddddot{\vec{r}}_2}{2}(-\Delta t_{32}\Delta t_{12}^2 + \Delta t_{12}\Delta t_{32}^2) \tag{2.154}$$

The equation can be simplified by expanding the t terms. The terms inside of the first parenthesis can be simplified knowing the following:

$$-(t_3 - t_2) + (t_1 - t_2) = -(t_3 - t_1) = -\Delta t_{31} = \Delta t_{13} \tag{2.155}$$

The terms inside of the second parenthesis can be simplified after taking out the common factor.

$$\Delta t_{12}\Delta t_{32}(-\Delta t_{12} + \Delta t_{32}) \tag{2.156}$$

This can be again be simplified using Eqn. (2.155). Thus, Eqn. (2.154) can be simplified to result in the following equation.

$$-\ddot{\vec{r}}_1 \Delta t_{32} + \ddot{\vec{r}}_3 \Delta t_{12} = \ddot{\vec{r}}_2(-\Delta t_{31}) + \frac{\ddddot{\vec{r}}_2}{2}(\Delta t_{12}\Delta t_{32}\Delta t_{31}) \tag{2.157}$$

This can be solved for the fourth derivative, resulting in:

$$\ddddot{\vec{r}}_2 = \frac{2}{\Delta t_{12}\Delta t_{32}\Delta t_{31}}(-\ddot{\vec{r}}_1\Delta t_{32} + \ddot{\vec{r}}_2\Delta t_{31} + \ddot{\vec{r}}_3\Delta t_{12}) \tag{2.158}$$

Returning to Eqns. (2.152) and (2.153), by multiplying by $(-\Delta t_{32}^2)$ and (Δt_{12}^2) respectively and taking the sum, the fourth derivative can be eliminated and leave the third derivative.

$$-\ddot{\vec{r}}_1\Delta t_{32}^2 + \ddot{\vec{r}}_3\Delta t_{12}^2 = \ddot{\vec{r}}_2(-\Delta t_{32}^2 + \Delta t_{12}^2) + \dddot{\vec{r}}_2(-\Delta t_{32}^2\Delta t_{12} + \Delta t_{12}^2\Delta t_{32}) \tag{2.159}$$

Again, the time differences need to be simplified. Expanding the terms inside of the first parenthesis, the following results can be found.

$$\begin{aligned}
-\Delta t_{32}^2 + \Delta t_{12}^2 &= -(t_3 - t_2)(t_3 - t_2) + (t_1 - t_2)(t_1 - t_2) \\
&= -(t_3 - t_2 + t_1 - t_1)(t_3 - t_2) + (t_1 - t_2 + t_3)(t_1 - t_2) \\
&= -(t_3 - t_1)(t_3 - t_2) - (t_1 - t_2)(t_3 - t_2) - (t_3 - t_1)(t_1 - t_2) \\
&\quad +(t_3 - t_2)(t_1 - t_2) \\
&= -(t_3 - t_1)[(t_3 - t_2) + (t_1 - t_2)] \\
&= -\Delta t_{31}(\Delta t_{32} + \Delta t_{12})
\end{aligned} \tag{2.160}$$

Similar to the simplification for the third order derivative, the following simplification for the terms of the second parenthesis of Eqn. (2.154) can be found.

$$\Delta t_{12}\Delta t_{32}(\Delta t_{12} - \Delta t_{32}) = \Delta t_{12}\Delta t_{32}\Delta t_{13} \tag{2.161}$$

Substituting in these resulting simplifications, the following equation is found.

$$-\ddot{\vec{r}}_1\Delta t_{32}^2 + \ddot{\vec{r}}_3\Delta t_{12}^2 = \ddot{\vec{r}}_2(-\Delta t_{31}[\Delta t_{32} + \Delta t_{12}]) + \dddot{\vec{r}}_2(\Delta t_{12}\Delta t_{32}\Delta t_{13}) \tag{2.162}$$

This equation is then solved for the third derivative.

$$\dddot{\vec{r}}_2 = \frac{1}{\Delta t_{12}\Delta t_{32}\Delta t_{13}}(-\ddot{\vec{r}}_1\Delta t_{32}^2 + \ddot{\vec{r}}_2(-\Delta t_{31}[\Delta t_{32} + \Delta t_{12}]) + \ddot{\vec{r}}_3\Delta t_{12}^2) \tag{2.163}$$

Substituting in the quantities for the third and fourth derivative, the following equation results.

$$\begin{aligned}\dot{\vec{r}}_2 &= \frac{1}{\Delta t_{12}\Delta t_{32}\Delta t_{13}}[\vec{r}_1\Delta t_{32}^2 + \vec{r}_2(-\Delta t_{32}^2 + \Delta t_{12}^2) - \vec{r}_3\Delta t_{12}^2] \\ &\quad -\frac{1}{6\Delta t_{31}}[\ddot{\vec{r}}_1\Delta t_{32}^2 + \ddot{\vec{r}}_2\Delta t_{31}(\Delta t_{32} + \Delta t_{12}) + \ddot{\vec{r}}_3\Delta t_{12}^2]\end{aligned} \tag{2.164}$$

The previous equation is then simplified.

$$\begin{aligned}\dot{\vec{r}}_2 &= \frac{\vec{r}_1\Delta t_{32}}{\Delta t_{12}\Delta t_{31}} - \frac{\vec{r}_2(\Delta t_{32} + \Delta t_{12})}{\Delta t_{12}\Delta t_{32}} - \frac{\vec{r}_3\Delta t_{12}}{\Delta t_{12}\Delta t_{31}} \\ &\quad +\ddot{\vec{r}}_1\left(\frac{\Delta t_{32}^2}{6\Delta t_{31}} - \frac{\Delta t_{32}(\Delta t_{32} + \Delta t_{12})}{12\Delta t_{31}}\right) \\ &\quad +\ddot{\vec{r}}_2\left(\frac{-\Delta t_{31}(\Delta t_{32} + \Delta t_{12})}{6\Delta t_{31}} + \frac{\Delta t_{31}(\Delta t_{32} + \Delta t_{12})}{12\Delta t_{31}}\right) \\ &\quad +\ddot{\vec{r}}_3\left(\frac{-\Delta t_{12}^2}{6\Delta t_{31}} + \frac{\Delta t_{12}(\Delta t_{32} + \Delta t_{12})}{12\Delta t_{31}}\right)\end{aligned} \tag{2.165}$$

$$\begin{aligned}\dot{\vec{r}}_2 &= \frac{\vec{r}_1\Delta t_{32}}{\Delta t_{12}\Delta t_{31}} - \frac{\vec{r}_2(\Delta t_{32} + \Delta t_{12})}{\Delta t_{12}\Delta t_{32}} - \frac{\vec{r}_3\Delta t_{12}}{\Delta t_{12}\Delta t_{31}} + \ddot{\vec{r}}_1\left(\frac{\Delta t_{32}(2\Delta t_{32} - \Delta t_{32} - \Delta t_{12})}{12\Delta t_{31}}\right) \\ &\quad +\ddot{\vec{r}}_2\left(\frac{-\Delta t_{31}(\Delta t_{32} + \Delta t_{12})}{12\Delta t_{31}}\right) + \ddot{\vec{r}}_3\left(\Delta t_{12}\frac{-2\Delta t_{12} + \Delta t_{32} + \Delta t_{12}}{12\Delta t_{31}}\right)\end{aligned} \tag{2.166}$$

The second derivative can be found by substituting in the fundamental equation of astrodynamics.

$$\ddot{\vec{r}} = -\frac{\mu}{r^3}\vec{r} \tag{2.167}$$

This results in the final equation, a function for the velocity vector at the second position in terms of the previously known quantities only.

$$\begin{aligned} \vec{v}_2 &= -\Delta t_{32}\left(\frac{1}{\Delta t_{21}\Delta t_{31}} + \frac{\mu}{12r_1^3}\right)\vec{r}_1 + (\Delta t_{32} - \Delta t_{21})\left(\frac{1}{\Delta t_{21}\Delta t_{32}} + \frac{\mu}{12r_2^3}\right)\vec{r}_2 \\ &\quad +\Delta t_{21}\left(\frac{1}{\Delta t_{32}\Delta t_{31}} + \frac{\mu}{12r_2^3}\right)\vec{r}_3 \end{aligned} \tag{2.168}$$

CHAPTER III

METHODOLOGY

A. Orbit Error Description

To compare the different methods, the estimated orbit must be compared to the true orbit. This has previously been accomplished in a number of ways.

An orbit can be fully defined by 6 parameters. Two common methods to define the orbit are the Cartesian coodinate systems and the Keplerian elements. The Cartesian coordinate system defines the orbit by giving the position and velocity, each of which has 3 elements. The difficulty with using Cartesian coordinates to define an orbit is it is extremely difficult to visualize the resulting orbit if just given the Cartesian elements. The advantage of Cartesian elements is they are more easily used for manuevers and other operations. Keplerian elements are very easily used to visualize the resulting orbit but the problem of comparing two orbits with so many (six) orbit error descriptors remain. The Keplerian elements use the following orbital parameters are: semi-major axis (a), eccentricity (e), inclination (i), right ascension of ascending node (Ω), argument of perigee (ω), and a time-varying parameter that can be selected between the true anomaly(φ), eccentric anomaly(E), and mean anomaly (M).

As the goal of this thesis is to compare orbits, merely using these element systems will not suffice. Comparing orbits using 6 different parameters is quite difficult and probably only useful for perhaps comparing between a few methods and a few scenarios, but this would be inconvenient for a large survey of methods and scenarios as the analyist would be overwhelmed by information. Thus, the number of param-

eters to be compared must be decreased. In previous works, this has been done in a number of ways. One method is to compare the scalar position and velocity errors. Again, this suffers from the difficulty of making it difficult to visualize how much it might effect the resulting orbit. Furthermore, if only the position is shown, while it might predict the position very well, if the velocity error was large, the orbit would have a drastically different shape. Others when comparing methods have also used angular error [15].

In Ref. [25], a new error method was proposed that reduced the parameters from 6 to 2. The first error parameter was the orbit shape error, d, which was used for this project and will be fully presented below. The second error parameter proposed, the orbit orientation, δ, is defined as below.

$$\cos\delta = \frac{1}{2}\left(\mathrm{tr}[C\tilde{C}^T] - 1\right) \tag{3.1}$$

where C_i denotes the rotation matrix and the axis about which the rotation occurs. $\tilde{C}$ denotes the estimated direction cosine matrix while C is the true direction cosine matrix. The rotation matrix is defined below as

$$C = R_3(\omega)\, R_1(i)\, R_3(\Omega) = [\,\hat{\mathbf{r}} \quad \vdots \quad \hat{\mathbf{h}} \times \hat{\mathbf{r}} \quad \vdots\, \hat{\mathbf{h}}\,]^T \tag{3.2}$$

This representation is modified in the current project. The previous orbit orientation definition was not incorporating any of the potential time-varying elements (such as the true anomaly) and was therefore incomplete and has the problem that ω is not defined for circular orbits. These two problems were previously identified and corrected by by Schaeperkoetter and Mortari [19].

Thus a new error representation was sought that similarly simplified the error representation with only a few, easy to understand error parameters that also in-

corporated all of the orbital elements. To accomplish this, the Keplerian elements were divided into two groups. The first group, made of i, Ω, and $\omega + \varphi$, identifies the orientation of a rotating orbital reference frame $[\hat{\mathbf{r}},\ \hat{\mathbf{t}},\ \hat{\mathbf{h}}]$, with respect to the inertial reference frame. The axes of this orbital frame are identified by the radius direction, $\hat{\mathbf{r}}$, the direction of the angular momentum, $\hat{\mathbf{h}}$, and the third axis to form a right-handed frame, $\hat{\mathbf{t}} \triangleq \hat{\mathbf{h}} \times \hat{\mathbf{r}}$. Therefore, the transformation matrix moving from inertial to the rotating reference frames can be written as:

$$C_{\mathrm{OI}} = R_3(\omega + \varphi)\ R_1(i)\ R_3(\Omega) = [\,\hat{\mathbf{r}} \quad \vdots \quad \hat{\mathbf{h}} \times \hat{\mathbf{r}} \quad \vdots\, \hat{\mathbf{h}}\,]^T \tag{3.3}$$

where R_1 and R_3 are the rotation matrices around the first and third coordinate axis, respectively.

The second group, which consists of a and the semi-minor axis, $b = a\sqrt{1-e^2}$ (or for hyperbolic orbits, the semi-minor axis is defined as $b = a\sqrt{e^2-1}$), identifies the shape of the orbit.

Two distinct parameters emerge from the groups and are introduced to describe two distinct aspects of the orbit error. These are:

- *Orientation Error.* This error is identified by an angle, Φ, that can be computed by the following relationship using the true (C_{OI}) and the estimated ($\tilde{C}_{\mathrm{OI}}$) transformation matrices between interital and rotating reference frames.

$$\cos\Phi = \frac{1}{2}\left(\mathrm{tr}[C_{\mathrm{OI}}\tilde{C}_{\mathrm{OI}}^T] - 1\right) \tag{3.4}$$

  From a mathematical point of view, Φ represents the principal angle of the corrective attitude matrix between the two attitudes matrices C_{OI} and $\tilde{C}_{\mathrm{OI}}$.

Specific error information can be easily derived from the orbit orientation er-

ror. These can be, a) the distance between estimated and true radii, $|\,\mathbf{r}-\tilde{\mathbf{r}}\,|$, to capture the ability to estimate the spacecraft position, and b) the angle between estimated and true angular momentum directions, $\hat{\mathbf{h}}$ and $\tilde{\hat{\mathbf{h}}}$, to capture the ability to estimate the orbit plane orientation.

- *Shape Error.* The orbit shape is here identified using the semi-major and semi-minor axes because they are dimensionally consistent parameters, as they can be measured in kilometers. Using these two parameters, the shape of an orbit can be identified as a point in the a-b plane. Thus the orbit shape error can be simply described by the distance (d) from estimated and true points in the a-b plane

$$d = \sqrt{(a-\tilde{a})^2 + (b-\tilde{b})^2} \tag{3.5}$$

Since the orientation and the shape orbit error parameters are dimensionally represented by an angle and a distance, they can be merged into a *single general orbital error descriptor*, which is represented by the following complex number

$$\boxed{\varepsilon = (E\{d\} + d)\, e^{i\,\phi}} \tag{3.6}$$

where $E\{d\}$ is a freely chosen value representing the expected value of the shape error.

To compare the display of errors between this new method and other error representations, the error results of a sample scenario are displayed below for a Monte Carlo simulation of 100 runs. The sample orbit was a moderately inclined orbit with small non-zero eccentricity. (a=9000 km, e=.2, i=45°, ω=20°, Ω=5°, φ=15°). In Figure 1, the orientation error and the shape error are shown as the new error representation. In Figure 2, the normalized error in the position and velocity is shown. In Figure 3, the error in the estimation of the Keplerian elements is shown. The

new error representation avoids the potentially overwhelming amount of data that cound be presented in Keplerian elements while still conveying helpful information about the orbit, unlike the Cartesian representation. Furthermore, this new error representation is capable of handling coplanar and circular orbits.

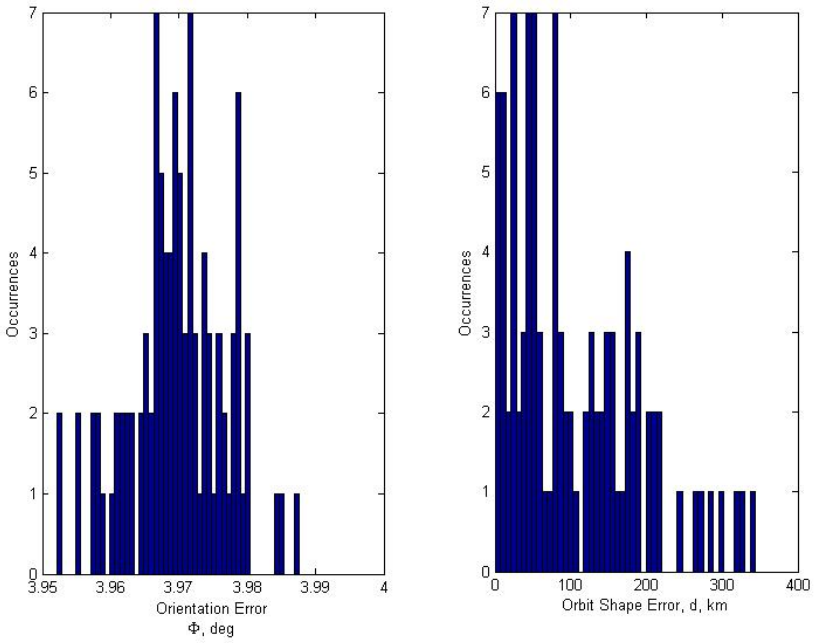

Figure 1: General Orbit Error Histograms

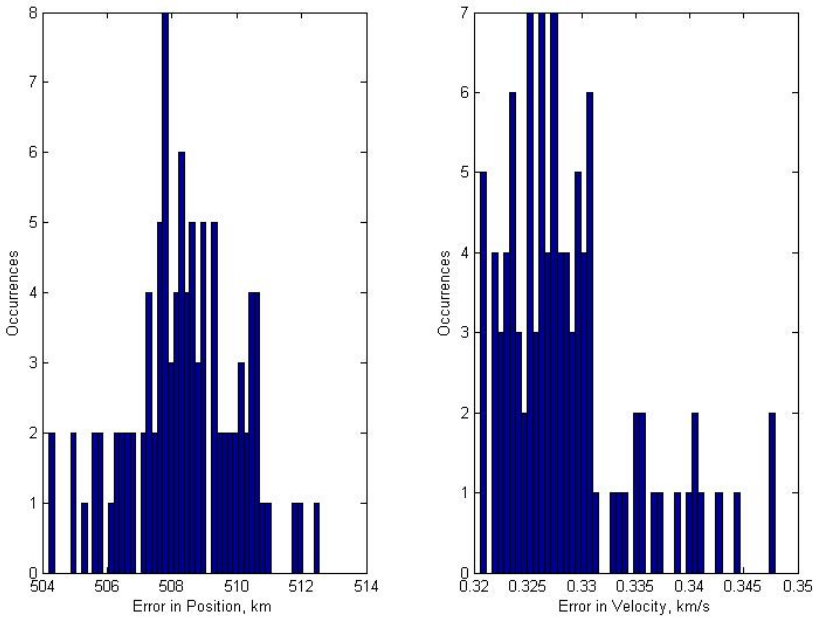

Figure 2: Cartesian Orbit Error Histograms

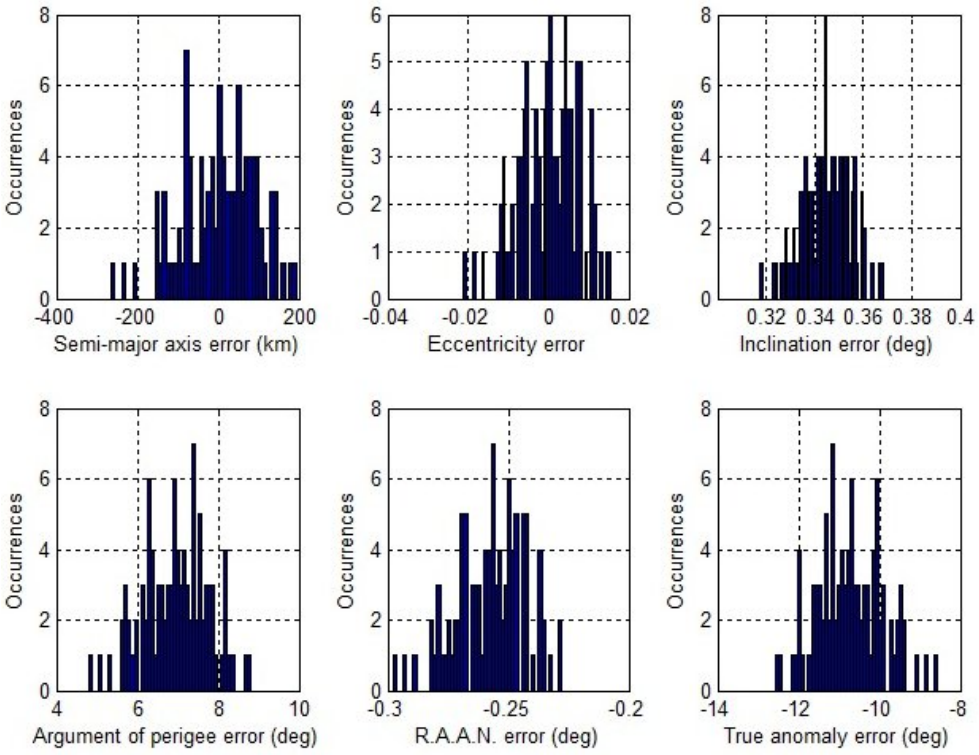

Figure 3: Keplerian Orbit Error Histograms

B. Test Scenarios

To identify the strengths and weaknesses of each IOD method, various distinct scenarios will be employed. These specific orbits are: *a)* Coplanar, *b)* Polar, *c)* Sun-Synchronous, *d)* Molniya while ascending, *e)* Molniya at apogee, and *f)* Geostationary (GEO). Additionally, a non-coplanar LEO orbit shall be utilized to study the changes when the semi-major axis, the inclination, and the observation interval are varied.

For each observation interval tested, 100 runs will be performed. For all studies, a line plot is used, where for each value of the varying parameters, the median of all the Monte Carlo runs is taken and the corresponding error is plotted on the Y-axis whereas the varying parameters will be on the X-axis. The median is chosen rather than the mean to ensure that the few very very inaccurate estimates will not have too large of an influence on the analysis.

Furthermore, each run, unless otherwise stated, does not use the perfect orbital parameters but rather adds a slight variation to each of them to best simulate real orbits. For example, in reality, there will be no truly polar orbit or truly equatorial orbit, for an orbit will have very small variations in it as a result of perturbations. To each initial radius is added a randomly orientated vector of modulus ν_1, which has a standard deviation equal to 1% of the radius. Likewise, to each initial velocity is added a randomly orientated vector of modulus ν_2, which has a standard deviation equal to 1% of the velocity. Thus, the initial position of the satellite, at the beginning of each run, exists in a Gaussian sphere, as does the velocity vector. In addition to this variation, the measurements are corrupted by noise to simulate real data. These adjustments to the orbit are performed in a Monte Carlo fashion.

For all scenarios, it is assumed that each observation is effected by noise with a standard deviation of $5''$, unless otherwise stated. This noise has a Gaussian dis-

tribution as a result of the centroiding process used to determine the position of the observed object on an optical photo. No error is assumed in the time measurements, and it is assumed that no corrections need to be made to account for the duration of the flight time of the light. It is important to outline that, particularly for satellites very far from the observer, light corrections would need to be made for accuracy (GEO are seen with a 0.12 sec delay). For this research, it is assumed that the light travels instantaneously from the satellite to the observer.

Both the Double R and Gooding methods require initial estimates. The Double R method requires an estimate of the initial and final radius. For all scenarios tested, the initial estimates were selected to be 50% of the true radius value. The Gooding method requires an estimate of the range at each observation time. For all scenarios, the initial estimate of the range was selected to be 50% of the true value of the middle range (thus the middle range estimate was used for initial, middle, and final range estimates). Additionally, for the Gooding method, an estimate of the orbit direction of the orbit is needed, estimating if the orbit is prograde or retrograde. When it is known that the orbit has a near-polar inclination, it is desirable that both the retrograde and prograde estimates be tested.

CHAPTER IV

RESULTS

A. Particular Orbit Analysis

All orbits, unless otherwise stated, were observed from 0° latitude, 0° longitude at sea level. For all three observations for each scenario, the observation time interval was held constant. No orbital perturbations, such as drag or J_2 effects, were included. Note that for the Monte Carlo runs, small variations were added to the baseline orbits, as explained previously.

1. Coplanar Orbit

The coplanar case has always proved to be extremely problematic for IOD solvers. For these runs, it was assumed that the observing location was at 0° latitude with the orbit having 0° inclination. Again, during the Monte Carlo runs the Gaussian variations were included in the orbit so the orbits were not perfectly coplanar. The baseline orbit was (a=9000 km, e=0, i=0 °, ω=-5°, Ω=0 °, φ=0 °).

Fig. 4 shows the results obtained. All of the methods resulted in several degrees of error in Φ except for the Gooding method, which had a median error of about 0.1°. The orbit shape error, d, was very large for all of the methods, typically on the order of thousands of kilometers. Additionally, the Double R method failed to converge a significant number of times, particularly for smaller observation intervals.

The case of the perfectly coplanar orbit was also examined, where no variations were added to the orbit. Additionally, no noise was added to the measurements either. Similarly, the performance was very poor and the algorithms failed to converge even

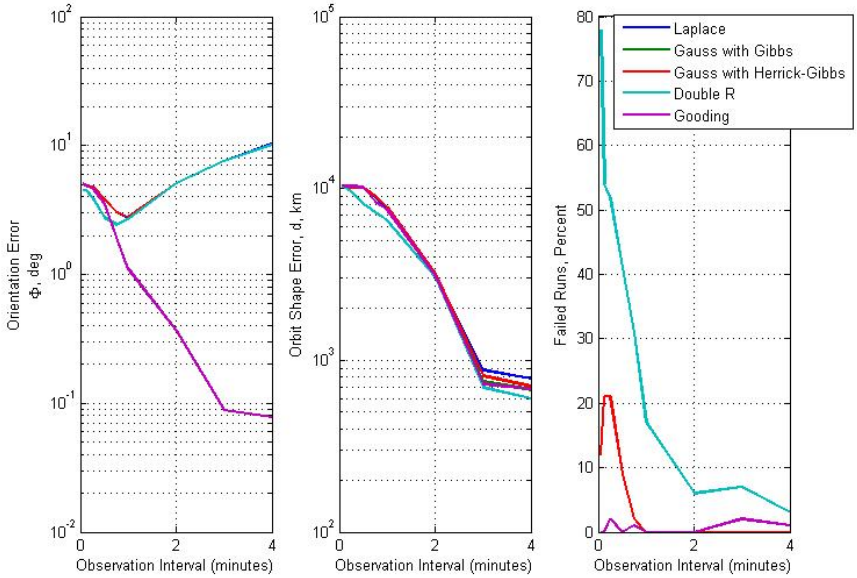

Figure 4: IOD Errors for the Coplanar Case

more frequently. These results can be seen in Fig. 5.

It should be noted that in an operational setting, since the plane of the orbit is well estimated and realize that this was a coplanar case, the user would know that the IOD method would fail to calculate the orbital shape with any kind of accuracy. This is good so that it is not assumed that all the parameters were estimated well.

2. Polar Orbit

Again, in the polar orbit case, variations were added to the baseline orbit in the Monte Carlo runs so the orbits were not perfectly polar. The baseline orbit was (a=7000 km, e=0, i=90°, ω=-5°, Ω=5°, φ=0°).

Fig. 6 shows the results obtained. All proposed methods worked relatively well. The Gooding method continues to be the best at analyzing for the plane and angular position of the satellite, with Φ being much smaller than the other methods. When

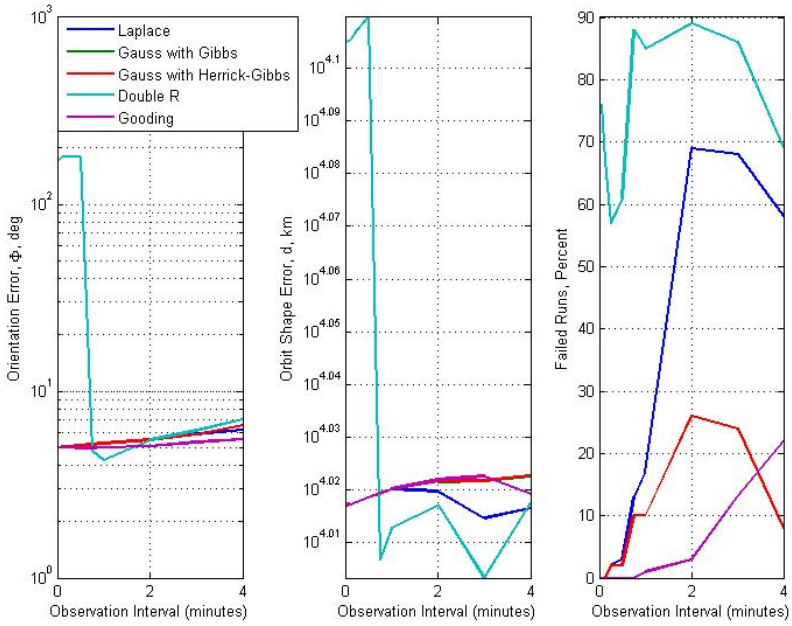

Figure 5: IOD Errors for the Perfect Coplanar Case

the observations were spaced more closely than 2 minutes (for an orbit of $a = 7,000$ km), the Gooding method failed to converge more frequently as the observations grew closer. As the observation interval grew larger than 2 minutes, the Gooding method did very poorly in both error parameters while the Double R method continued to grow in its accuracy of d.

The case of the perfectly polar orbit was also examined. Furthermore, no noise was added to the measurements. The Laplace and Gauss methods failed completely. The Gooding method did well until around a 2 minutes interval (though it had convergence problems for observation intervals of less than a minute). When the interval increased, the estimates very rapidly decreased in accuracy. Simultaneously, the Double R method continued to perform well. These results can be seen in Fig. 7.

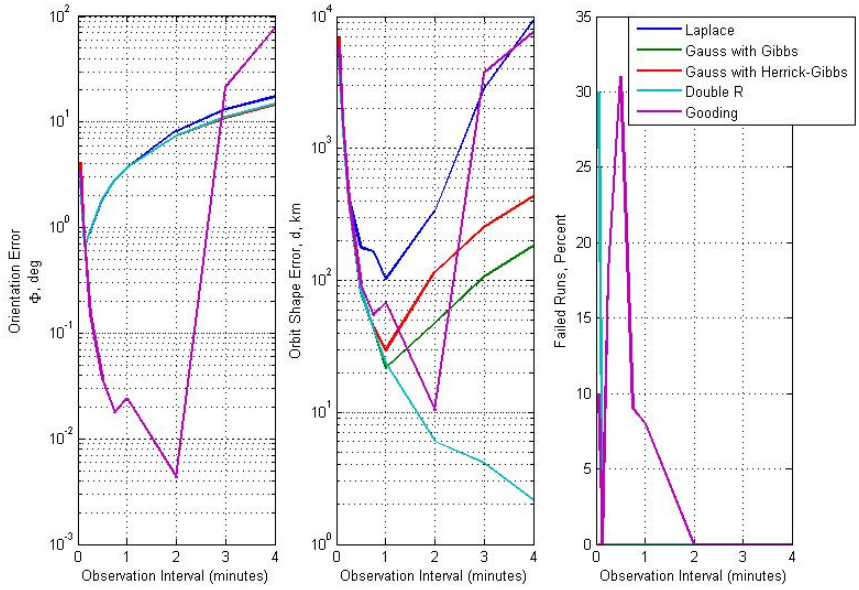

Figure 6: IOD Errors for the Polar Case

3. Sun-Synchronous Orbit

The sun-synchronous orbit is an important orbit for many scientific studies, enabling the satellite to always be in view of the sun. The baseline orbit was (a=7264 km, e=0, i=98.4°, ω=-5°, Ω=10°, φ=0°). Consequently, the orbit is retrograde, which for the Gooding method must be estimated at the beginning. Fig. 8 shows the results obtained. Most of the methods had only a few degrees of error in Φ while the Gooding method again had fractions of a degree in error. The Gooding method failed increasingly as the observations were less than 2 minutes apart, failing almost 50% of the time when spaced .5 minutes apart. The error d decreases for both Gooding and Double R as the interval increases.

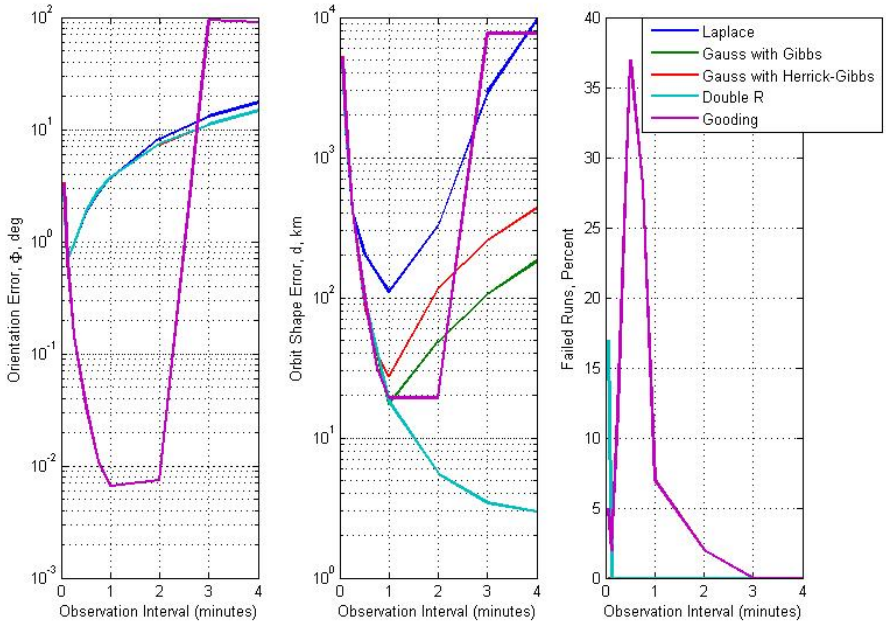

Figure 7: IOD Errors for the Perfect Polar Case

4. Molniya Orbit

Two different portions of the Molniya orbit were examined. It was decided to study when the satellite was ascending through the equatorial plane and when the satellite was near apogee.

The study of when the satellite is ascending in the Molniya orbit is particularly interesting for several reasons. The satellite has passed perigee and is rapidly rising towards apogee. Furthermore, the Molniya orbit is at a relatively high inclination and has a large eccentricity. When the satellite goes through the ascending node, the radius is rapidly increasing. The baseline orbit was (a=26610 km, e=.722, i=63.4°, ω=-90°, Ω=0°, φ=70°).

Laplace's estimate of d grew steadily worse as the observations were spread apart. More interestingly, the Gauss-Gibbs method more rapidly decreased in accuracy than

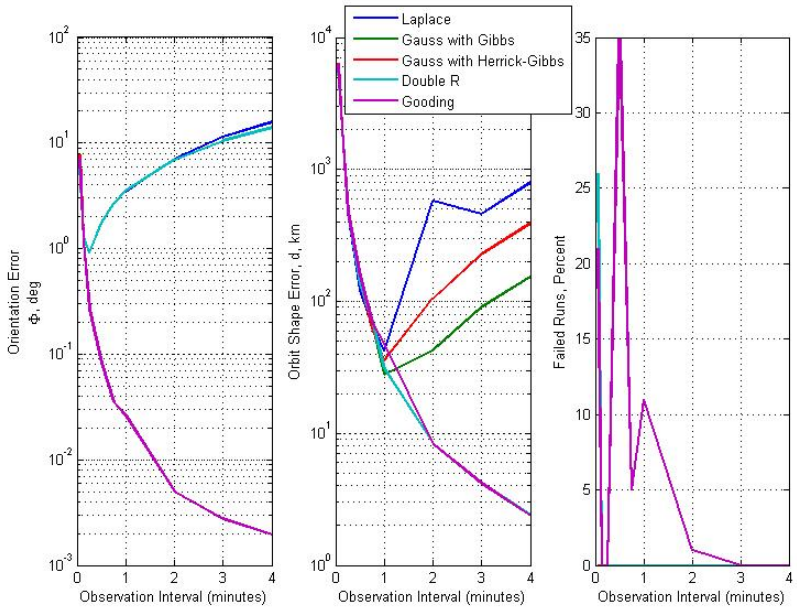

Figure 8: IOD Errors for the Sun-Synchronous Case

the Gauss-Herrick-Gibbs method, contrary to what would be traditionally expected. Double R and Gooding both did very well estimating d, increasing with accuracy as the observation interval grew.

Fig. 9 shows the results obtained. Also while all the methods (including Gooding) continued to run well and converge upon a solution, Double R failed to converge as the observations grew closer together. All methods decreased in accuracy when the observations were closer than 5 minutes apart.

Next, the case when the satellite is near apogee was examined. The baseline orbit was (a=26610 km, e=.722, i=63.4°, ω=-90°, Ω=-80°, φ=175°). Fig. 10 shows the results obtained. Interestingly, all methods but the Gooding and Double R method failed to converge at nearly all times. When the observations were spaced 10 minutes or less, the other methods began to converge on solutions that were completely wrong. Both the Double R and Gooding methods determined d at roughly the same accuracy

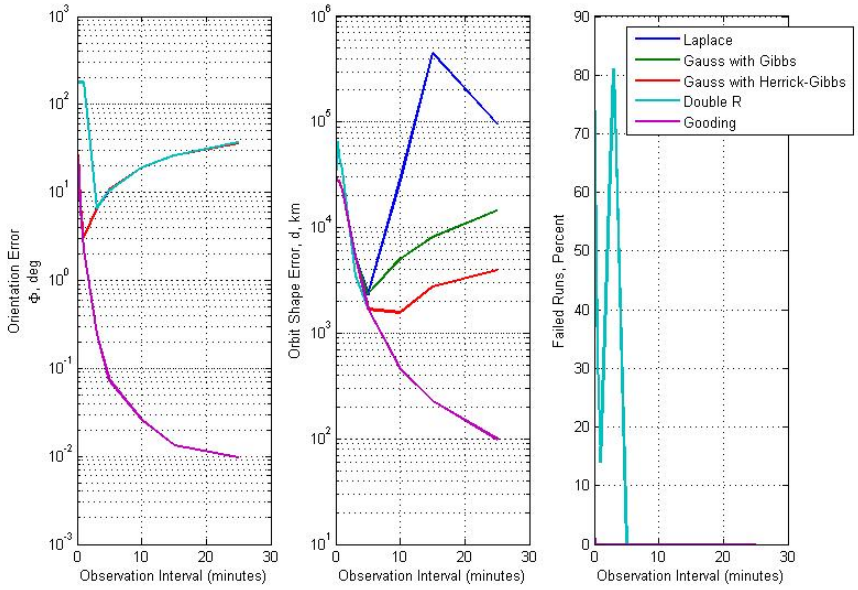

Figure 9: IOD Errors for the Ascending Molniya Case

for all observation spacings, though at very large intervals Double R was mostly unable to converge. Again, Gooding determined Φ much better than Double R.

For both cases, Φ is best determined by the Gooding method by several orders of magnitude.

5. GEO Orbit

Next the case of the geostationary orbit (GEO) was examined. The baseline orbit was (a=42241 km, e=0, i=0 °, ω=0°, Ω=0 °, φ=0 °). To avoid it being a variation of the coplanar problem, the observer location was changed to be 20° latitude.

Fig. 11 shows the results obtained. First, the Double R method actually had the best accuracy in Φ for observations extremely close together, 3 minutes and less, though it did fail to converge nearly 50% of all the runs. At about 6 minutes, the Gooding method resumed being the best at estimating Φ by a significant margin.

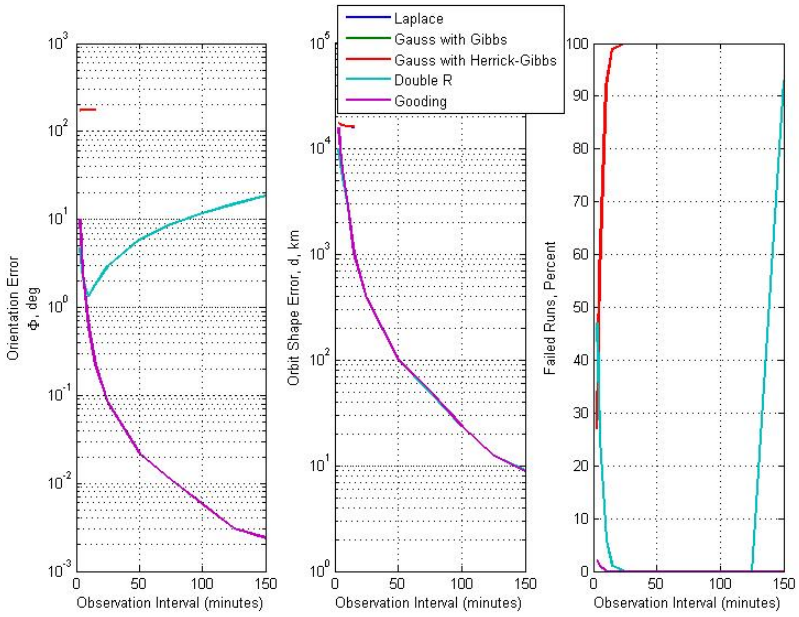

Figure 10: IOD Errors for the Apogee Molniya Case

All of the methods had the same accuracy in d with observations closer than 25 minutes apart. The Gauss methods using Gibbs performed comparably to Gooding and Double R for observations less than 100 minutes apart. Starting around 100 minutes and more, the Double R and Gooding methods estimated d about the same until near 400 minutes, when the Double R method started performing poorly. The Gooding method gave good accuracy for both parameters until the spacing grew past 700 minutes, at which point it became inaccurate for d. These results remained consistent when the true anomaly of the spacecraft was varied.

B. General Orbit Analysis

In this section, a general orbit was examined, varying the observation spacing, semi-major axis, and inclination. The observer, unless otherwise stated, was at the equator at 0° longitude with observation intervals 1 minute apart. Unless the parameter was

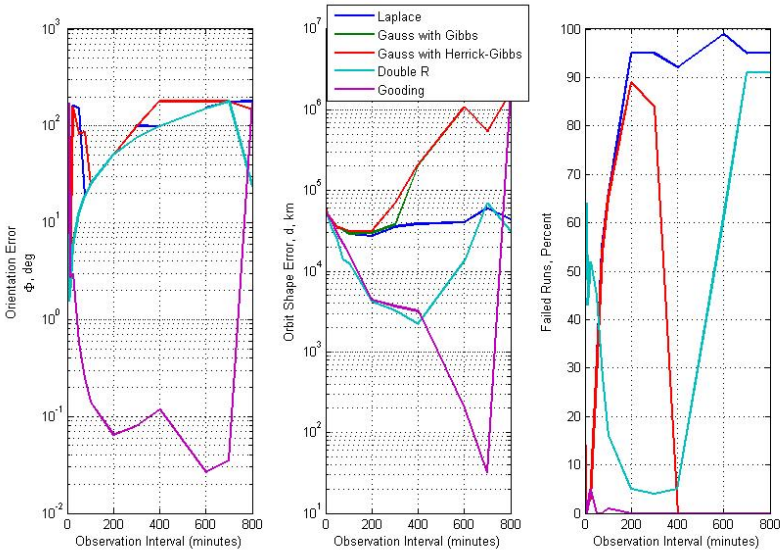

Figure 11: IOD Errors for Geostationary Case

being varied, the baseline orbit was (a=7800 km, e=0, i=25°, ω=0°, Ω=-5°, φ=5 °).

1. Observation Interval

The results of this test are shown in Fig. 12. This study reveals more generally that the Gooding method will increase in accuracy for both parameters, while the Double R method increased in the accuracy of only d, with accuracy comparable to the Gooding method. The other methods all perform significantly worse. All methods converged for all observation intervals except when the interval became extremely small.

2. Semi-Major Axis

The results of this test are shown in Fig. 13. All of the methods have around the same accuracy for the determination of d. Additionally, the Gooding method starts very well off estimating Φ, but near 20,000 km, the Gooding method has an accuracy

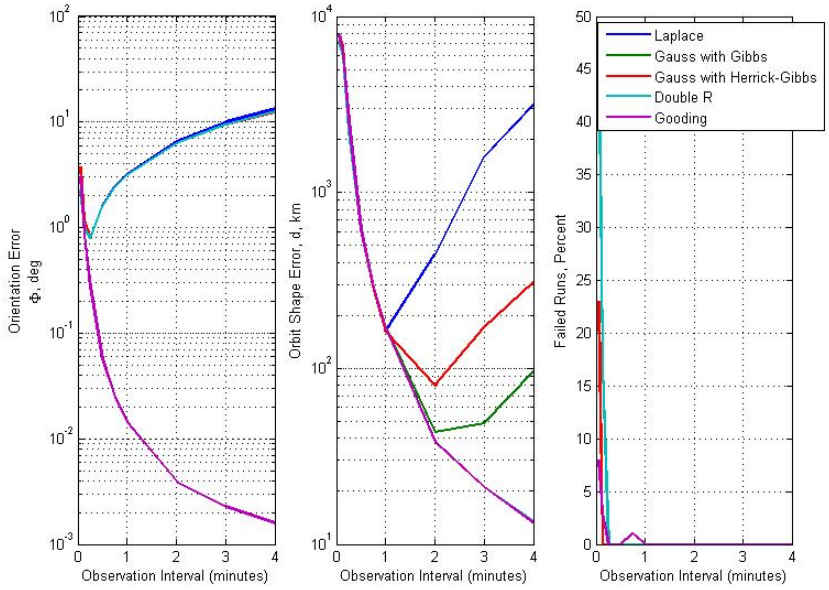

Figure 12: IOD Errors in LEO by Varying Observation Interval

comparable to the others. The Double R method rapidly deteriorated in its ability to converge when the semi-major axis was greater than 10,000 km. For larger semi-major axis, the Gooding method, and to a lesser extent Gauss, failed to converge a small amount, as seen in Fig. 13. Again, the observation interval was 2 minutes.

3. Inclination

It is important to remember that this intial study occurs with the observer at 0° latitude. The results of this test are shown in Figs. 14 and 15. This study shows that all the methods determine Φ at constant accuracies except for the Gooding method, which does worse as the inclination is increased, with an additional spike occurring near 90°. The observation interval also has an impact. When the interval is 1 minute, all methods are comparable to each other for determining the orbit shape. However, when the interval is increased to 3 minutes, the Gooding and Double R methods

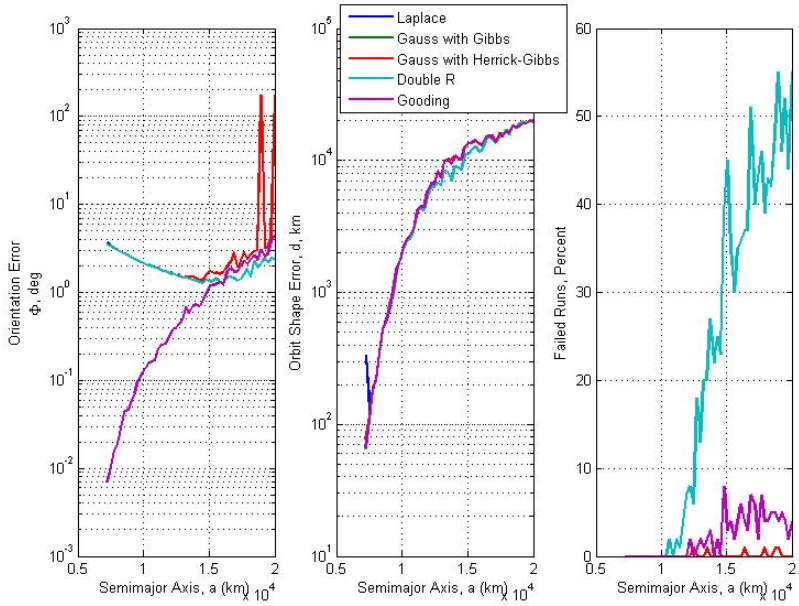

Figure 13: IOD Errors in LEO Varying Semi-Major Axis

do the best again at determining d. Near the coplanar cases, all the methods do comparably except for Laplace which is significantly worse. The Gooding method again has a spike at 90° while the Double R method, which is comparable in accuracy to Gooding for all other inclinations, does the best job at estimating the shape at 90° inclination.

It was also decided to repeat the test from a different observer location at 20° latitude. The results of this test are shown in Figs. 16 and 17. This revealed that the problems at the equator were most likely a result of the orbit approaching the coplanar case. Unexpectedly, the error spiked even higher for all the methods at an inclination of 90°. For all inclinations other than near the polar orbit, the Gooding method was the most successful at determining Φ while for d, at closer intervals all methods had roughly the same accuracy. At larger intervals Double R and Gooding were best. The Double R method failed to converge for nearly all the runs near the

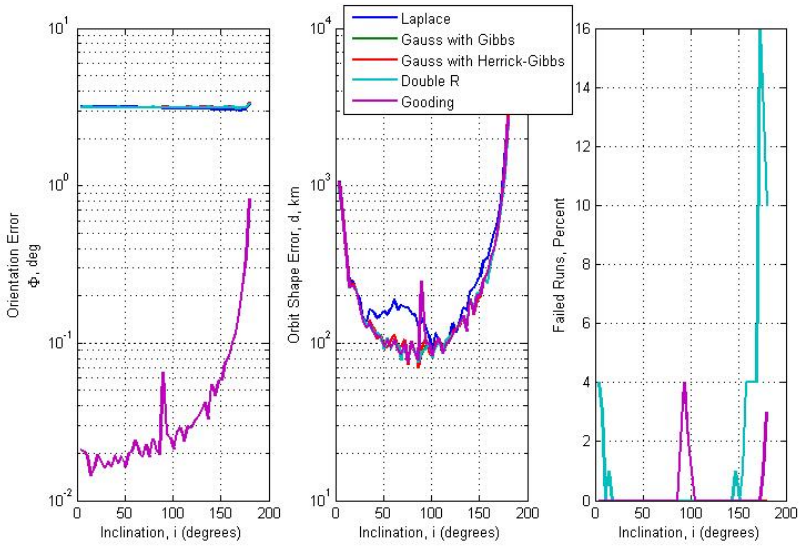

Figure 14: IOD Errors in LEO Varying Inclination (1 min Observation Interval)

polar case.

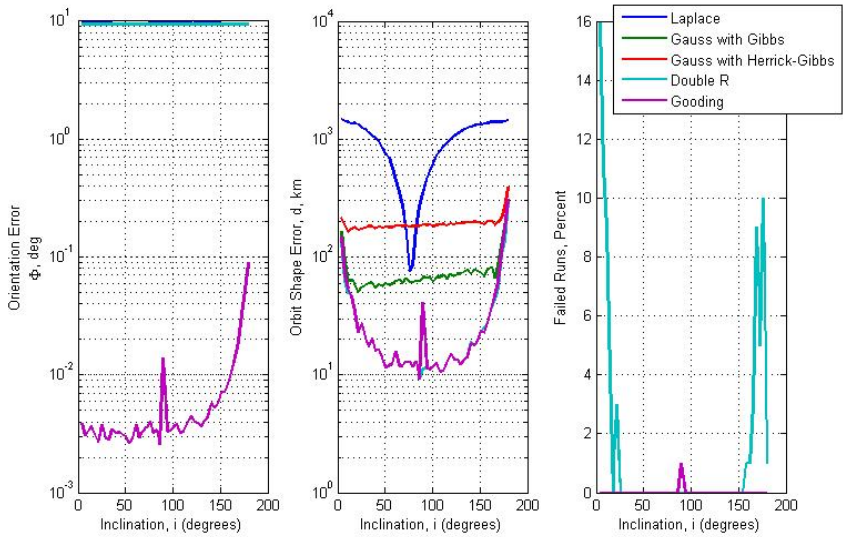

Figure 15: IOD Errors in LEO Varying Inclination (3 min observation interval)

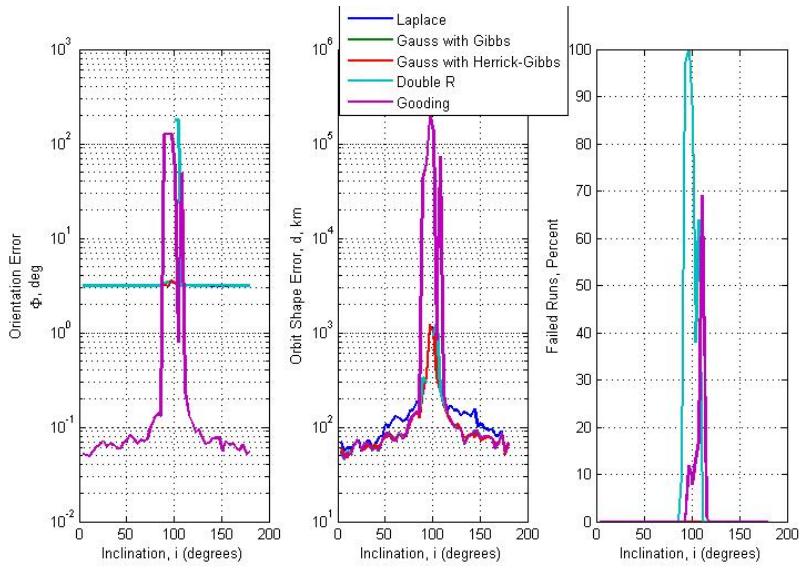

Figure 16: IOD Errors in LEO Varying Inclination from 20° Latitude (1 min time interval)

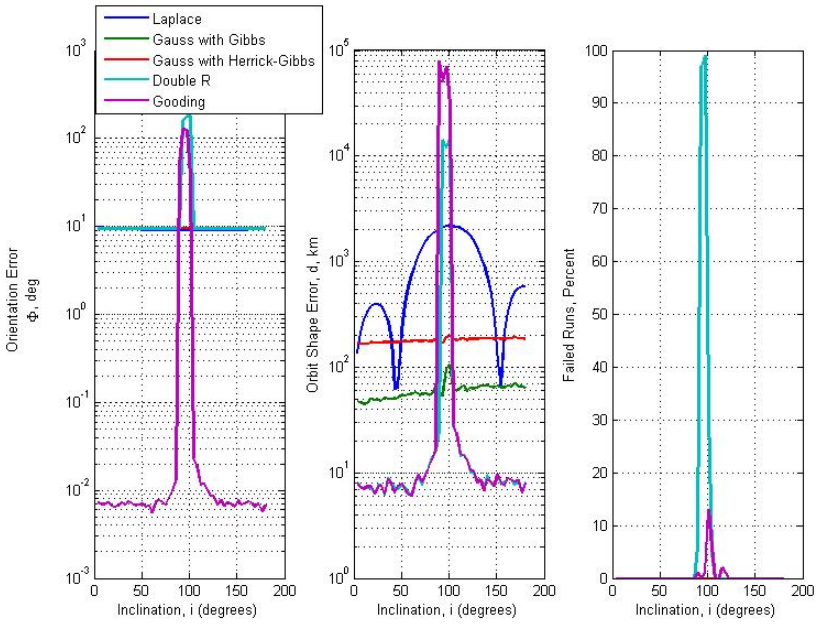

Figure 17: IOD Errors in LEO Varying Inclination from 20° Latitude (3 min time interval)

C. Tests for Robustness

It is desirable to determine how robust the different methods are. There are two components that must be considered when analyzing the robustness of a particular method. The first component is the sensitivity of the method to the initial guess required by the method. The second component is the sensitivity to measurement error.

Both Gauss and Laplace require no initial estimates so the first component of the robustness tests do not apply to them; however, both the Gooding method and the Double R method require initial estimates. The Gooding method requires estimates of the range from the observer to the satellite at each of the three times, while the Double R method requires an estimate of the radius for the first and the third observation. The previous analysis was all conducted with the estimates being 50

The following section will be divided into two portions. The first portion will discuss the robustness of the Double R method and the second potion will discuss the robustness of the Gooding method. Following this discussion, another section will present analysis of all of the methods sensitivity to growing noise in the measurements.

1. Robustness of the Double R Method with Respect to the Initial Estimate

The Double R method shows a surprising degree of robustness with respect to the initial estimate. The initial estimate appears to have very little effect on the accuracy of the estimations or the number of runs that failed to converge. This was shown to be true in all cases previously examined (polar, sun-synchronous, GEO, coplanar, Molniya ascension and apogee, and LEO). The results for all the initial estimates seem to give nearly the same orientation error exactly. Some minimal variation in the

orientation error was present at mid-interval ranges for the coplanar case and larger intervals for GEO. The orbit shape error had more variation but in general followed the same trend. There does not appear to be any correlation between the accuracy of the final estimate and the accuracy of the initial guess.

These plots, Figures 18 - 24, are shown below.

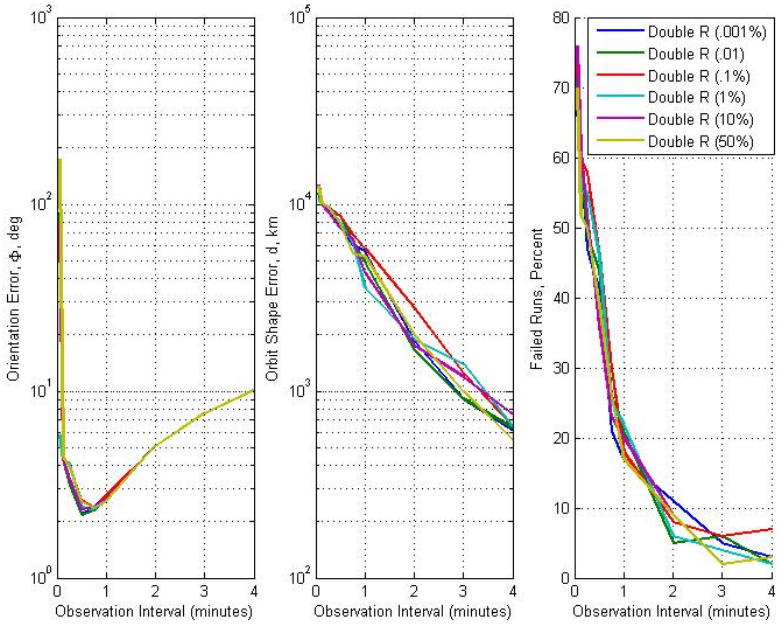

Figure 18: Effects of Initial Guesses on Orbital Estimate for Coplanar Orbit Using Double R Method

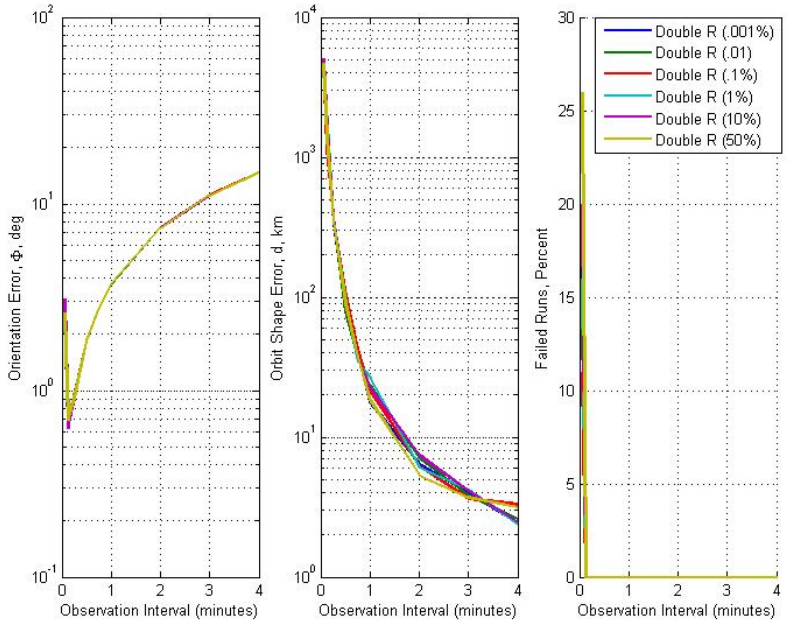

Figure 19: Effects of Initial Guesses on Orbital Estimate for Polar Orbit Using Double R Method

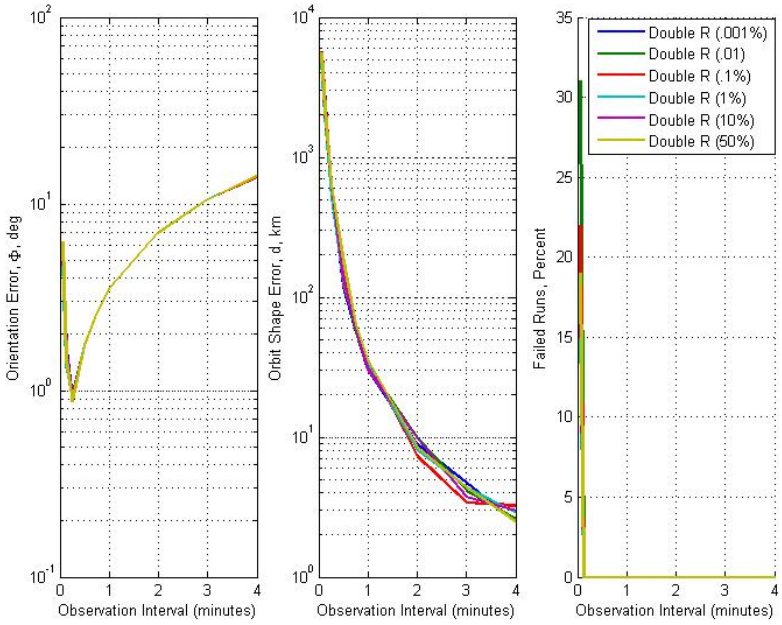

Figure 20: Effects of Initial Guesses on Orbital Estimate for Sun-synchronous Orbit Using Double R Method

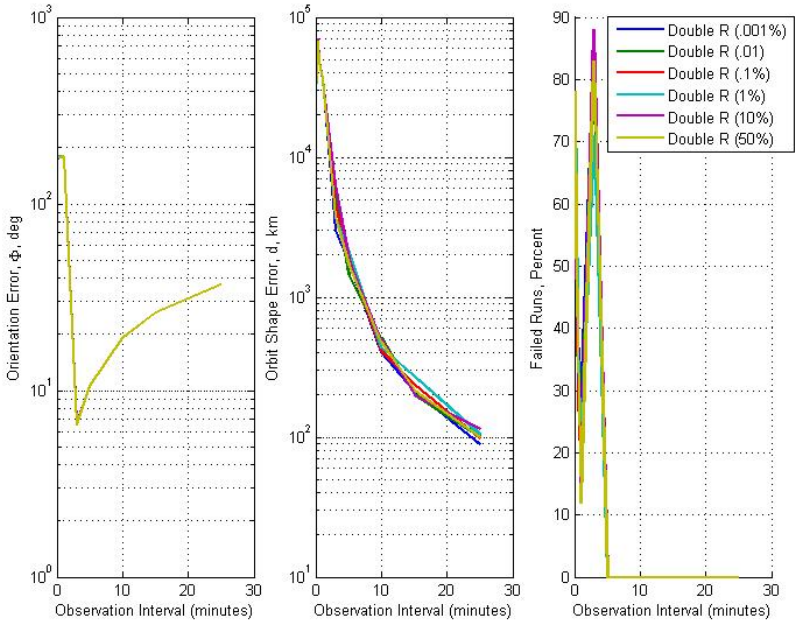

Figure 21: Effects of Initial Guesses on Orbital Estimate for Ascension on Molniya Orbit Using Double R Method

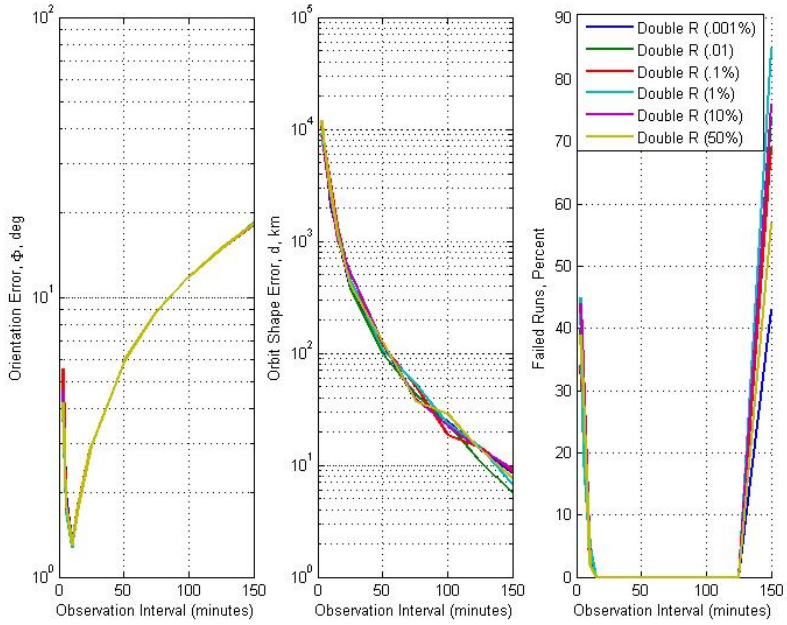

Figure 22: Effects of Initial Guesses on Orbital Estimate for Perigee on Molniya Orbit Using Double R Method

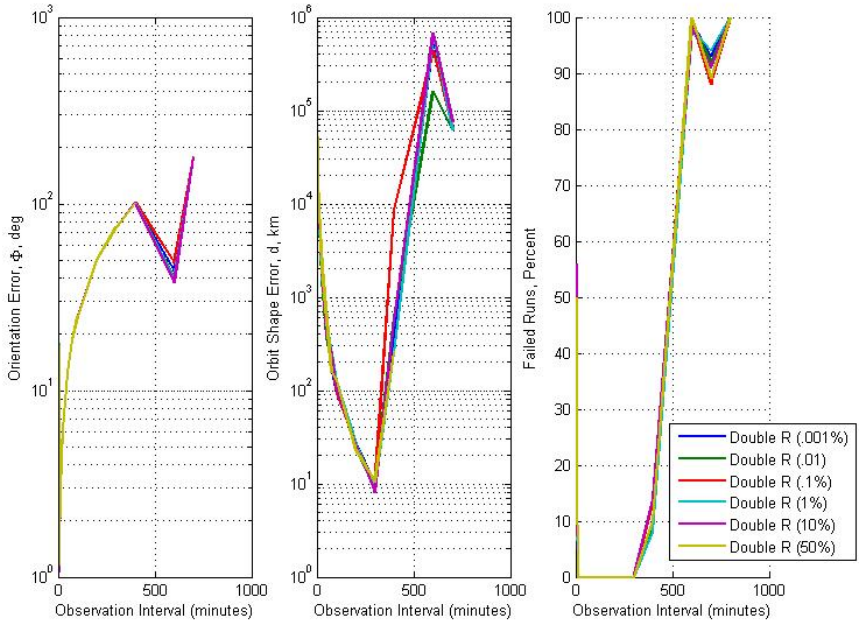

Figure 23: Effects of Initial Guesses on Orbital Estimate for GEO Orbit Using Double R Method

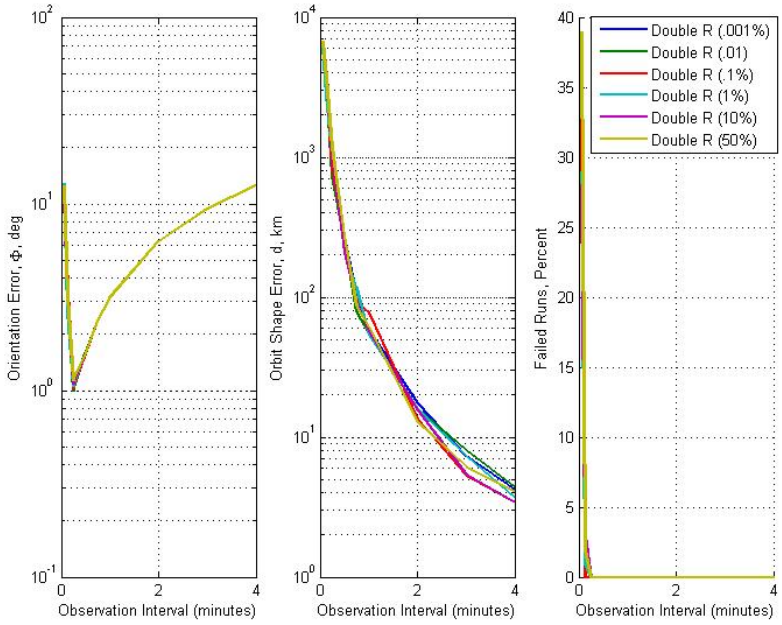

Figure 24: Effects of Initial Guesses on Orbital Estimate for LEO Orbit Using Double R Method

2. Robustness of the Gooding Method with Respect to the Initial Estimate

The Gooding method is robust as well, though not quite as robust as the Double R method. While the final estimates have some range with respect to the initial guess, they all follow the same general trend typically but don't match each other as closely as the Double R method. The polar case had the most variability between the different initial guesses, with some methods at some intervals even completely breaking the trend. There does not seem to be a correlation between the initial guess and the accuracy of the final estimate. The polar case variability is not surprising as the Gooding method had a great deal of difficulty converging upon a good final estimate. Both the polar case and the sun-synchronous case had a great deal of variability in their ability to converge, being highly dependent upon the initial guess with no final correlation between the initial guess and the final estimate.

The plots, Figures 25 - 31, are shown below.

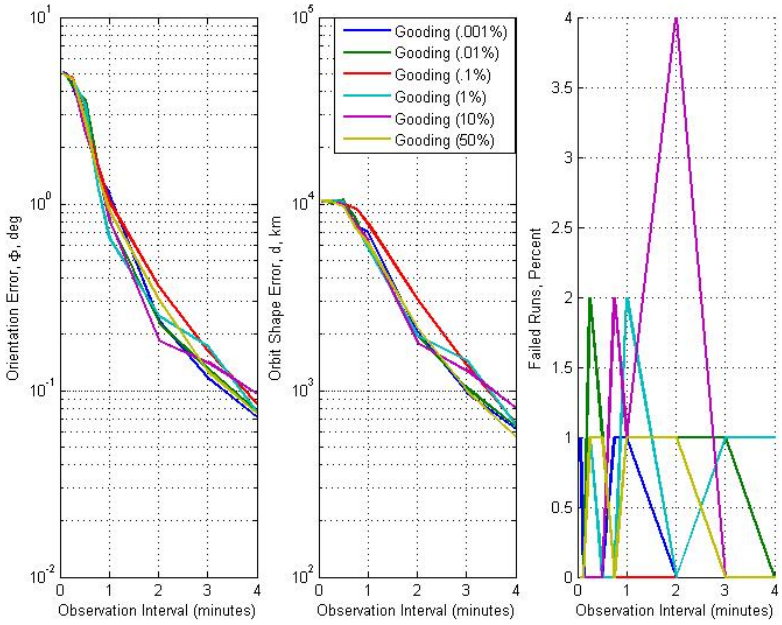

Figure 25: Effects of Initial Guesses on Orbital Estimate for Coplanar Orbit Using Gooding Method

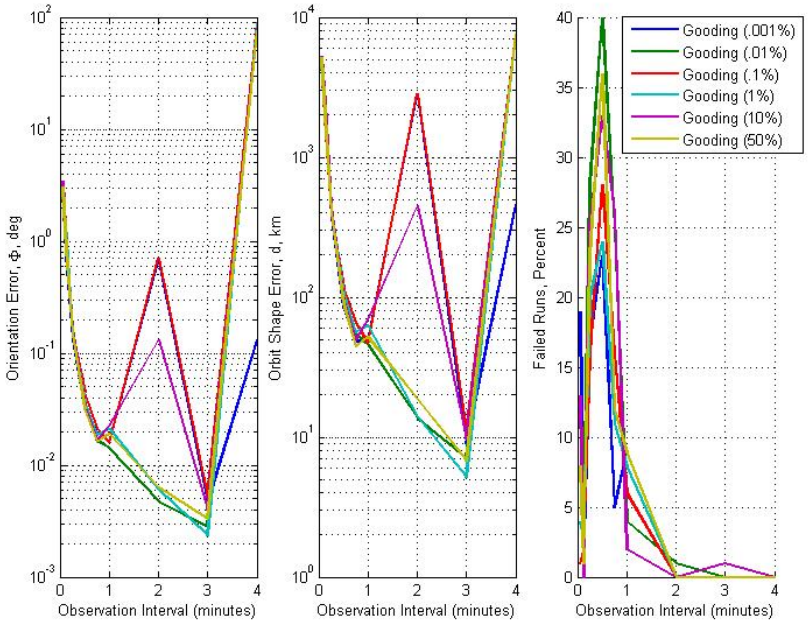

Figure 26: Effects of Initial Guesses on Orbital Estimate for Polar Orbit Using Gooding Method

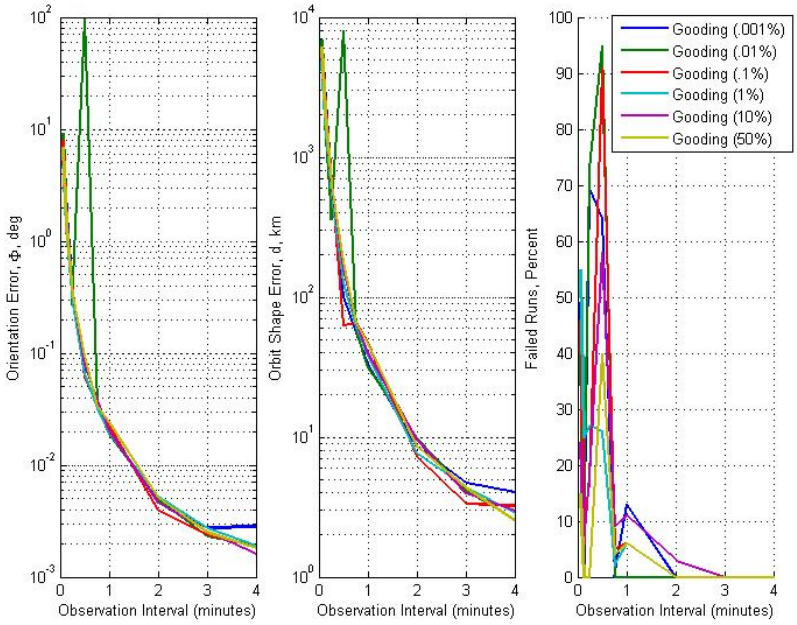

Figure 27: Effects of Initial Guesses on Orbital Estimate for Sun-synchronous Orbit Using Gooding Method

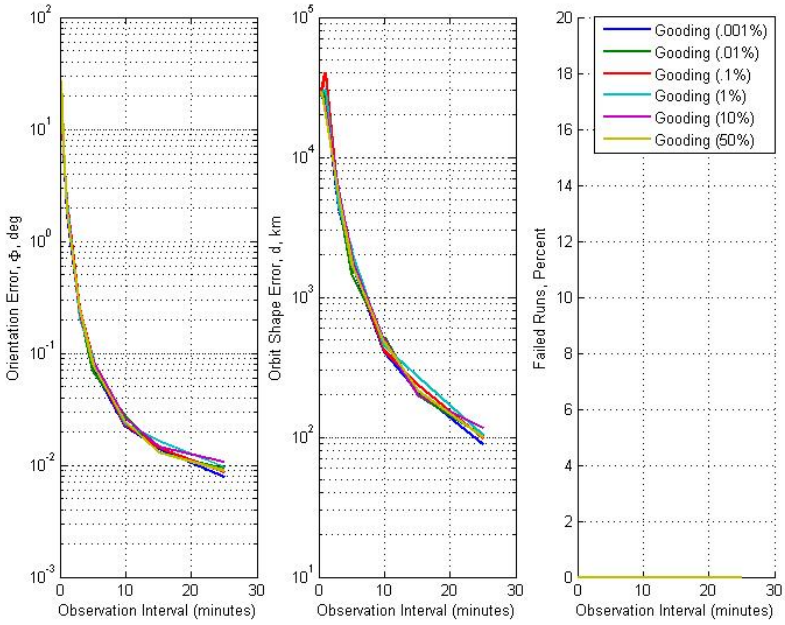

Figure 28: Effects of Initial Guesses on Orbital Estimate for Ascension on Molniya Orbit Using Gooding Method

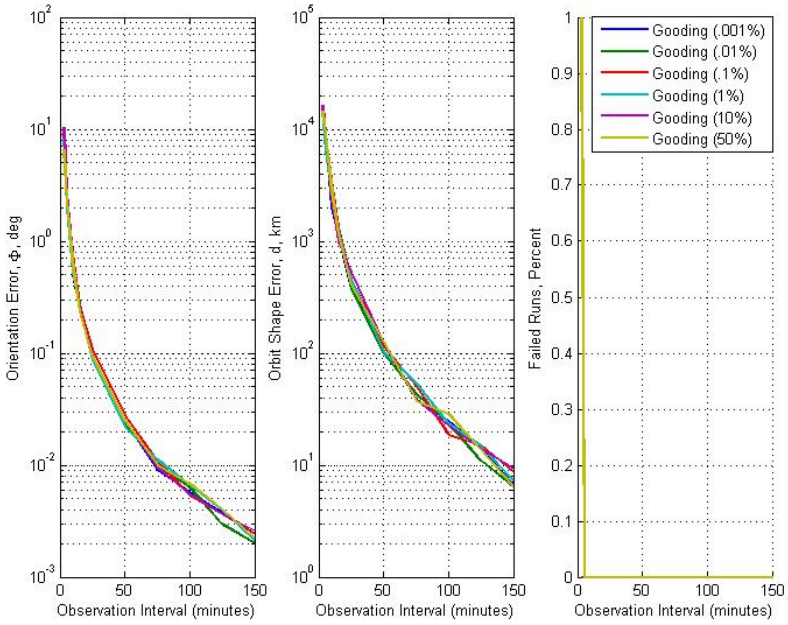

Figure 29: Effects of Initial Guesses on Orbital Estimate for Perigee on Molniya Orbit Using Gooding Method

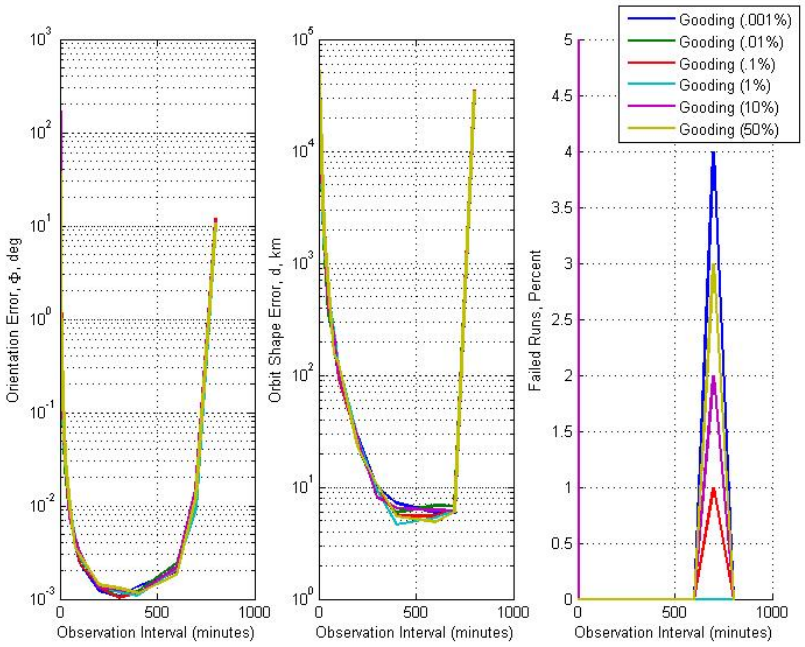

Figure 30: Effects of Initial Guesses on Orbital Estimate for GEO Orbit Using Gooding Method

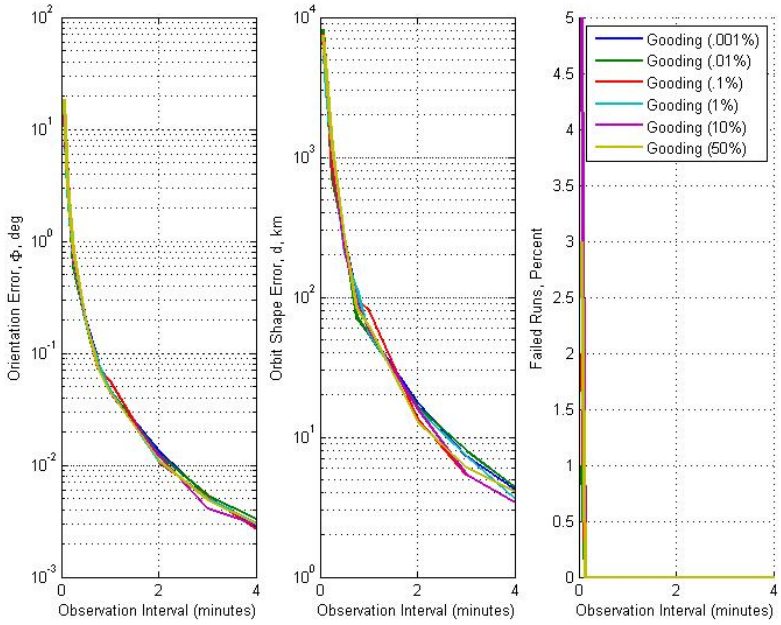

Figure 31: Effects of Initial Guesses on Orbital Estimate for LEO Orbit Using Gooding Method

3. Robustness of the Methods with Respect to the Measurement Error

Previous analysis all assumed that the measurement errors were 5". For the analysis to be more generalized, it is important to understand how the different methods will respond if the measurement error is increased or decreased. The measurement errors used in this analysis were 0", 2", 5", 10", and 20".

In nearly all cases, the measurement errors had almost not effect on the final estimates with no correlation found between the measurement errors and the final estimate.

The Laplace and both Gauss methods always converged upon nearly the same final estimate regardless of the measurement error. Frequently there would be a slight divergence in the orbit shape error near the interval where the error was minimum. The same thing was only minimally observed in the Double R results. The Gooding method had a slight divergence for both the orbit shape error and the orientation error. Again, no correlation was found. Unsurprisingly, all methods had a much larger spread of results for the coplanar case.

As an example, the general LEO plots are shown below, Figures 32 - 36. The remainder of these plots can be found in the appendix.

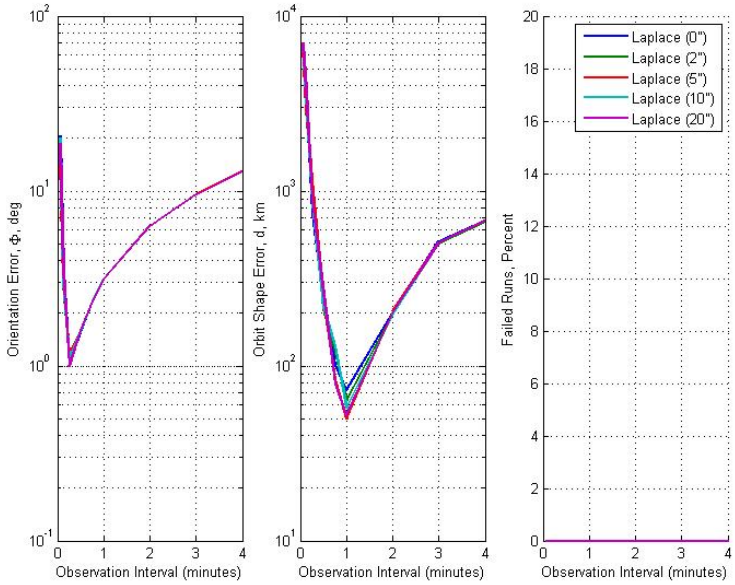

Figure 32: Effects of Measurement Errors on Orbital Estimate for LEO Orbit Using the Laplace Method

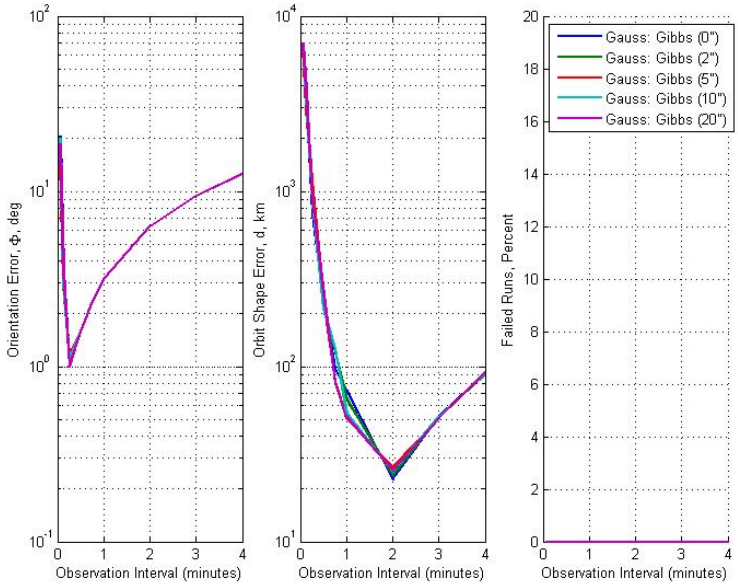

Figure 33: Effects of Measurement Errors on Orbital Estimate for LEO Orbit Using the Gauss Method with the Gibbs Method

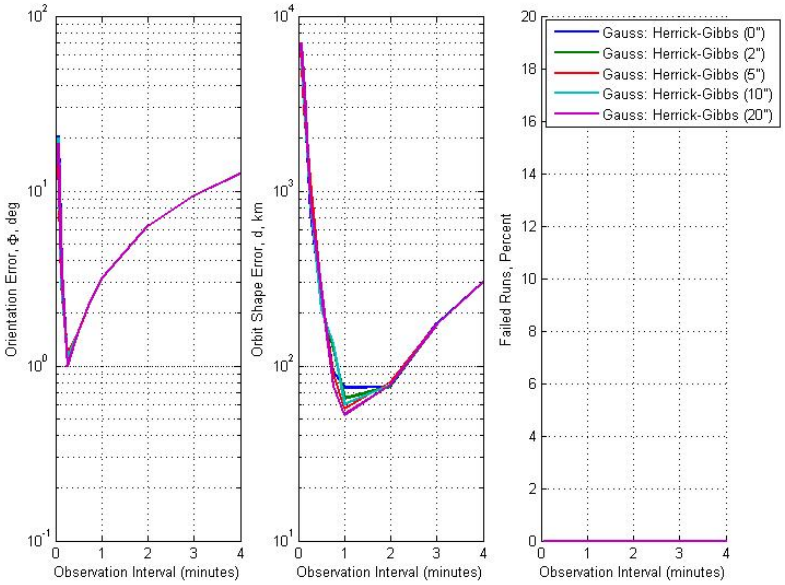

Figure 34: Effects of Measurement Errors on Orbital Estimate for LEO Orbit Using the Gauss Method with the Herrick-Gibbs Method

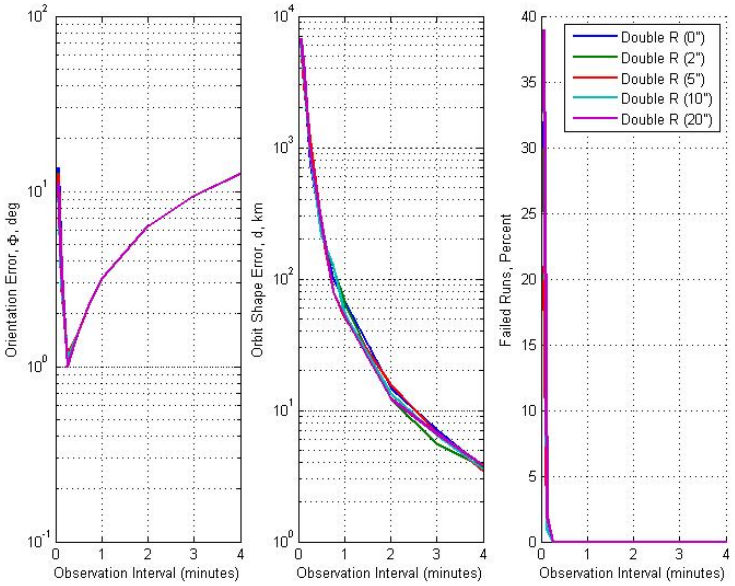

Figure 35: Effects of Measurement Errors on Orbital Estimate for LEO Orbit Using the Double R Method

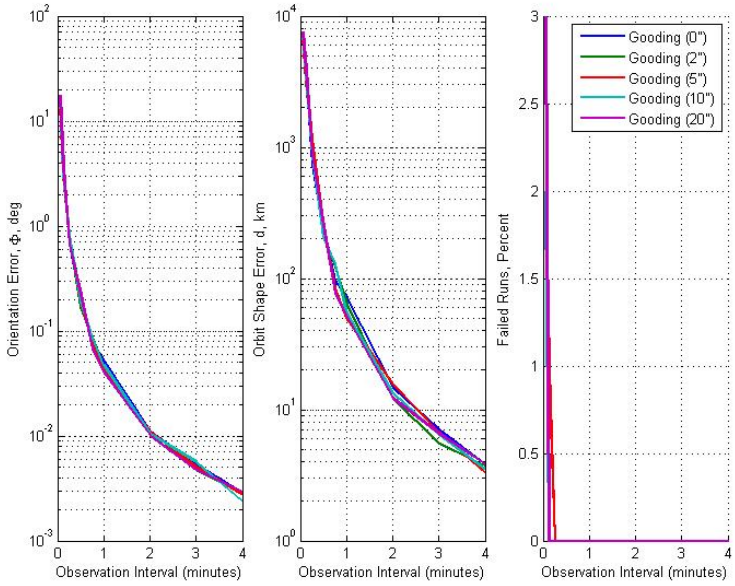

Figure 36: Effects of Measurement Errors on Orbital Estimate for LEO Orbit Using the Gooding Method

D. Tests of Multiple Observation Site Scenarios

It sometimes occurs that one particular site does not capture all of the necessary observations, but rather that multiple observation locations are utilized. For the multiple observation site study to be effective, the locations must not share the same plane. For example, if all observations occurred on the equator by different sites evenly spaced, it would be as if the earth's rotation were at a different speed, a parameter which the algorithms are largely independent of.

To accomplish this and to cover a large range of possibilities, the latitude of the observation site was randomly varied between 10 degrees south and 30 degrees north for each observation (the lop-sided latitudes were chosen since in the cases analyzed the satellite had just passed the ascending node at the initial time). The longitude was varied by a slightly more complex method. Inside the algorithm, to ensure the longitude between observation sites was spaced large enough to have the desired effect of different observation sites (because if the longitudes are very close together, the effect is not very large and poorly simulates what multiple observation sites would be like, it just makes the final results a little less accurate), the algorithm is adjusted in the following way. Previously, the program was operated such that for each observation, the original site would be rotated about the Z-axis as determined by the time from the initial location to the desired observation time. To spread the sites across a range of longitudes, a random number between 7.5 and 12.5 was multiplied by the change in time between observations, which was then used to calculate the size of the rotation about the Z-axis.

This change in the observer location is done for each observation of the Monte Carlo run. As can be seen, both the Laplace and Gauss methods decreased in accuracy quite rapidly. Furthermore, the Double R method became slightly less accurate in d

than the Gooding method, while also failing a large portion of time as the observation interval decreased. The Laplace method failed to converge more frequently as the observation interval increased. Thus, the methods are adequately tested for a variety of observation sites. For simplicity, the general LEO case will be presented below in Fig. 37. Note that the X-axis of Fig. 37 goes beyond the intervals previously used.

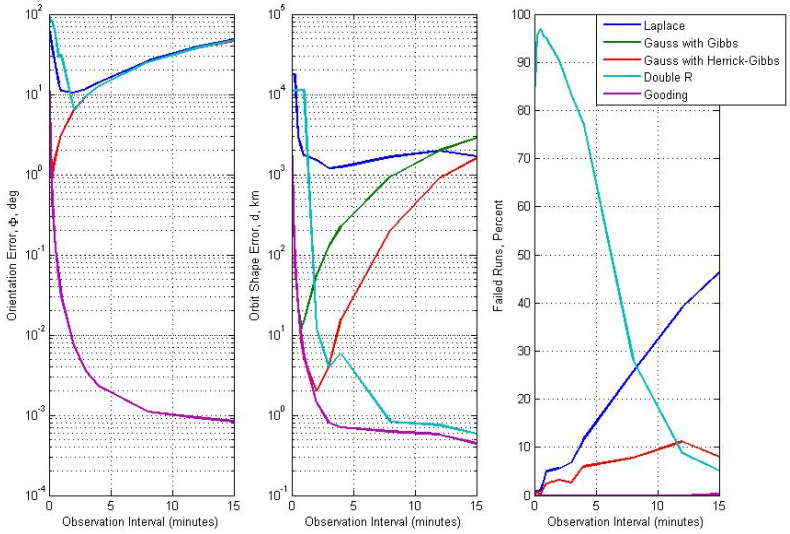

Figure 37: Effects of Multiple Observation Sites on Orbital Estimate for LEO Orbit

E. Test of Unequally Spaced Observations

All of the previous results have been analysis of scenarios when the observations had equal durations of time between each observation. It was desirable to determine what effect observations that were unequally spaced in time would have on the estimation of the orbit. Thus for this study, it was still desirable that the total time between the initial and last observation be the same so that the total arc length would be the same. Thus, a time was chosen to be the average time interval (these are the times shown on

the X-axis in Fig. 38). The time between the first and second observations was 50% of the average time and the time interval between the second and third observations was 150% of the average time. The unequally spaced observations appeared to have little effect on the majority of the methods. The only method that appeared to be significantly effected was Laplace method, which declined in accuracy more rapidly than previously. Analysis was also performed with the first interval being 150% and the second interval being 50% with nearly the same results.

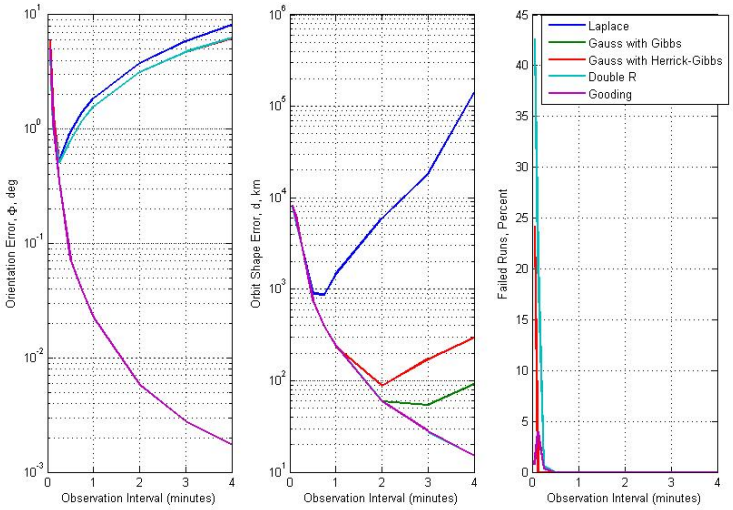

Figure 38: Effects of Unequal Observation Intervals on Orbital Estimate for LEO Orbit

F. Space-based Initial Orbit Determination

Next, the case of satellite-based observer was analyzed for initial orbit determination. Space-based orbit determination was then tested using two satellites. Due to the complexity in ensuring feasible orbits for both of them, only simple cases were examined. First, a case where the satellites had significant differences in semi-major axis to just prove the concept. The observed orbit is (a=8000 km, e=0, i=45°, ω=0°, Ω=0°, φ=0 °). The observed orbit is (a=9000 km, e=0, i=20°, ω=0°, Ω=0°, φ=-10 °).

Generally, the Gooding and Double R methods would converge upon the trivial solution of the observer's own orbit. This is expected, as the space-based observer's orbit is a valid solution if the range to the satellite was 0 km. The space-based observer's orbit will also absorb all measurement errors in the observations as well, while still being entirely valid. Some algorithms have been proposed [5] to handle this problem. One such method proposes a modification to the Gooding method that enforces a penalty to the cost function when the range drops below some determined amount, for example 20 km. In this paper, however, only the previous algorithms will be tested for the sake of simplicity.

For the Gauss and Laplace methods, multiple solutions were frequently found in the process of the algorithm when solving the roots of the 8^{th} order polynomial. As programmed for the all the previous analysis, these methods ceased operation and declared the run a failure. It is possible however, that if each of these solutions could be followed, additional solutions would be found, one being the satellite's orbit and the other being the observer's orbit. If more than the two solutions appear viable, for only 3 observations, one could not determine with certainty which orbit was the satellite's. In this case, a fourth observation would need to be used. It should be

noted that these methods are frequently used with success to determine the orbits of celestial objects such as asteroids with heliocentric orbits. The scenarios are similar in that the observer of the heliocentric orbit is on a heliocentric orbit as well (Earth's orbit).

When the algorithm was run, the Laplace and Gauss methods would produce 3 different viable orbits. One orbit could usually be eliminated for having a relatively large eccentricity. This left two orbits that were near circular. Very frequently, one of the remaining orbits would have an inclination near the observer's inclination and the other orbit would have an inclination near the observed satellite's inclination. In an operational setting, the selected orbit would be the orbit that had the most dissimilar inclination compared to the observer. Thus the appropriate orbit was selected and the errors analyzed.

When the appropriate solution was selected among the possible solutions for the Laplace and Gauss methods, the error for both parameters was on average lower. The Laplace solutions did very well for both parameters. The Gauss method faired all right, not excelling, but declined in accuracy as the observation interval grew larger. For the Gooding and the Double R method, it was decided the initial estimate of the ranges and radii respectively should be larger rather than smaller than the true value. Thus the initial guesses were 150% of the true value. It was decided to see if the initial guess would result in a better final estimate. Thus the initial guess was changed to 120%. This had a major influence on the Gooding method, with virtually no effect on the Double R method. The Gooding method became much more accurate, with behavior similar to the previous results presented. Various estimates were tried between 120% and 150% to see when this impact began to take place and with an estimate as close as 140% the impact made the Gooding method the most accurate overall. These results can be seen in Fig. 39.

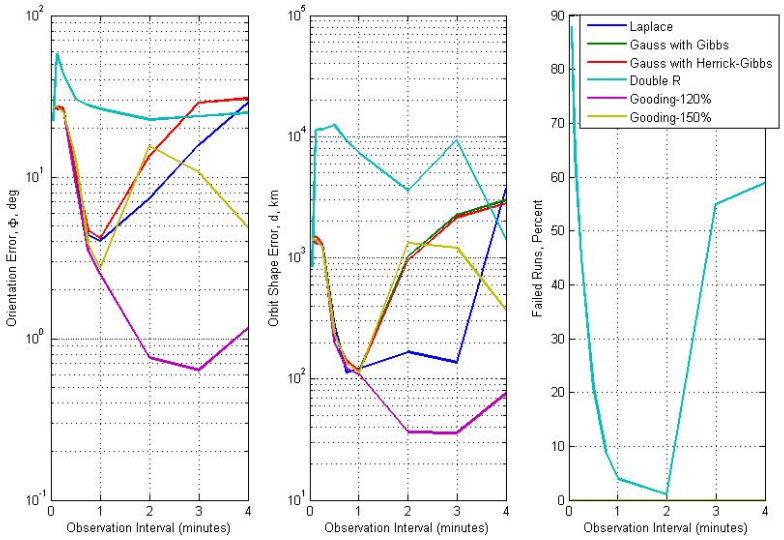

Figure 39: IOD Errors for Space-based Observer

A test was also done for a case when the semi-major axis were nearer to each other. In this case, the observed orbit's semi-major axis was changed to 8100 km. Both the Gooding and Double R were shown to be very good for this case, having results similar to previous ground-based results, while the Laplace and Gauss methods all did very poorly. This is seen in Fig. 40.

A test was done for the case with the same inclination. This case failed because the orbits were coplanar. Φ was estimated with some success while d was poor for all intervals. These results are seen in Fig. 41.

Lastly, a test was done for the case of similar inclinations, with the observer being at 40° and the observed satellite having an inclination of 45°. Both the Gooding and the Laplace methods performed comparably, with Laplace estimating Φ better at shorter observation intervals and Gooding estimating Φ better at larger observation interals. The Double R method did well for the parameter d but poorly for the parameter Φ. The Gauss method did well for Φ but poorly for d. These results are

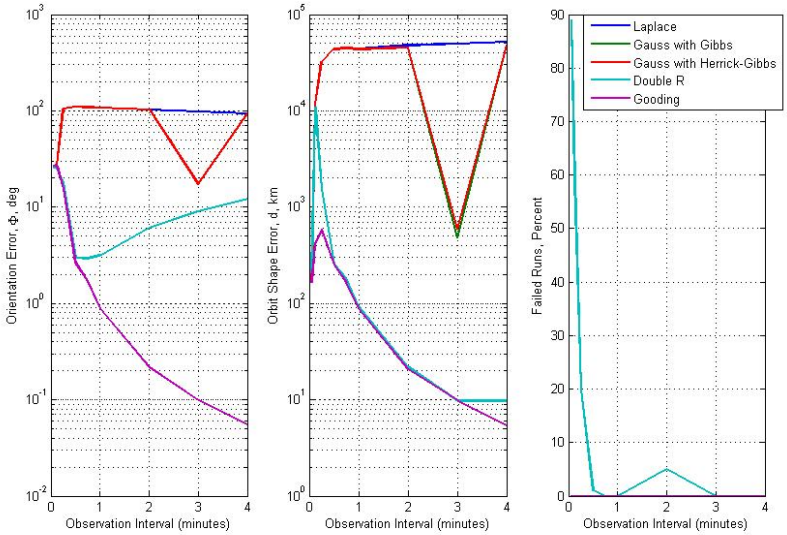

Figure 40: IOD Errors for Space-based Observer with Similar Orbit Shapes

seen in Fig. 42.

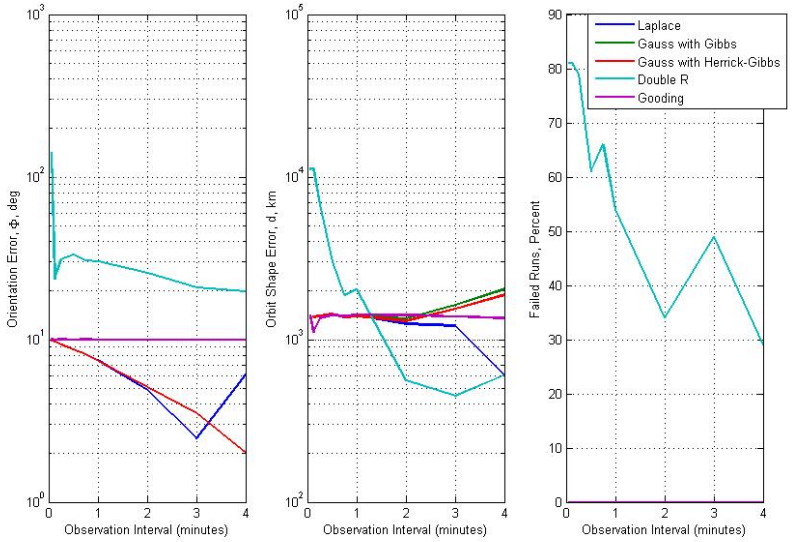

Figure 41: IOD Errors for Space-based Observer which is Coplanar

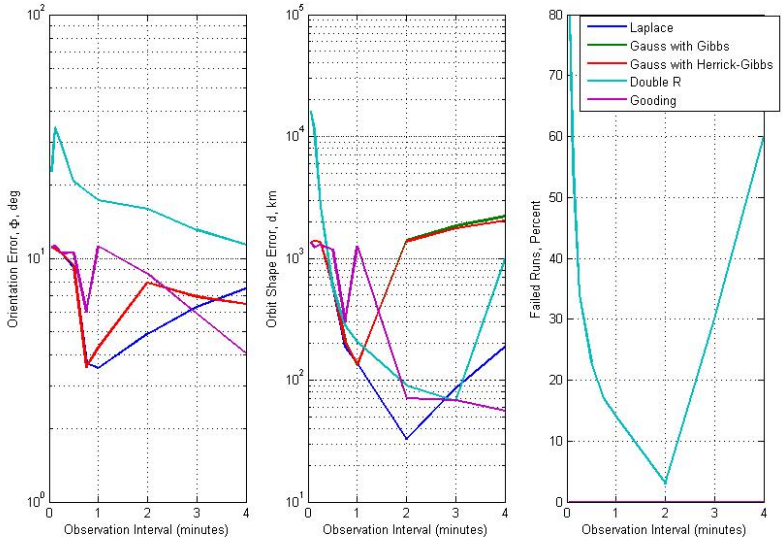

Figure 42: IOD Errors for Space-based Observer with Nearly Similar Inclination

CHAPTER V

CONCLUSIONS

Laplace, Gauss, and Double R methods all estimate the orbit orientation error, Φ, with about the same decreasing accuracy as the observation interval is increased, with Laplace declining in accuracy slightly more rapidly. The Gooding method increases in accuracy as the observation interval is increased, reaching several orders of magnitude better than the other methods. For observations very close together, closer than 2-5° separation, all of the methods do increasingly worse and perform similarly.

As for the orbit shape error, d, Double R and Gooding do nearly exactly the same in most scenarios. Both increase in accuracy as the observation interval is increased, while in contrast Laplace and Gauss decrease in accuracy. Also, as would be expected, when the Gibbs method is used for larger observation intervals, the accuracy is better for the determination of the orbit shape. However, as the observations grow closer together, the Gooding and Double R methods decrease in accuracy until all the methods have similarly poor results.

This paper demonstrated that the Gauss and Laplace methods are not the ideal choices for estimating any of the desired parameters. For all cases examined, the Gooding method consistently estimated Φ more accurately, usually by at least an order of magnitude or more. The Double R method and the Gooding method both had comparable accuracy in d in nearly all but a few cases. Additionally, the Double R method would more frequently fail to converge, though the Gooding method too did fail to converge in a few particular scenarios. Near polar inclinations, the Gooding method would need to run twice, once assuming prograde and another assuming retrograde.

This study reveals the capability of the Gooding method to estimate nearly all orbits. Double R also nearly always does well for both parameters, though it struggles to converge upon a solution frequently for observations very close for nearly all cases and for observations very far apart for the Molynia apogee case. At the very least, the Gooding method should always be used to determine the orbit orientation, except when the orbit is nearly polar and the observation interval is larger. The shape of the orbit is often best determined by either the Double R method or the Gooding method. The only case when the Double R method was consistently better at estimating the shape was the polar orbit case for larger observation intervals. All methods do poorly for when the coplanar orbit case is approached. In an operational setting, the orientation can be relatively well determined the Gauss and Gooding methods with a high rate of convergence, so it will be known the coplanar case is being approached. While both the Double R and Gooding methods are hindered with a requirement to provide an initial estimate for the radii and the ranges respectively, a range of initial guesses could be used to increase the likelihood of convergence.

Various parameters were also adjusted to view the effects on the accuracy of the method. A LEO orbit was selected to be control specimen. The increase in semi-major axis made all the methods less accurate, but this is believed to be a result of the decreasing arc length for the given observation interval. When the inclination was varied, the greatest problems occurred when the coplanar case was approached (when the observation site was on the equator). Furthermore, the case when the inclination approached 90° also proved to be problematic, particularly for the Gooding and Double R methods.

The robustness of the different methods was also tested. In general, the initial guesses of the range and the radii for the Gooding and Double R methods respectively had little effect on the final initial orbit estimation. Additionally, the measurement

error seemed to have little effect on any of the methods for a measurement error as high as 20". Thus, all of the methods are shown to be quite robust.

The case of multiple ground-based observing sites was tested. The Laplace method's accuracy significantly decreased in accuracy overall. Additionally, while the Double R method was still one of the more accurate methods, the Double R did not perform as well as the Gooding method for the shape error, in contrast to the results of the majority of other runs where they were generally very nearly the same. Lastly, the case when the observations were unequally spaced was examined. The only major effect was that the Laplace method decreased in accuracy more rapidly as the average observation interval increased.

Lastly, the capabilities of the methods were tested for space-based initial orbit determination. The Laplace and Gauss methods produced more than 1 solution (typically 3). If educated guesses can be made of the observed object (such as the eccentricity or orbital plane), these potential solutions can be narrowed. The Laplace method was shown to be the best method when the Gooding method did not have a good range estimate. If the Gooding method did have a good range estimate, the Gooding method frequently had by far the best orientation estimate and a significantly better shape estimate. When the observed orbit and observer's orbit have similar shapes, the Double R and Gooding methods were by far the best with Laplace and the Gauss methods being just acceptable. In the case when the two orbits have nearly the same inclination, all the methods performed poorly.

In conclusion, the Gooding method is nearly always the best method to use for initial orbit determination, irregardless of the scenario, when the sole criteria for selecting a method is accuracy. The only scenarios where the Gooding method struggled were the near polar orbit cases and cases of space-based IOD when the range estimates were not well-known (in this case it is best to use the Laplace method). The

Gooding method was always by far the best by usually several orders of magnitude in estimating the orientation error, Φ. For the shape error, both the Gooding and Double R method performed nearly equally well, with only a few cases when the Gooding method would be better. No statement about efficiency has been made, computational times were not analyzed.

Several recommendations are made for future work. First, future work should measure the computational times for each of these methods in the various scenarios to determine how computationally intensive each method is. The computational intensity of the methods is particularly important for space-based IOD when computing power is very expensive on a satellite.

Additionally, more measurements should be incorporated into the analysis. As previous research as pointed out, the majority of time in an operational setting additional observations would be available. Both the Laplace and Gooding methods can be expanded to N-measurements, thus enabling greater accuracy. Furthermore, IOD is nearly always followed by the method of least-squares or a filter to refine the estimate through the use of additional measurements. These follow-up methods require a good enough initial estimate to ensure convergence. No statement has been made in this research as to if the achieved estimates for any of the methods would be good enough to ensure convergence for one of these follow-up methods. Future research should endeavor to make statements as to how good of an estimate is required for convergence to be reached.

Future research should analyze more randomly generated orbits to allow for a stronger generalized statement. The difficulty with creating this orbits is ensuring that the orbit can be feasibly viewed from the observer's location. These randomly generated orbits should hold the elements constant that are of interest (such as the inclination for a polar orbit) while randomizing the other orbital elements. Further-

more, more work should be done for the unequal observation intervals and analyze more cases with a greater range of interval percentages.This work should also be expanded to run test cases of interest to astronomers, test cases that include highly elliptical and highly inclined asteroids and parabolic comets. Additional high altitude satellites and highly eccentric satellites should be studied as well.

Finally, no statement was made as to the frequency a good estimate is achieved. The median was used instead of the mean due to the desire to avoid the influence of tremendously bad estimates. Since the mean cannot be used, the standard deviation is unhelpful as well. Future work should perhaps incorporate a kind of mean and standard deviation that doesn't include the extreme estimates.

REFERENCES

[1] ESCOBAL, P. R., *Methods of Orbit Determination*, John Wiley and Sons, Inc., New York, 1965.

[2] GOODING, R.H., "A New Procedure for the Solution of the Classical Problem of Minimal Orbit Determination from Three Lines of Sight," *Celestial Mechanics and Dynamical Astronomy*, Vol. 66, No. 4, 1997, pp. 387-423.

[3] VALLADO, D. A., *Fundamentals of Astrodynamics and Applications*, Microcosm Press, El Segundo, CA, 2001.

[4] TAFF, L.G., "The Resurrection of Laplace's Method of Initial Orbit Determination," Lincoln Laboratory, Lexington, MA, 1983, Technical Report 628.

[5] HENDERSON, T. A. and MORTARI, D., "Modifications to the Gooding Algorithm for Angles-Only Initial Orbit Determination," presented as paper AAS 10-238 at the 20th AAS/AIAA Space Flight Mechanics Meeting Conference, San Diego, CA, February 14-18, 2010.

[6] HERGET, P., "Computation of Preliminary Orbits," *The Astronomical Journal*, Vol. 70, No. 1, 1955, pp. 1-3.

[7] KARIMI, R. R. and MORTARI, D., "Initial Orbit Determination using Multiple Observations," *Celestial Mechanics and Dynamical Astronomy*, Vol. 109, 2011, pp. 167-180.

[8] KRISTENSEN, L.K., "Single Lunation N-observation Orbits," *Celestial Mechanics and Dynamical Astronomy*, Vol. 105, No. 4, 2009, pp. 275-287.

[9] LENZ, S. M., BOCK, H.G., and SCHLÖDER, J. P., "Multiple Shooting Method for Initial Satellite Orbit Determination," *Journal of Guidance, Control, and Dynamics*, Vol. 33, No. 5, 2010, pp. 1334-1346.

[10] KARIMI, R. R. and MORTARI, D., "An Adaptive Scheme on Optimal Number

of Observations and Time Intervals for an Initial Orbit Determination Problem," presented as paper AAS 10-152 at the 20th AAS/AIAA Space Flight Mechanics Meeting Conference, San Diego, CA, February 14-17, 2010.

[11] GAPOSCHKIN, E. M., VON BRAUN, C., and SHARMA, J., "Space-based Space Surveillance with the Space-Based Visible," *Journal of Guidance, Control, and Dynamics*, Vol. 23, No. 1, 2000, pp. 148-152.

[12] MULLIKIN, T.L.,"Rapid Determination and Ephemeris Prediction of Satellite Orbits from an Earth-Orbiting Platform," presented as paper AIAA-84-2033 at the AIAA/AAS Astrodynamics Conference, Seattle, WA, August 20-22, 1984.

[13] CELLETTI, A. and PINZARI, G., "Four Classical Methods for Determining Planetary Elliptic Elements: A Comparison," *Celestial Mechanics and Dynamical Astronomy*, Vol. 93, 2005, pp. 1-52.

[14] CELLETTI, A and PINZARI, G., "Dependence on the Observational Time Intervals and Domain of Convergence of Orbital Determination Methods," *Celestial Mechanics and Dynamical Astronomy*, Vol. 95, 2006, pp. 327-344.

[15] TAFF, L.G., RANDALL, P.M.S., and STANSFIELD, S.A., "Angles-Only, Ground-Based, Initial Orbit Determination," Lincoln Laboratory, Lexington, MA, 1984, Technical Report 618.

[16] TAFF, L.G., "On Initial Orbit Determination," *The Astronomical Journal*, Vol. 89, No. 9, 1984, pp. 1426-1428.

[17] BRANHAM, R. L., "Laplace Orbit Determination and Differential Corrections," *Celestial Mechanics and Dynamical Astronomy*, Vol. 93, 2005, pp. 53-68.

[18] LONG, A.C., CAPPELLARI, J.O., JR, VELEZ, C.E., and FUCHS, A.J., "Goddard Trajectory Determination System (GTDS) Mathematical Theory (Revision 1)," Goddard Space Flight Center: National Aeronautics and Space Administration, Greenbelt, MD, 1989.

[19] SCHAEPERKOETTER, A. and MORTARI, D., "A Comprehensive Comparison between Angles-Only Initial Orbit Determination Techniques," presented as paper AAS 11-116 at the 21st AAS/AIAA Space Flight Mechanics Meeting Conference, New Orleans, LA, February 13-17, 2011.

[20] KARIMI, R. R. and MORTARI, D., "On Laplace's Orbit Determination Method: Some Modifications," presented as paper AAS 11-121 at the 21st AAS/AIAA Space Flight Mechanics Meeting Conference, New Orleans, LA, February 13-17, 2011.

[21] PRUSSING, J. E. and CONWAY, B. A., *Orbital Mechanics*, Oxford Press, New York, 1993.

[22] GIBBS, J. W., "On the Determination of Elliptical Orbits from Three Complete Observations," *Memoires National Academy of Science*, Vol. 4, No. 2, 1889, pp. 79-104.

[23] HERRICK, S., *Astrodynamics: Orbit Determination, Space Navigation, Celestial Mechanics- Vol. 1*, Van Nostrand Reinhold Co., London, 1971.

[24] BATE, R. M., MUELLER, D. D., and WHITE, J. E., *Fundamentals of Astrodynamics*, Dover Publications, New York, 1971.

[25] MORTARI, D., SCURO, S. R., and BRUCCOLERI, C., "Attitude and Orbit Error in n-Dimensional Spaces," *The Journal of the Astronautical Sciences*, Vol. 54, No. 3-4, 2006, pp. 467-484.

APPENDIX A

ADDITIONAL RESULTS FROM ANALYSIS

Robustness of Methods with Respect to Measurement Errors

For the sake of brevity, only the LEO orbit analysis was presented within Chapter IV. Below, the complete results are shown for all the previously analyzed orbit cases.

Below are the results for the coplanar case in Figures A.1 - A.5.

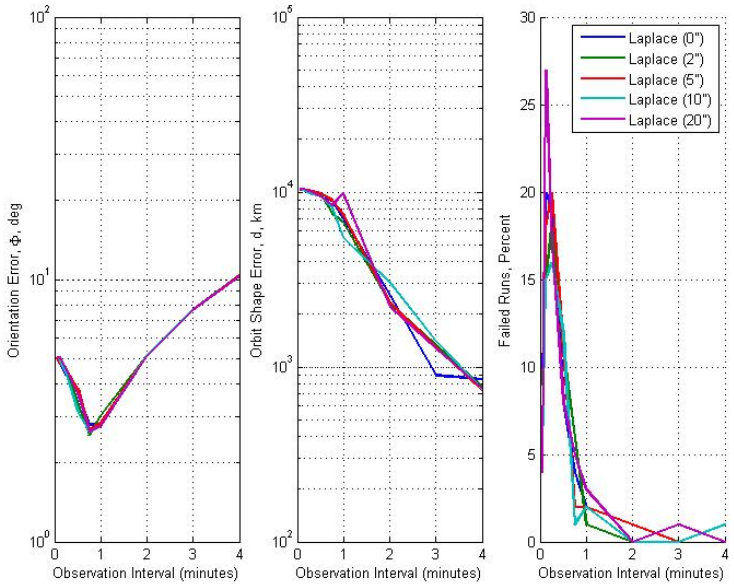

Figure A.1: Effects of Measurement Errors on Orbital Estimate for Coplanar Orbit Using the Laplace Method

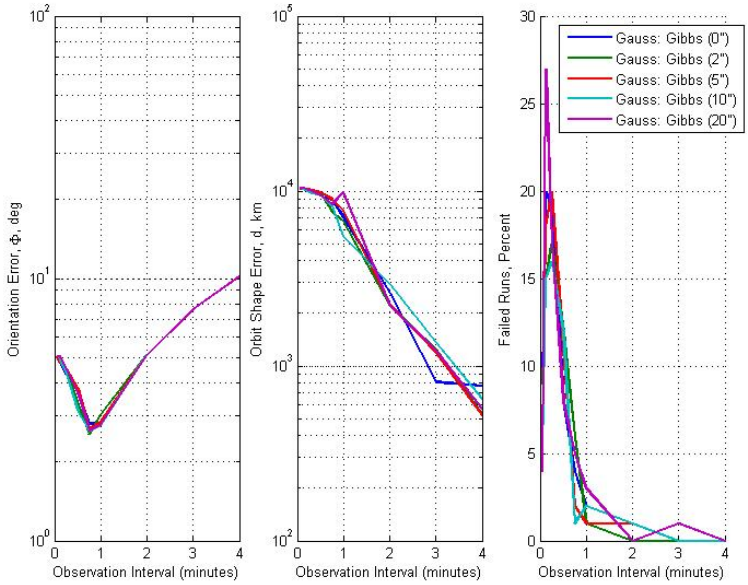

Figure A.2: Effects of Measurement Errors on Orbital Estimate for Coplanar Orbit Using the Gauss Method with the Gibbs Method

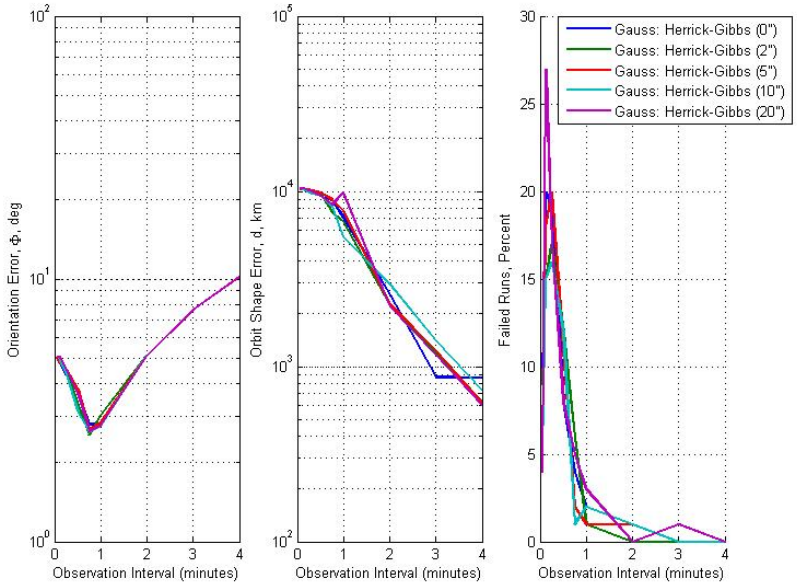

Figure A.3: Effects of Measurement Errors on Orbital Estimate for Coplanar Orbit Using the Gauss Method with the Herrick-Gibbs Method

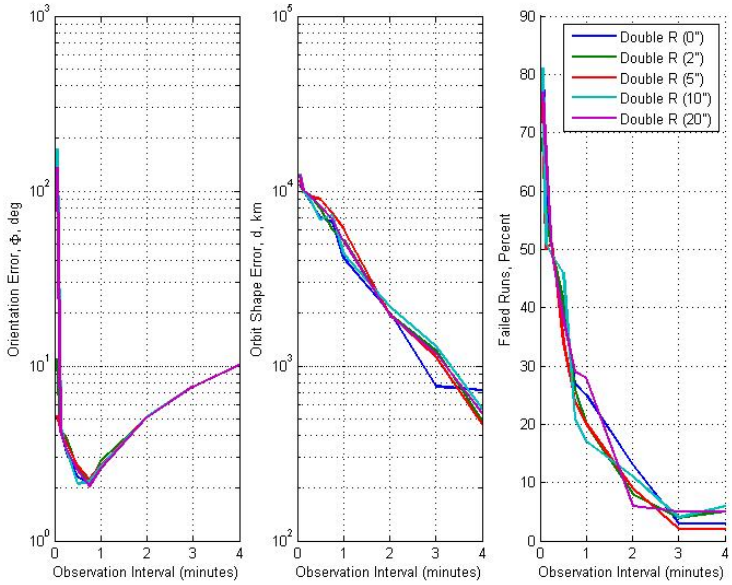

Figure A.4: Effects of Measurement Errors on Orbital Estimate for Coplanar Orbit Using the Double-R Method

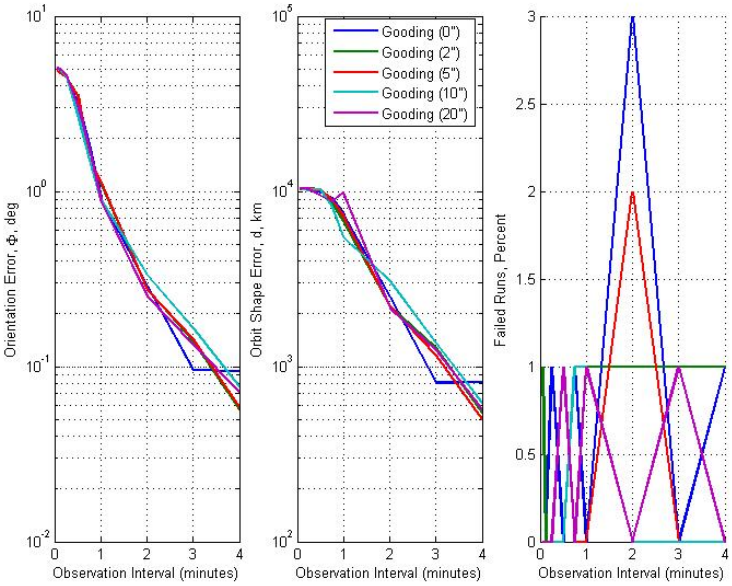

Figure A.5: Effects of Measurement Errors on Orbital Estimate for Coplanar Orbit Using the Gooding Method

Below are the results for the polar case in Figures A.6 - A.10.

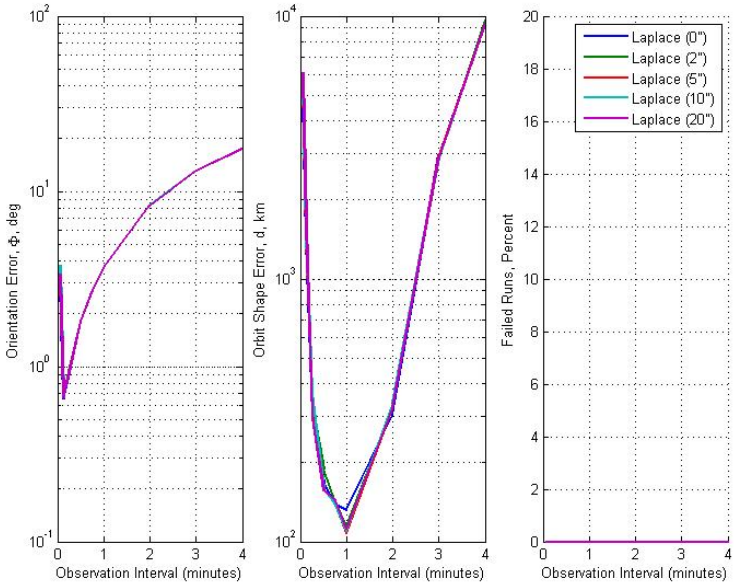

Figure A.6: Effects of Measurement Errors on Orbital Estimate for Polar Orbit Using the Laplace Method

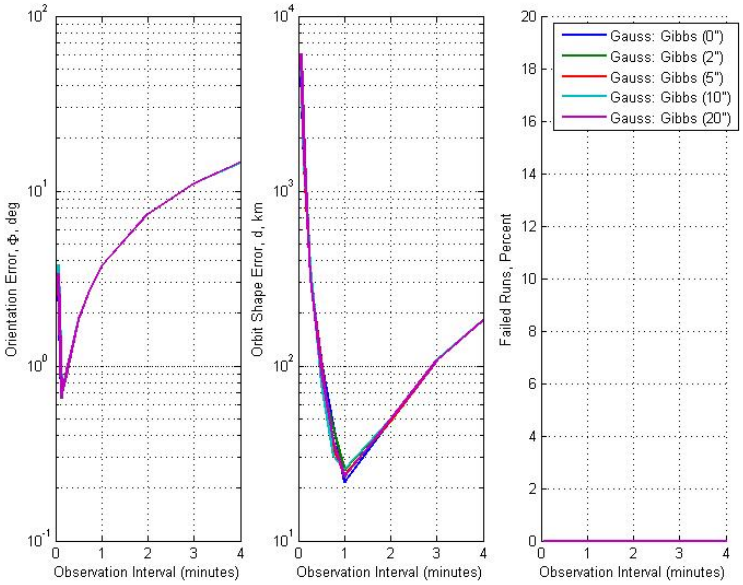

Figure A.7: Effects of Measurement Errors on Orbital Estimate for Polar Orbit Using the Gauss Method with the Gibbs Method

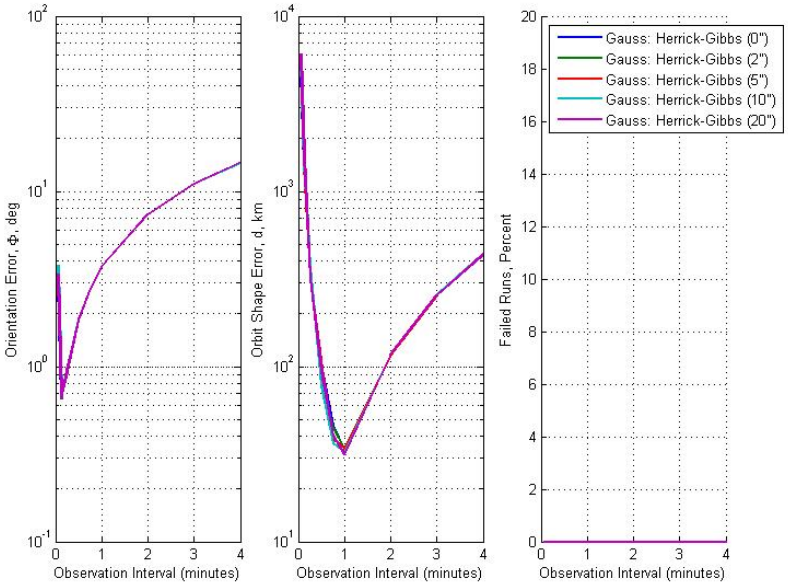

Figure A.8: Effects of Measurement Errors on Orbital Estimate for Polar Orbit Using the Gauss Method with the Herrick-Gibbs Method

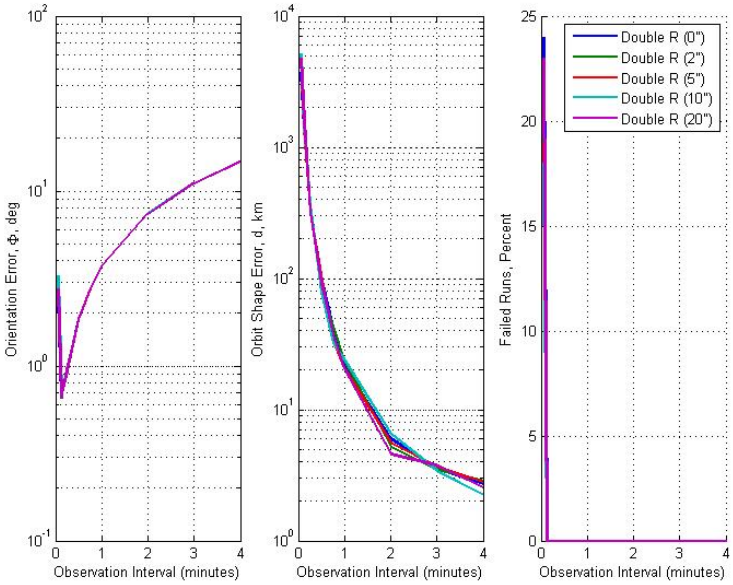

Figure A.9: Effects of Measurement Errors on Orbital Estimate for Polar Orbit Using the Double-R Method

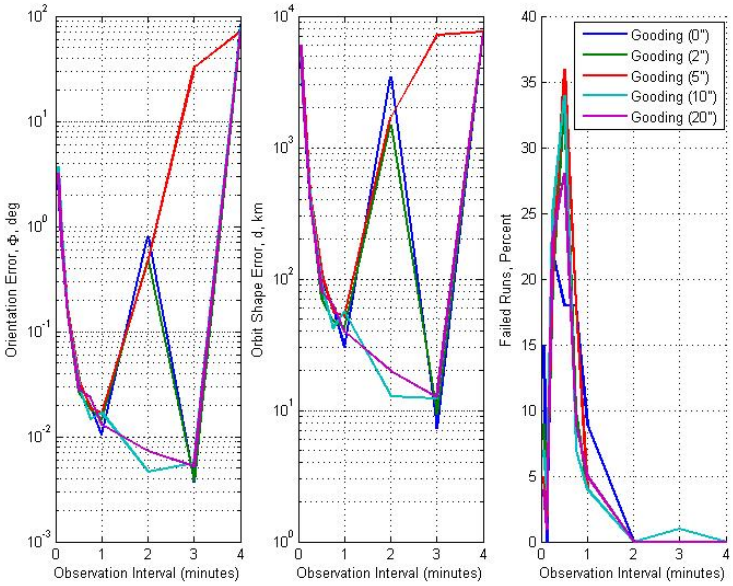

Figure A.10: Effects of Measurement Errors on Orbital Estimate for Polar Orbit Using the Gooding Method

Below are the results for the sun-synchronous case in Figures A.11 - A.15.

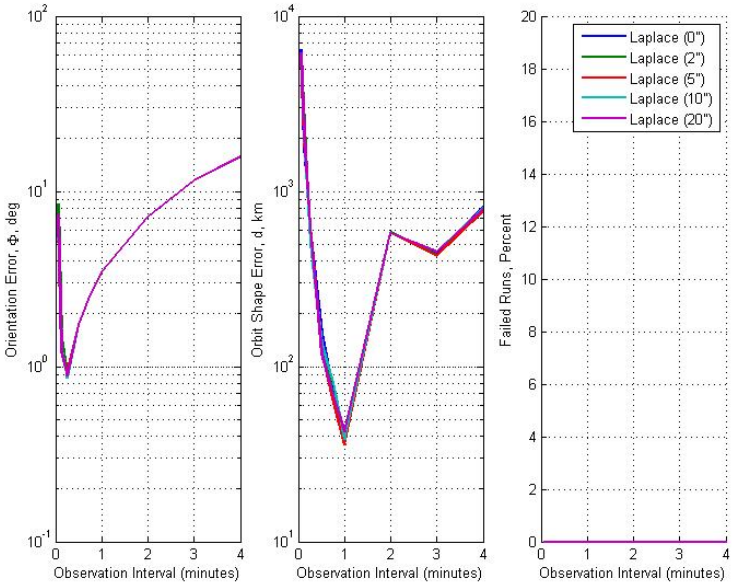

Figure A.11: Effects of Measurement Errors on Orbital Estimate for Sun-Synchronous Orbit Using the Laplace Method

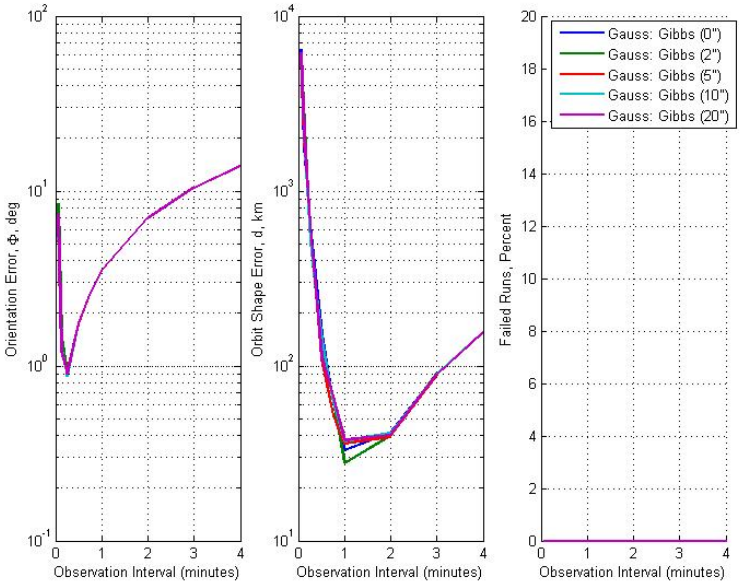

Figure A.12: Effects of Measurement Errors on Orbital Estimate for Sun-Synchronous Orbit Using the Gauss Method with the Gibbs Method

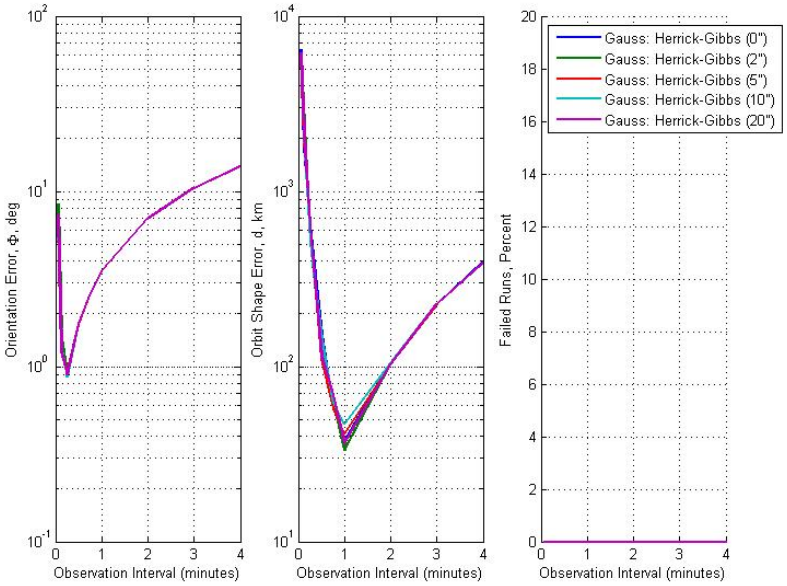

Figure A.13: Effects of Measurement Errors on Orbital Estimate for Sun-Synchronous Orbit Using the Gauss Method with the Herrick-Gibbs Method

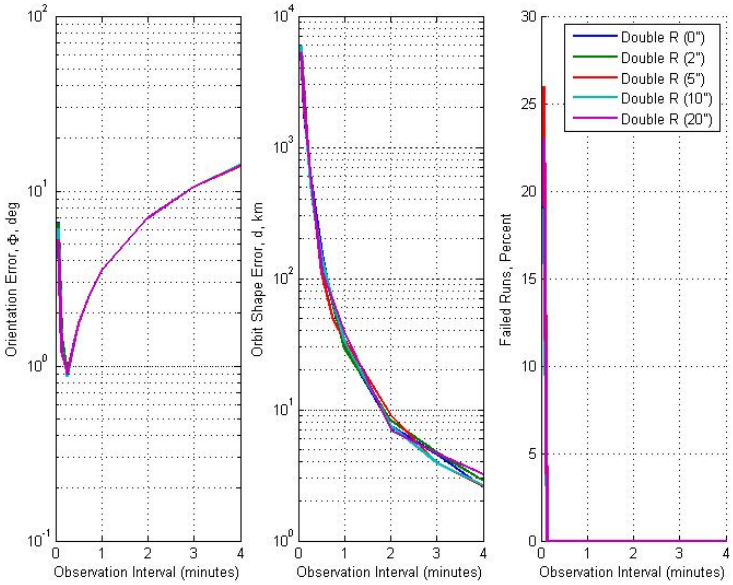

Figure A.14: Effects of Measurement Errors on Orbital Estimate for Sun-Synchronous Orbit Using the Double-R Method

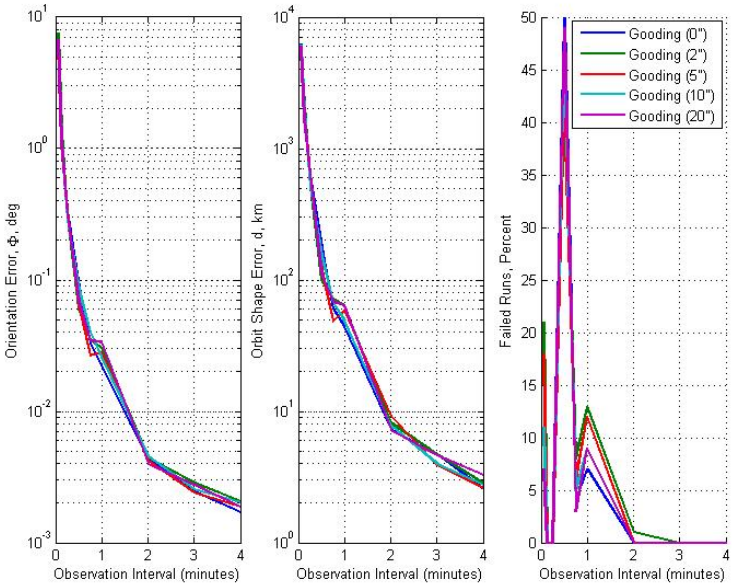

Figure A.15: Effects of Measurement Errors on Orbital Estimate for Sun-Synchronous Orbit Using the Gooding Method

Below are the results for the Molniya case at ascension in Figures A.16 - A.20.

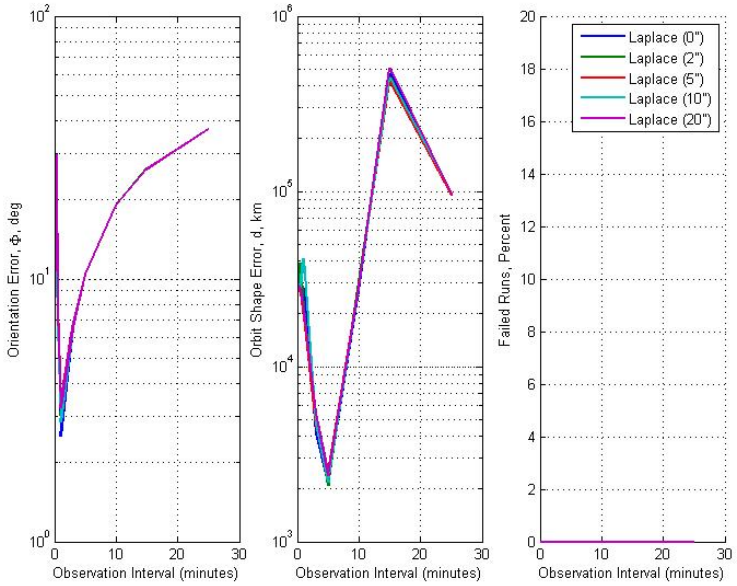

Figure A.16: Effects of Measurement Errors on Orbital Estimate for Molniya Orbit at Ascension Using the Laplace Method

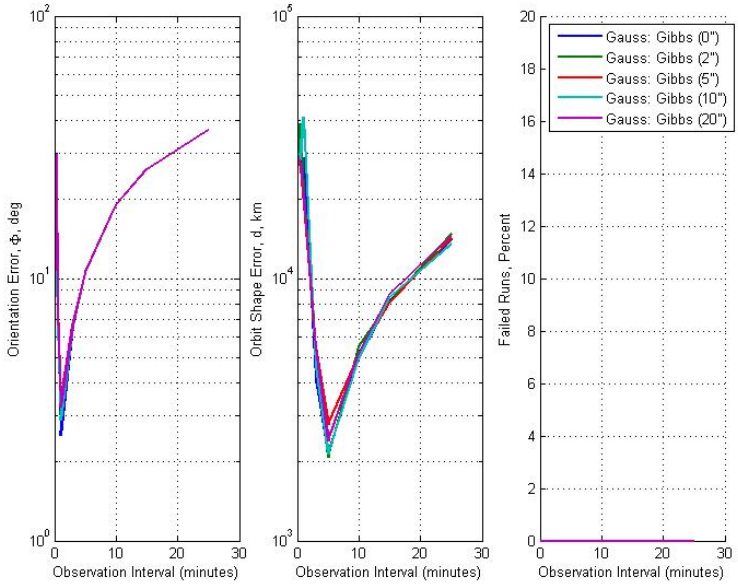

Figure A.17: Effects of Measurement Errors on Orbital Estimate for Molniya Orbit at Ascension Using the Gauss Method with the Gibbs Method

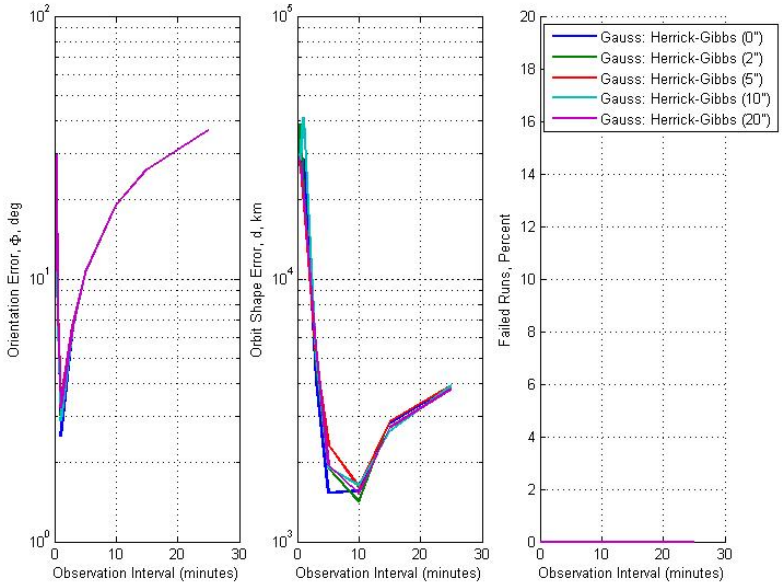

Figure A.18: Effects of Measurement Errors on Orbital Estimate for Molniya Orbit at Ascension Using the Gauss Method with the Herrick-Gibbs Method

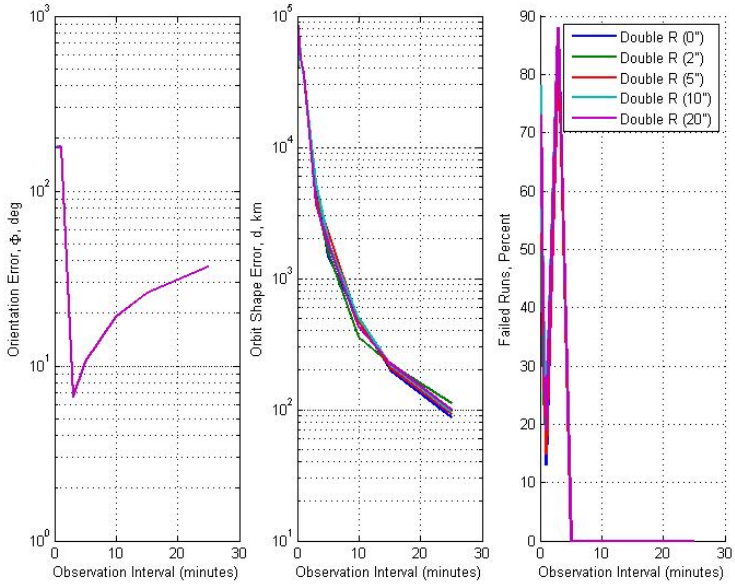

Figure A.19: Effects of Measurement Errors on Orbital Estimate for Molniya Orbit at Ascension Using the Double-R Method

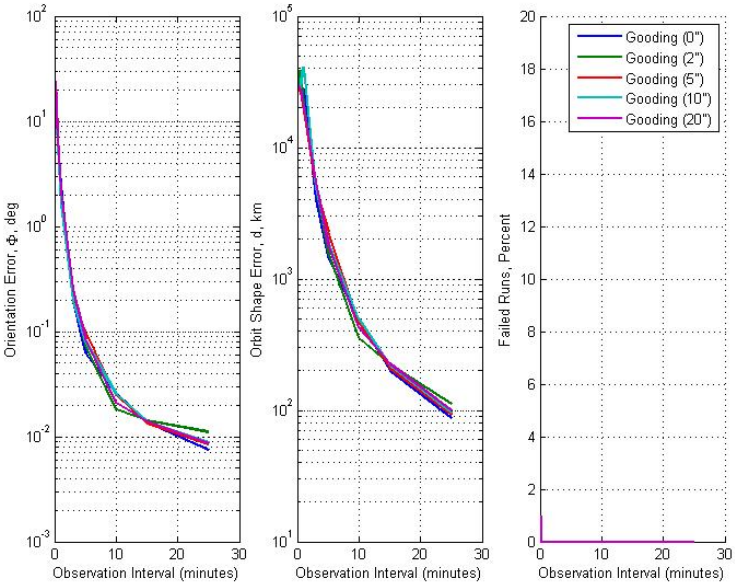

Figure A.20: Effects of Measurement Errors on Orbital Estimate for Molniya Orbit at Ascension Using the Gooding Method

Below are the results for the Molniya case at apogee in Figures A.21 - A.25.

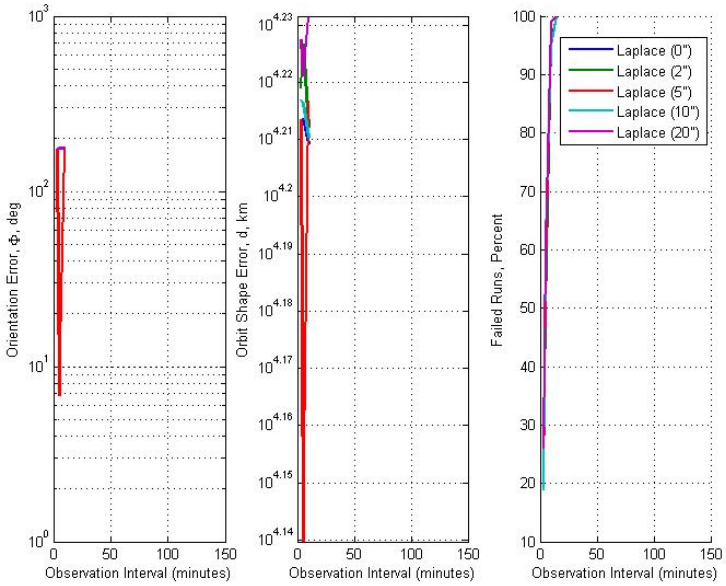

Figure A.21: Effects of Measurement Errors on Orbital Estimate for Molniya Orbit at Apogee Using the Laplace Method

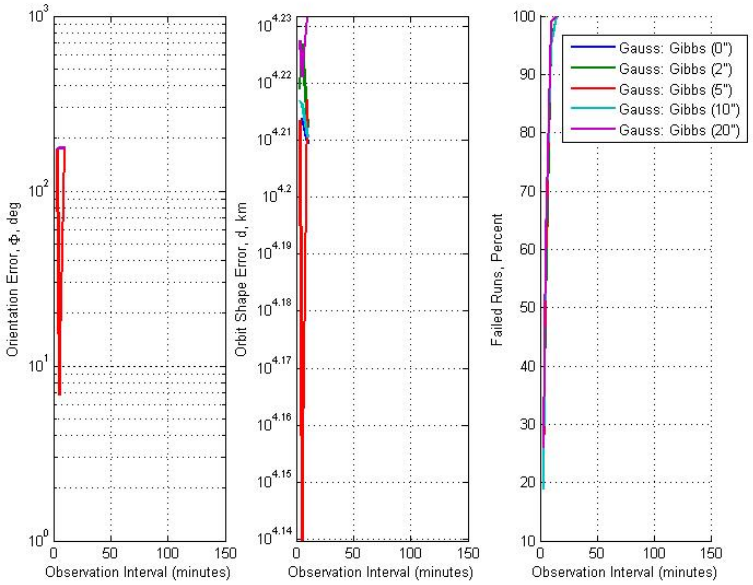

Figure A.22: Effects of Measurement Errors on Orbital Estimate for Molniya Orbit at Apogee Using the Gauss Method with the Gibbs Method

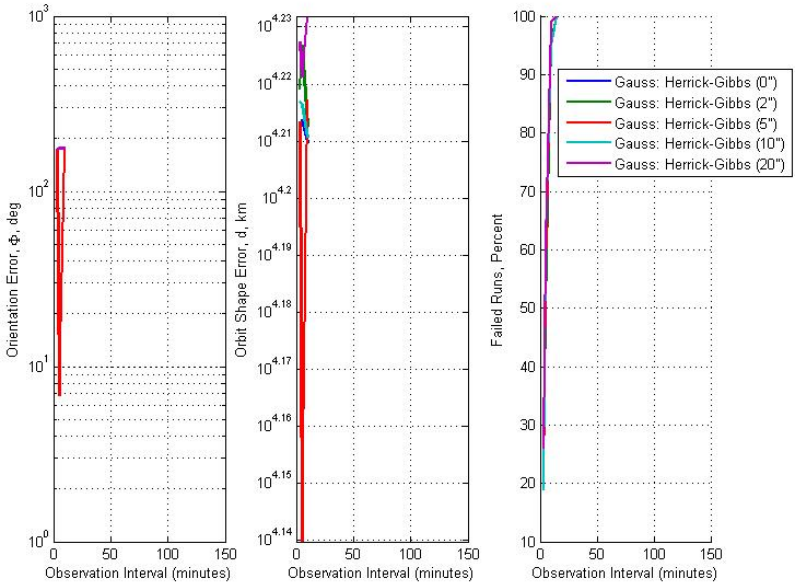

Figure A.23: Effects of Measurement Errors on Orbital Estimate for Molniya Orbit at Apogee Using the Gauss Method with the Herrick-Gibbs Method

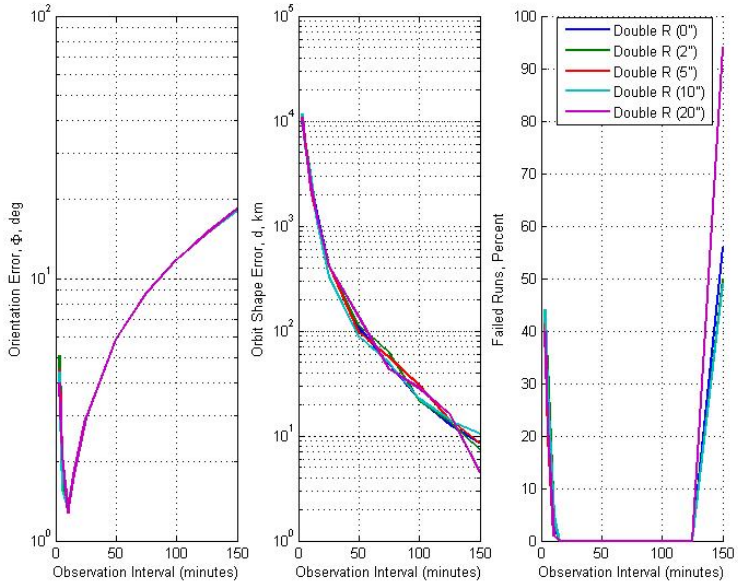

Figure A.24: Effects of Measurement Errors on Orbital Estimate for Molniya Orbit at Apogee Using the Double-R Method

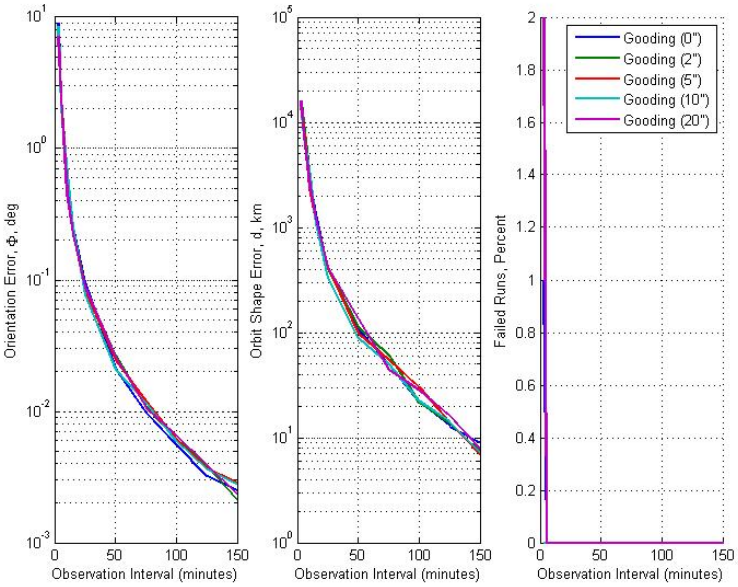

Figure A.25: Effects of Measurement Errors on Orbital Estimate for Molniya Orbit at Apogee Using the Gooding Method

Below are the results for the GEO case in Figures A.26 - A.30.

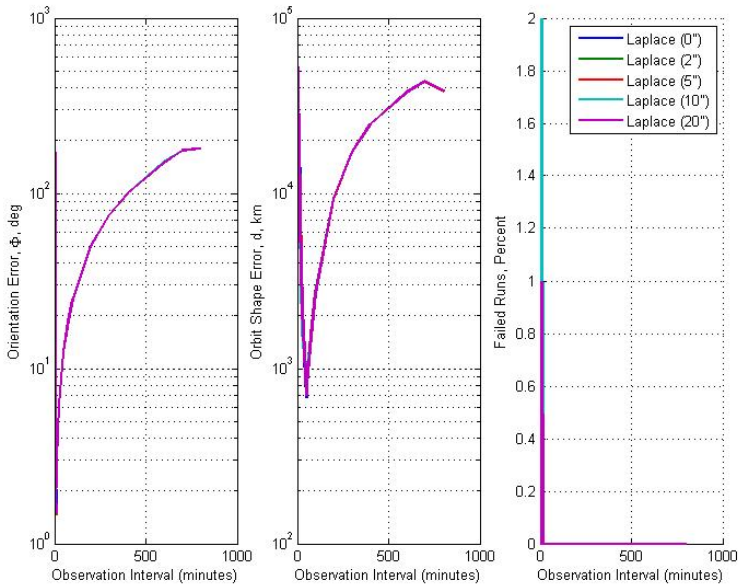

Figure A.26: Effects of Measurement Errors on Orbital Estimate for GEO Orbit Using the Laplace Method

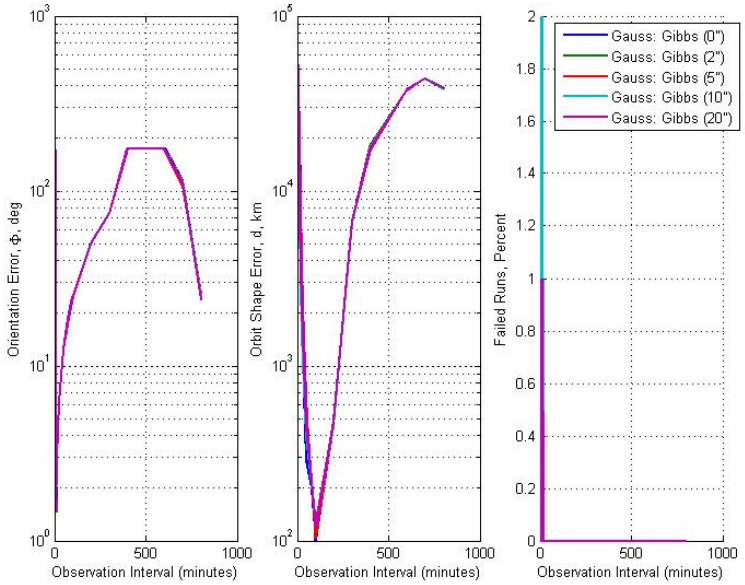

Figure A.27: Effects of Measurement Errors on Orbital Estimate for GEO Orbit Using the Gauss Method with the Gibbs Method

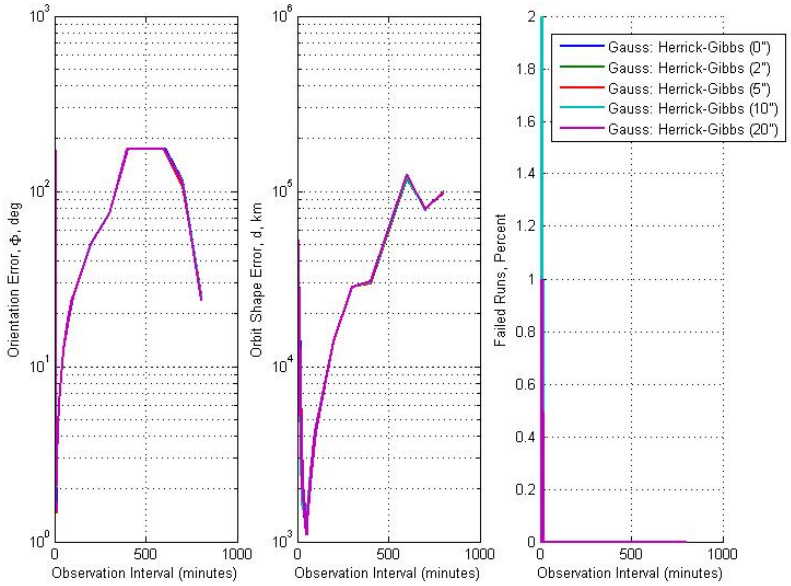

Figure A.28: Effects of Measurement Errors on Orbital Estimate for GEO Orbit Using the Gauss Method with the Herrick-Gibbs Method

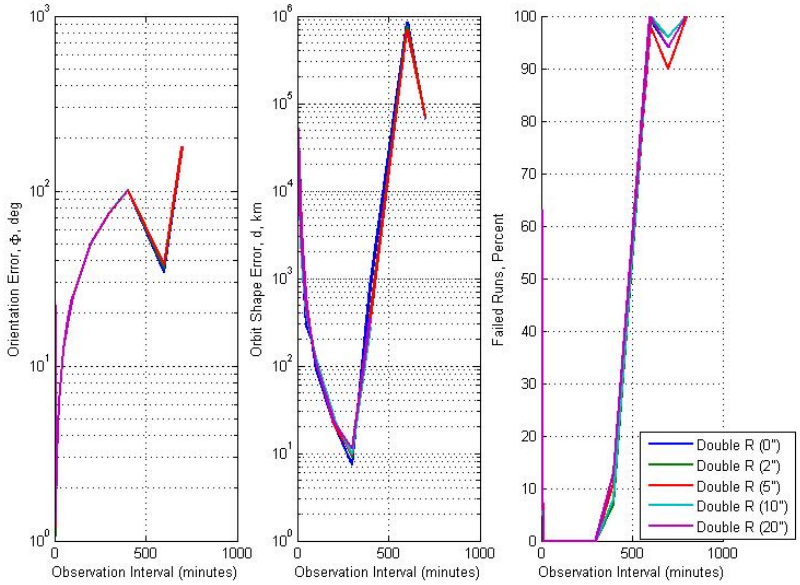

Figure A.29: Effects of Measurement Errors on Orbital Estimate for GEO Orbit Using the Double-R Method

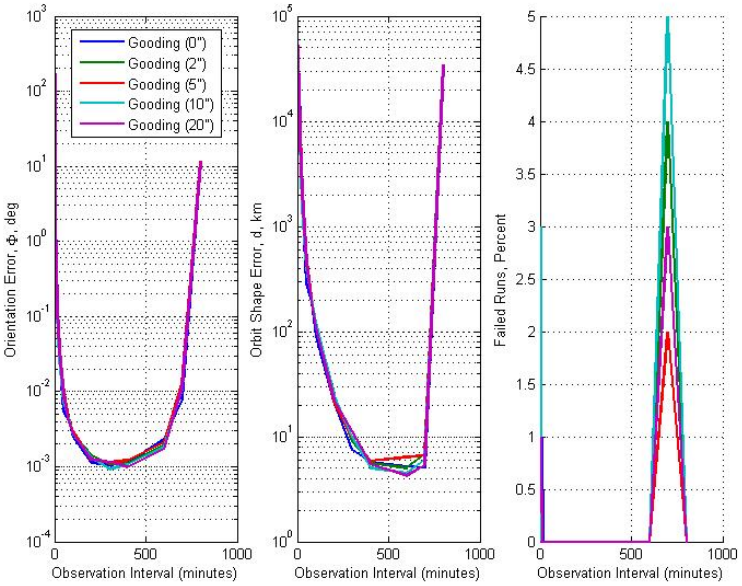

Figure A.30: Effects of Measurement Errors on Orbital Estimate for GEO Orbit Using the Gooding Method

VITA

Andrew Vernon Schaeperkoetter was born in St. Louis, Missouri. He received his Bachelor of Sceince degree in aerospace engineering from the University of Kansas, Lawrence , Kansas in May 2009.

He began his graduate study at Texas A&M University in August 2009 and received his Master of Science degree in aerospace engineering in December 2011. His research interests focused on astrodynamics, particularly on comparing and contrasting different algorithms for initial orbit determination.

Andrew Vernon Schaeperkoetter's email address is aschaepe@gmail.com. He can be reached at:

Department of Aerospace Engineering

c/o Dr. Daniele Mortari

Texas A&M University

H.R. Bright Building, Ross Street - TAMU 3141

College Station, TX 77843-3141

The typist for this thesis was Andrew Schaeperkoetter.